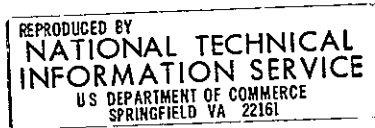




Submitted to
 JET PROPULSION LABORATORY
 Pasadena, California

ATMOSPHERIC PREDICTION
 MODEL SURVEY

Final Report



Prepared Under

Contract No. 954547
 (Subcontract under NASA Contract No. NAS7-100,
 Task Order No. RD-151)

December 1976

{NASA-CR-157217}	ATMOSPHERIC PREDICTION	N78-29697
MODEL SURVEY Final Report {Ocean Data Systems, Inc.)	HC A10/MF A01 CSCL 04B	
		Unclas
		G3/47 15076



OCEAN DATA SYSTEMS, INC.

2400 GARDEN ROAD MONTEREY CALIFORNIA 93940 • 408/649-1133

Submitted to
JET PROPULSION LABORATORY
Pasadena, California

ATMOSPHERIC PREDICTION

MODEL SURVEY

Final Report

Prepared Under

Contract No. 954547
(Subcontract under NASA Contract No. NAS7-100,
Task Order No. RD-151)

December 1976

Prepared by
Robert E. Wellck
OCEAN DATA SYSTEMS, INC.
Monterey, California

ABSTRACT

As part of the SEASAT Satellite program of NASA, a survey of representative primitive equation atmospheric prediction models that exist in the world today was written for the Jet Propulsion Laboratory under Contract No. 954547 (Subcontract under NASA Contract No. NAS7-100, Task Order No. RD-151). Seventeen models developed by eleven different operational and research centers throughout the world are included in the survey. The surveys are intended to be tutorial in nature describing the features of the various models in a systematic manner.

TABLE OF CONTENTS

	<u>Page</u>
Abstract	11
I. Introduction	I-1
II. Atmospheric Prediction Models	II-1
A. AFGWC 6-Layer Hemispheric Operational Model (Air Force Global Weather Central, USA)	
B. FNWC 5-Layer Hemispheric Operational Model (Fleet Numerical Weather Central, USA)	
C. FNWC 5-Layer Global Model (Fleet Numerical Weather Central, USA)	
D. GFDL 9-Layer Global Model (Geophysical Fluid Dynamics Laboratory, NOAA, USA)	
E. GFDL 18-Layer Global Model (Geophysical Fluid Dynamics Laboratory, NOAA, USA)	
F. GISS 9-Layer Global Model (Goddard Institute for Space Studies, NASA, USA)	
G. NCAR Multi-Layer Second Generation Global Model (National Center for Atmospheric Research, USA)	
H. NCAR Multi-Layer Limited Area Model (National Center for Atmospheric Research, USA)	
I. NCAR Multi-Layer Third Generation Global Model (National Center for Atmospheric Research, USA)	
J. NMC 6-Layer Hemispheric Operational Model (National Meteorological Center, USA)	
K. NMC 6-Layer Limited Area Operational Model (National Meteorological Center, USA)	
L. NMC 8-Layer Global Model (National Meteorological Center, USA)	
M. UCLA 12-Layer Global Model (University of California at Los Angeles, USA)	

- N. ANMRC 5-Layer Hemispheric, Spectral Model
(Australian Numerical Meteorological Research
Center, Australia)
- O. Canadian 5-Layer Hemispheric, Spectral Operational
Model
(Atmospheric Environment Service, Canada)
- P. Deutscher Wetterdienst 6-Layer Hemispheric Operational
Model
(Deutscher Wetterdienst, Federal Republic of Germany)
- Q. Japan Meteorological Agency 6-Layer Limited Area
Operational Model
(Japan Meteorological Agency, Japan)

III. Summary III-1

I. Introduction

At the request of the Jet Propulsion Laboratory and in support of the SEASAT satellite program of NASA, Ocean Data Systems, Inc. has conducted a survey of representative atmospheric prediction models in use at operational and research centers throughout the world. These surveys are intended to be tutorial in nature describing the features of the various models in a systematic manner.

When conducting a survey on some subject, one is immediately faced with the problem of choosing the items to be surveyed. If the survey is to be exhaustive, then the only problem is making sure that it is truly exhaustive. Since this atmospheric prediction model survey was not intended to be exhaustive, but to be representative of the types of primitive equation atmospheric prediction models that exist in the world today, criteria for model selection was required.

This survey has attempted to include models from many different organizations, models with a wide range of applications - research to operational, models of varying types - gridpoint and spectral, and models of varying areal coverage - global to limited area. In addition, the availability of literature describing the models, a desire to avoid

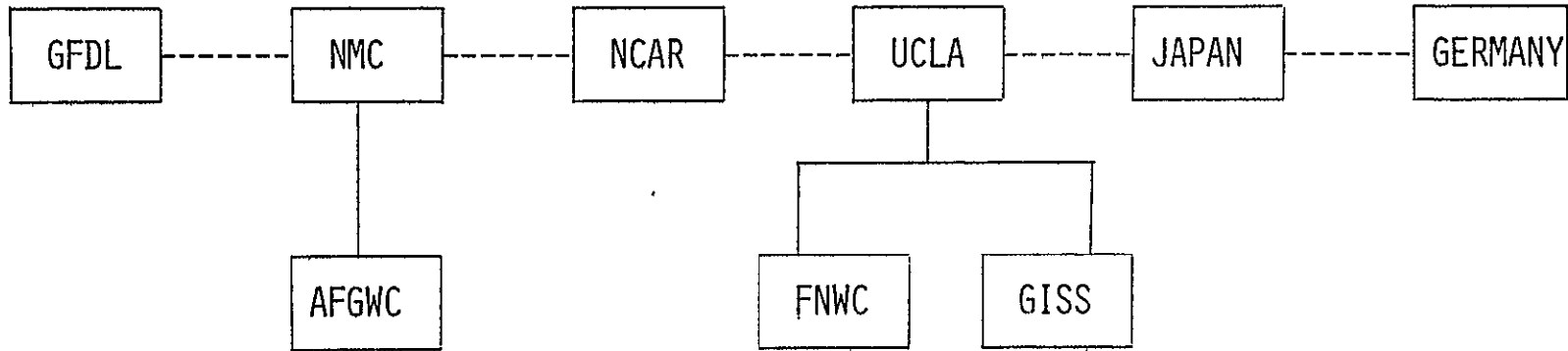
repetition that would be caused by surveying quite similar models, and an attempt for the survey to be representative of atmospheric prediction models in the world today, influenced the model selections.

The accompanying chart represents a crude attempt to describe the "genealogy" of the various models surveyed. The models are denoted by the organizations that developed them and have been divided into two basic categories - gridpoint and spectral. The solid lines represent direct descendents while the dotted lines represent interchange of procedures and ideas. While there are not very many direct descendents, there is a tremendous amount of interchange of ideas within the modelling community.

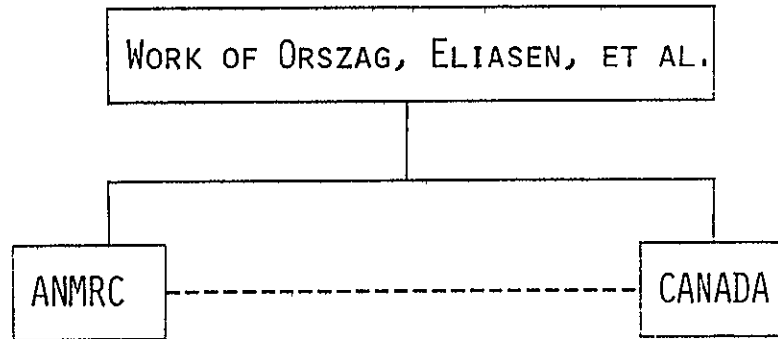
Seventeen different models from the eleven different organizations shown on the chart were included in the survey. Where multiple models from a single organization were included, they are ususally quite similar and differ only in numerical techniques or in areal extent (e.g., a limited area model).

A standard format was devised for the model surveys in order that features of the various models can more easily be compared. That is, the description of the variables, areal coverage, physical and dynamical processes, numerical methods, and so forth, are presented in the same order, topic by topic for each prediction model.

GRID POINT MODELS -



SPECTRAL MODELS -



I-3

"GENEALOGY" CHART OF THE ATMOSPHERIC PREDICTION MODELS CONSTITUTING THE SURVEY

Finally, it should be pointed out that some of the model surveys are more detailed than others. This, of course, reflects the amount of information that was available concerning the model. Also, all of the model descriptions represent a snapshot of the various prediction models at some point in time defined by a combination of the source material available and the knowledge of the author concerning the particular model. While the availability and accuracy of the source material heavily impacts the accuracy of a given model description, the ultimate responsibility for the accuracy of the model description rests with the author of the surveys.

The following Section, Section II, contains the surveys of the models included in this atmospheric prediction model survey. Section III discusses the inclusion of SEASAT Satellite data in the forecast models in relation to the analysis problem. Mention is also made of the boundary layer parameterization problem as related to the use of SEASAT Satellite data.

II. Atmospheric Prediction Model Surveys

This section contains the atmospheric prediction model surveys. Each model is presented in a standard format as a subsection in order to more easily compare the features of the various models.

III. Summary

The previous section contains surveys of seventeen different atmospheric prediction models developed by eleven different organizations. These models are representative of the types of primitive equation atmospheric prediction models that exist in the world today. Included are models from many different organizations, models with a wide range of applications - research to operational, models of varying types - gridpoint and spectral, and models of varying areal coverage - global to limited area.

In the descriptions of the models, the initial data is either treated as input to the program in the case of the forecast models, or as being self-generated in the case of the general circulation (climate simulation) models. The descriptions of the inputs to the forecast models usually make reference to an analysis procedure which produces data for use by the forecast model. Thus, the model descriptions only very indirectly make reference to the analysis problem. This is, of course, reasonable since discussion of analysis procedures is beyond the scope of this survey. However, in order to make a forecast an initial state is required and some mention should be made of the analysis problem including data sources.

Historically, the analysis data cycle has been geared to those times at which upper-air observations (rawinsondes) are made (0000 and 1200 GMT, mainly). Analyses of pertinent atmospheric parameters are made at these times for the entire three-dimensional domain of interest. However, with the availability in recent years of satellite temperature/moisture profiles (SIRS, VTPR) derived from radiance measurements, considerable attention has been given to methods for incorporating these "off-time" data into atmospheric analysis structures.

The satellite data available today is spread through both space and time. Satellites in polar orbits produce data in strips corresponding to orbits around the earth and the width of the field of view of the sensors. Satellites in other types of orbits also produce data that is distributed in space and time in a manner dependent upon the orbit and the sensor characteristics; but, not as the classical analysis cycle would prefer it - global coverage at the canonical times of 0000 and 1200 GMT.

SEASAT will add to the amount of data available for analysis by producing large amounts of data over the oceans including wave heights, surface winds and ocean temperatures. This data will, of course, be "off-time" data as is other satellite data and methods will have to be found to incorporate the data into the analysis structure.

In addition, SEASAT data will all be at the ocean surface which will introduce a different class of problem in the utilization of the data. With the exception of variables such as surface pressure, forecast models carry data at levels above the surface. In fact, in most models, surface values of many variables are obtained through diagnostic boundary layer calculations. SEASAT data will present the inverse of this problem - many surface values will be available from measurements and boundary layer parameterizations must be devised to couple this information into the levels above the surface.

The previous paragraphs have given a brief discussion of the analysis problem since the forecast problem cannot be addressed without at least mentioning the related analysis problem. In particular, the problem of incorporating "off-time", strip data and data at "inconvenient" levels into the analysis structure has been pointed out. These problems are all being actively investigated and the solutions or, at least, partial solutions will certainly be included as part of future atmospheric analysis/prediction systems.

A. AFGWC 6-Layer Hemispheric Operational Model

The Air Weather Service atmospheric prediction model (AWSPE) is currently executed twice daily to produce three day forecasts for the Northern Hemisphere. The model is an adaptation of the NMC model without moisture (Flattery, 1975). Since the forecast model is continually being modified, the description that follows is, thus, a snapshot of the state of the model as of mid-1976.

MODEL DESCRIPTION

1.0 Variables

1.1 Independent

The independent variables are x and y derived from a polar stereographic map projection in the horizontal, σ in the vertical defined as:

$$\sigma = \frac{P - P_U}{P_L - P_U} \quad [A.1]$$

where P_U is the pressure at a given quasi-horizontal surface above some point and P_L is the pressure at a surface below, and time, t .

1.2 Dependent

1.2.1 Prognostic

The prognostic variables are the x wind component, u ; the y wind component, v ; the potential temperature, θ ; and the vertical pressure gradient, $\frac{\partial P}{\partial \sigma}$, at the three interfaces (between the planetary boundary layer and the troposphere, between the troposphere and the stratosphere, and between the stratosphere and the constant θ layer) as shown in Figure A-2.

1.2.2 Diagnostic

The diagnostic variables are the geopotential, Φ , and the vertical velocity, $w \equiv -\dot{\sigma}$.

2.0 Domain

2.1 Horizontal

The horizontal domain is a polar stereographic projection (true at 60°N) of the Northern Hemisphere using x-y coordinates with map factor

$$m = \frac{1 + \sin 60^\circ}{1 + \sin \phi} \quad [\text{A.2}]$$

The grid resolution is 381 km at 60°N and the grid dimensions are 53 x 57 which covers virtually the entire

Northern Hemisphere as shown in Figure A-1. (The standard octagon is also shown.) There is no staggering of variables in the horizontal.

2.2. Vertical

The vertical coordinate is sigma as defined by Equation [A.1]. Figure A-2 shows the vertical structure of the model with the four distinct sigma domains. The variables u , v and θ are carried at the midpoints of the various sigma layers and the variables ϕ , π and p are carried at the layer interfaces. The vertical velocity, $\dot{\sigma}$, is defined at layer interfaces, but at the center of a horizontal gridpoint square.

ORIGINAL PAGE IS
OF POOR QUALITY

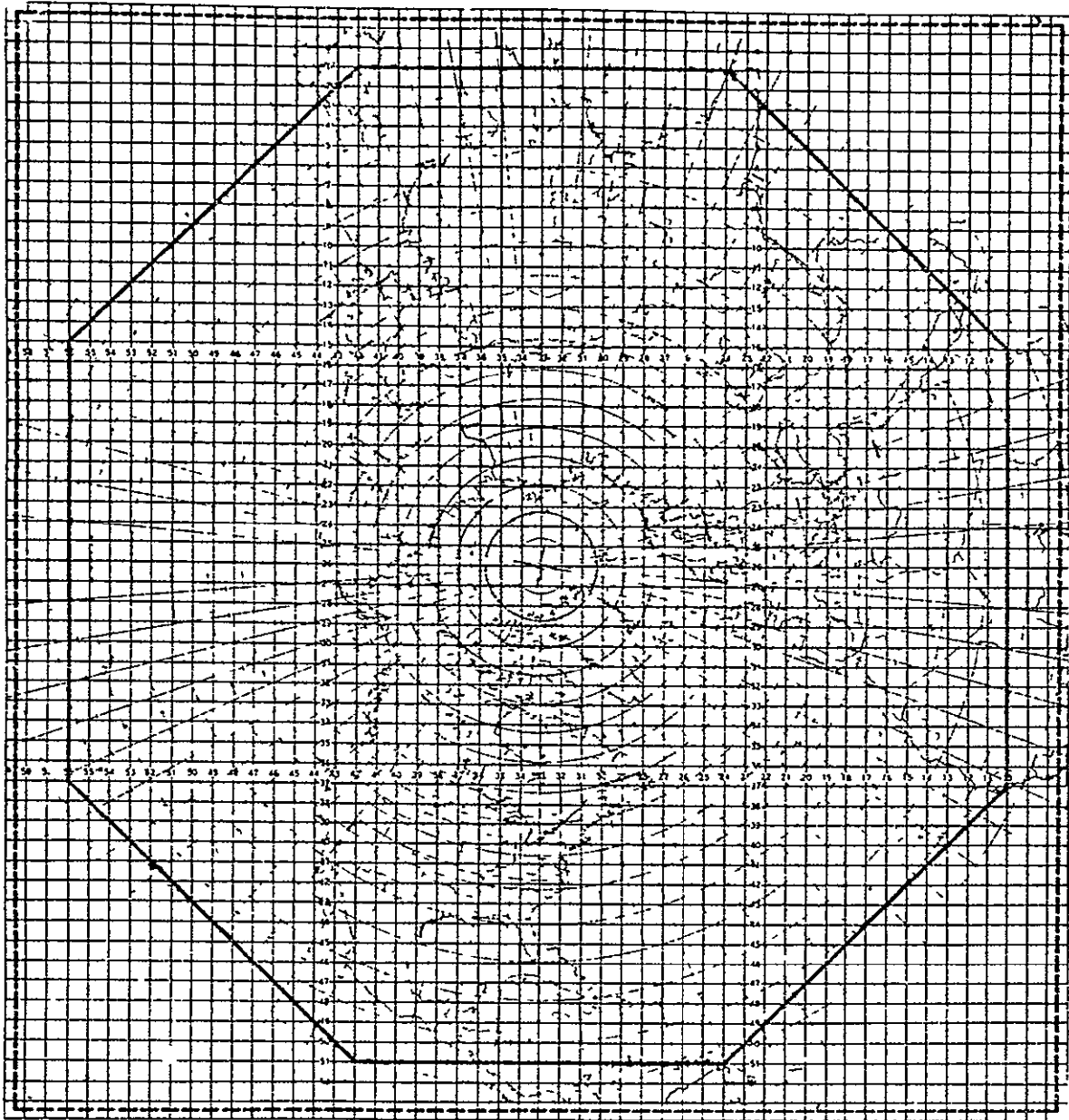


Figure A-1

AWS Northern Hemisphere Polar Stereographic Grid

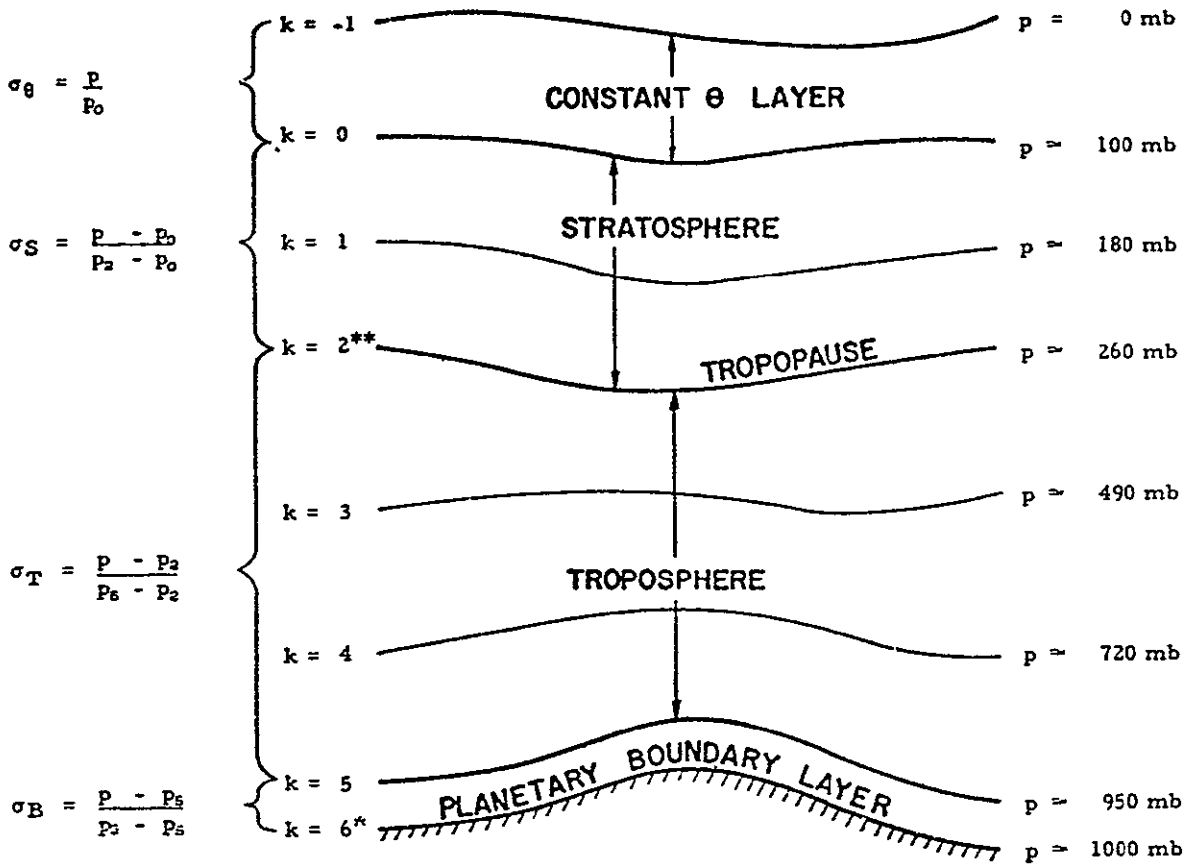


Figure A-2

Vertical Structure of the AWS Atmospheric Prediction Model

2.3 Temporal

Two time levels of data are required (except during the startup step) since a centered time differencing scheme is used with a twenty minute time step. There is no staggering of variables in time.

3.0 Governing Equations

The governing partial differential equations, written for an x-y map projection with map factor m, are listed below.

Wind component in the x direction:

$$\begin{aligned} \frac{\partial u}{\partial t} = & -m \left[u \frac{\partial u}{\partial x} + v \frac{\partial u}{\partial y} \right] - m \left[\frac{\partial \phi}{\partial x} + C_p \theta \frac{\partial \pi}{\partial x} \right] - \dot{\sigma} \frac{\partial u}{\partial \sigma} \\ & + v \left[f - v \frac{\partial m}{\partial x} + u \frac{\partial m}{\partial y} \right] + F_x \end{aligned} \quad [A.3]$$

Wind component in the y direction:

$$\begin{aligned} \frac{\partial v}{\partial t} = & -m \left[u \frac{\partial v}{\partial x} + v \frac{\partial v}{\partial y} \right] - m \left[\frac{\partial \phi}{\partial y} + C_p \theta \frac{\partial \pi}{\partial y} \right] - \dot{\sigma} \frac{\partial v}{\partial \sigma} \\ & - u \left[f - v \frac{\partial m}{\partial x} + u \frac{\partial m}{\partial y} \right] + F_y \end{aligned} \quad [A.4]$$

Thermodynamic energy equation:

$$\frac{\partial \theta}{\partial t} = -m \left[u \frac{\partial \theta}{\partial x} + v \frac{\partial \theta}{\partial y} \right] - \dot{\sigma} \frac{\partial \theta}{\partial \sigma} + H \quad [A.5]$$

Pressure tendency equation:

$$\begin{aligned} \frac{\partial}{\partial t} \left(\frac{\partial p}{\partial \sigma} \right) = & -m \left[\frac{\partial}{\partial x} \left(\frac{\partial p}{\partial \sigma} u \right) + \frac{\partial}{\partial y} \left(\frac{\partial p}{\partial \sigma} v \right) \right] - \frac{\partial}{\partial \sigma} \left(\frac{\partial p}{\partial \sigma} \dot{\sigma} \right) \\ & + \frac{\partial p}{\partial \sigma} \left(u \frac{\partial m}{\partial x} + v \frac{\partial m}{\partial y} \right) \end{aligned} \quad [A.6]$$

Hydrostatic equation:

$$\frac{\partial \Phi}{\partial \sigma} = -C_p \theta \frac{\partial \pi}{\partial \sigma} \quad [\text{A.7}]$$

Exner function:

$$\pi = \left(\frac{P}{1000}\right)^\kappa \quad [\text{A.8}]$$

In the above equations,

u = x direction wind component

v = y direction wind component

θ = potential temperature

Φ = gz = geopotential

p = pressure

f = Coriolis parameter

$\dot{\sigma}$ = $\frac{d\sigma}{dt}$ = vertical velocity

F_x, F_y = stress components

H = diabatic heating/cooling term

C_p = specific heat of dry air at constant pressure

R = gas constant for dry air

$\kappa = \frac{R}{C_p}$

4.0 Numerics

Finite difference methods are used to approximate the solution of the forecast model equations.

4.1 Spacial Differencing

Centered, second-order differencing using Shuman's (1968) horizontal space averaging technique is used to approximate the x and y derivatives in the various sigma domains. The vertical derivatives are also approximated by second-order differences.

4.2 Temporal Differencing

Centered time differencing with Shuman's pressure gradient force time averaging is used to obtain a time step of twenty minutes. The computation is started with a forward time step.

4.3 Boundary Conditions

The horizontal boundary conditions consist of insulated, slippery walls placed on the grid as shown in Figure A-1. That is, no heat or momentum flow is permitted through the wall, but a parallel flow is permitted along the wall.

The vertical boundary condition that $\dot{\sigma} = 0$ for a material surface is specified: at the top of the model; the boundary surface between the topmost computational layer and the stratosphere; the tropopause; and the earth's surface. As a consequence of the above approach, no mass exchange takes place among the isentropic, stratospheric and tropospheric domains. However, mass exchange can take place between the boundary layer and the troposphere.

5.0 Processes and Effects

5.1 Dynamics

Terms representing the horizontal and vertical advection and convergence/divergence of heat and momentum are included as are terms representing the pressure gradient and Coriolis forces in the momentum equations.

Orography that is rough but consistent with the grid resolution is included to add realism to the flows.

Horizontal stress according to Shuman (1968) is applied at the lowest level to simulate vertical momentum transport at the surface.

5.2 Heat Sources/Sinks

Sensible heating in the planetary boundary layer over the oceans is included. The ocean temperature is spatially varying, but held constant during the forecast.

A dry convective adjustment procedure is included to preclude hydrostatic instability of the model atmosphere.

5.3 Moisture Sources/Sinks

There are none since a dry, adiabatic fluid is considered.

6.0 Inputs

The forecast model initial data is obtained from hemispheric analyses of the mass structure (temperature and geopotential) between 1000 mb and 100 mb. The analyses are performed by a program called MULTAN which is the AFGWC objective analysis program and is based on the work of NMC.

The initial wind fields are derived from the linear balance equation solved on the mandatory pressure surfaces.

The analyzed and derived fields on pressure surfaces are then interpolated (linearly in $\ln p$) to obtain initial data on the model sigma surfaces.

The sea surface temperature is obtained from Fleet Numerical Weather Central analyses.

7.0 Outputs

Fields on the standard pressure surfaces are produced by interpolation from the model sigma surfaces to the pressure surfaces during an output cycle. Various filters are used to render the output fields more visually pleasing.

8.0 Computer Information

The forecast model is run on a Univac 1110 Computer System and is normally executed twice daily. The model is largely programmed in Fortran V (Univac dialect of FTN IV) with some routines in assembly language.

9.0 References

Flattery, T.W., "The Air Weather Service Primitive Equation Model", AFGWC User Documentation, May 1975.

Shuman, F.G. and J.B. Hovermale, "An Operational Six-Layer Primitive Equation Model", Journal of Applied Meteorology, Vol. 7, No. 4, August 1968, pp. 525-547.

B. FNWC 5-Layer Hemispheric Operational Model

The FNWC operational atmospheric prediction model is executed twice daily to produce three day forecasts for the Northern Hemisphere. The model was designed and developed for operational use by Kesel and Winninghamoff (1972) during the period 1969-72. Since that time many changes have been made to the model to improve the quality of the forecasts produced and to better utilize the available computer resources. The description that follows is, thus, a snapshot of the state of the model as of mid-1976.

MODEL DESCRIPTION

1.0 Variables

1.1 Independent

The independent variables are x and y derived from a polar stereographic map projection in the horizontal, σ in the vertical defined as

$$\sigma = \frac{P}{\pi} \quad [B.1]$$

where π is the local terrain pressure, and time, t .

1.2 Dependent

1.2.1 Prognostic

The prognostic variables are the terrain pressure, π , the temperature, T , the water vapor pressure, q , the x wind component, u , and the y wind component, v . A secondary prognostic variable is the precipitation, Pr , obtained from both the large scale precipitation algorithm and the cumulus parameterization.

1.2.2 Diagnostic

The diagnostic variables are the geopotential, Φ , and the vertical velocity, $w \equiv -\dot{\sigma}$.

2.0 Domain

2.1 Horizontal

The horizontal domain is a polar stereographic projection (true at 60°N) of the Northern Hemisphere using x-y coordinates with map factor:

$$m = \frac{1 + \sin 60^\circ}{1 + \sin \phi} \quad [\text{B.2}]$$

The horizontal grid resolution is 381 km at 60°N resulting in a 63 x 63 grid as shown in Figure B-1. There is no staggering of variables in the horizontal.

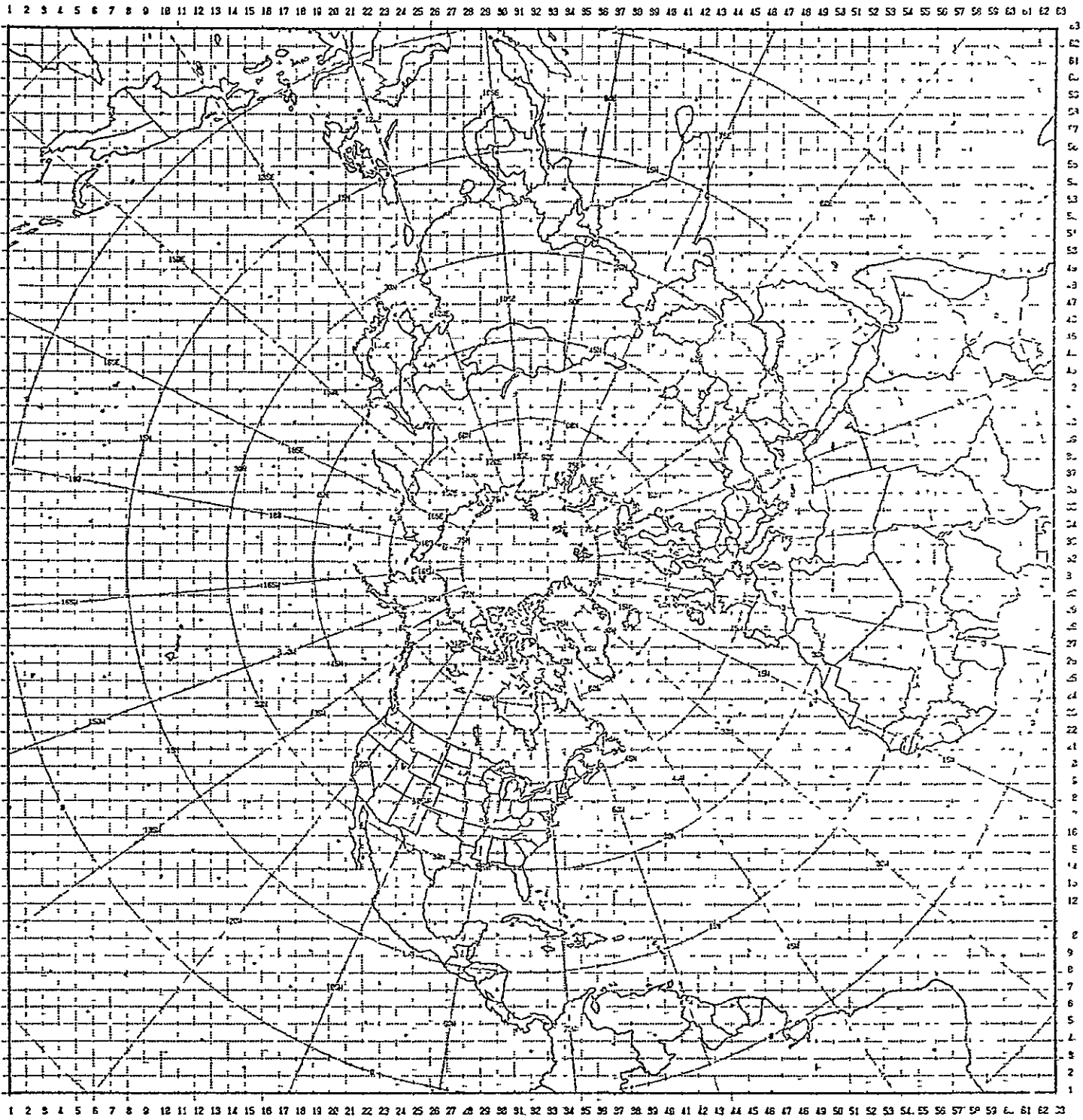


Figure B-1: Northern Hemisphere Polar Stereographic Grid.
The pole to equator distance is 31.205 grid lengths.

3.0 Governing Equations

The governing partial differential equations, written in flux form for an x-y map projection with map factor m, are listed below.

Momentum equation in the x direction:

$$\begin{aligned} \frac{\partial(\pi u)}{\partial t} = & -m^2 \left[\frac{\partial}{\partial x} \left(\frac{uu\pi}{m} \right) + \frac{\partial}{\partial y} \left(\frac{uv\pi}{m} \right) \right] + \pi \frac{\partial(wu)}{\partial \sigma} & [B.3] \\ & + \pi v f - m \left(\pi \frac{\partial \Phi}{\partial x} + RT \frac{\partial \pi}{\partial x} \right) + F_x + D_u \end{aligned}$$

Momentum equation in the y direction:

$$\begin{aligned} \frac{\partial(\pi v)}{\partial t} = & -m^2 \left[\frac{\partial}{\partial x} \left(\frac{uv\pi}{m} \right) + \frac{\partial}{\partial y} \left(\frac{vv\pi}{m} \right) \right] + \pi \frac{\partial(wv)}{\partial \sigma} & [B.4] \\ & - \pi u f - m \left(\pi \frac{\partial \Phi}{\partial y} + RT \frac{\partial \pi}{\partial y} \right) + F_y + D_v \end{aligned}$$

Thermodynamic energy equation:

$$\begin{aligned} \frac{\partial(\pi T)}{\partial t} = & -m^2 \left[\frac{\partial}{\partial x} \left(\frac{\pi u T}{m} \right) + \frac{\partial}{\partial y} \left(\frac{\pi v T}{m} \right) \right] + \pi \frac{\partial(wT)}{\partial \sigma} & [B.5] \\ & + H\pi + \frac{RT}{c_p \sigma} \left\{ -w\pi + \sigma \left[\frac{\partial \pi}{\partial t} + m \left(u \frac{\partial \pi}{\partial x} + v \frac{\partial \pi}{\partial y} \right) \right] \right\} + D_T \end{aligned}$$

Moisture conservation equation:

$$\begin{aligned} \frac{\partial(\pi q)}{\partial t} = & -m^2 \left[\frac{\partial}{\partial x} \left(\frac{\pi u q}{m} \right) + \frac{\partial}{\partial y} \left(\frac{\pi v q}{m} \right) \right] + \pi \frac{\partial(wq)}{\partial \sigma} & [B.6] \\ & + Q\pi + D_q \end{aligned}$$

Pressure tendency equation:

$$\frac{\partial \pi}{\partial t} = -m^2 \int_0^1 \left[\frac{\partial}{\partial x} \left(\frac{u\pi}{m} \right) + \frac{\partial}{\partial y} \left(\frac{v\pi}{m} \right) \right] d\sigma \quad [\text{B.7}]$$

Hydrostatic equation:

$$\frac{\partial \phi}{\partial \sigma} = - \frac{RT}{\sigma} \quad [\text{B.8}]$$

In the above equations,

u = x direction wind component

v = y direction wind component

π = terrain pressure

T = temperature

q = vapor pressure

w = $-\frac{d\sigma}{dt}$ = vertical velocity

f = Coriolis parameter

F_x, F_y = stress components

D_u, D_v, D_T, D_q = diffusion terms

H = diabatic heating/cooling term

Q = moisture source/sink term

ϕ = gz = geopotential

R = gas constant for dry air

C_p = specific heat of dry air at constant pressure

4.0 Numerics

Finite difference methods are used to approximate the solution of the forecast model equations.

4.1 Spacial Differencing

Centered, fourth-order differencing of the horizontal advection and pressure gradient force terms is used to reduce the phase propagation error. All other derivatives are approximated by centered, second-order differences.

The lateral diffusion terms shown in the momentum and thermodynamic energy equations take the form of diffusion of the departures from the initial state, while the lateral diffusion term in the moisture equation is based on the diffusion of the moisture only. Thus, the term D_T is defined as:

$$D_T = \frac{Km^2}{d^2} \Delta^2 (\pi^{\circ T^{\circ}} - \pi^{\tau T^{\tau}}) \quad [B.9]$$

where K is the diffusion coefficient, Δ^2 represents the Laplacian operator, the superscript zero denotes the initial value and the superscript τ denotes the current value.

4.2 Temporal Differencing

Centered time differencing with Shuman's pressure-gradient force time averaging is used to offset the more stringent linear stability requirements of fourth-order differencing resulting in a time step of ten minutes.

Robert time filtering of the solutions is also done to control computational noise.

The computation is started with an Euler-backward (or Matsuno) step. This procedure is repeated every six hours after each output cycle.

4.3 Boundary Conditions

The horizontal boundary conditions are of the restoration type; that is, persistence below 7.5°N, a blend of persistence and prediction between 7.5° and 15°N, and total prediction above 15°N.

The vertical boundary conditions are $w \equiv 0$ at $\sigma = 0$ and 1.

5.0 Processes and Effects

5.1 Dynamics

Terms representing the three-dimensional flux divergence of heat, moisture and momentum are included as are terms representing the pressure gradient and Coriolis forces in the momentum equations. Adiabatic temperature changes are also modeled.

The Kurihara local pressure surface technique is used to calculate the pressure gradient force terms in order to reduce computational noise over high, irregular terrain.

Orography that is rough but consistent with the grid resolution is included to add realism to the flows. The

terrain gradients are limited to 2000 meters per grid interval and the terrain is smoothed.

Friction according to Shuman is included in the lowest layer ($\sigma = 1.0$ to 0.8).

5.2 Heat Sources/Sinks

Both solar and terrestrial radiation are included in a manner similar to that of the Mintz and Arakawa model of the late sixties. Moisture is included only in the lower three sigma layers, and heating rates are evaluated for two gross layers only, from $\sigma = 1.0$ to 0.6 and from $\sigma = 0.6$ to 0.2 . Clouds are included at the $\sigma = 0.7$ level using a parameterization due to Smagorinsky.

Sensible heating in the Arakawa type constant flux, gross boundary layer is evaluated for the lowest sigma layer and a land-sea-ice discriminator is included. The ocean temperature is spatially varying, but held constant during the forecast.

Release of latent heat due to large scale precipitation is included in the moisture carrying layers.

A parameterization of cumulus ensembles (moist convective adjustment) based on the 1968 version by Arakawa et al redistributes heat and moisture in the vertical when the appropriate conditions prevail (conditional instability of the layers). A dry convective adjustment procedure is included to preclude hydrostatic instability.

5.3 Moisture Sources/Sinks

The large scale precipitation process removes supersaturated states from the model atmosphere and may result in evaporation in layers below the supersaturated layer.

The moist convective adjustment process can result in the evaporation/condensation of moisture in the lower layers.

Evaporation from the surface in the constant flux, gross boundary layer is also included in the lowest sigma layer.

6.0 Inputs

The forecast model initial data is obtained from hemispheric analyses of the mass structure between 1000 mb and 100 mb. The analyses are performed using a technique called Fields by Information Blending (FIB) devised by Holl (1972). The 50 mb level heights and temperatures are obtained through linear regression formulae using the 100 mb heights and temperatures. Dewpoint depression, sea level pressure and sea surface temperature analyses are also made using the FIB technique.

The rotational component of the winds is derived from the solution of the balance equation on pressure surfaces in which the nonlinear terms are approximated geostrophically.

The analyzed fields on pressure surfaces are interpolated (linearly in $\ln(p)$) to obtain initial data on the model sigma surfaces.

7.0 Outputs

A normal output cycle is made every six forecast hours. The sea level pressure, precipitation, and heights and temperatures at standard pressure levels from 1000 mb to 100 mb are output. The fields on pressure surfaces are produced by interpolation (or extrapolation algorithms below the terrain) from the sigma surface data. Various filters are used to render the output fields more visually pleasing.

Numerous other fields (winds, heating rates, etc) are available during the output cycle.

8.0 Computer Information

The forecast model is run on two Control Data Corporation 6500 computer systems (four processors) coupled through extended core memory. (See Morenoff, et al. 1972.) The model is normally executed twice per day and requires about ninety minutes to produce a seventy-two hour forecast.

The software system is slightly modified CDC and the model is written mainly in Fortran with some routines in assembly language. Various special purpose routines peculiar to FNWC are also used by the model.

9.0 References

- Arakawa, Akio, Akira Katayama and Yale Mintz, "Numerical Simulation of the General Circulation of the Atmosphere", Proceedings of the WMO/IUGG Symposium on Numerical Weather Prediction, Tokyo, Japan, November 26 - December 4, 1968, Japan Meteorological Agency, Tokyo, March 1969, pp. IV-1 - IV-14.
- Holl, M.M. and B.R. Mendenhall, 1972, "Fields by Information Blending", Sea-Level Pressure Version, U.S. Navy Fleet Numerical Weather Central Technical Note No. 72-2, Monterey, CA, 66 pp.
- Kaitala, J.E., "Heating Functions and Moisture Source Terms in the FNWC Primitive Equation Models", unpublished manuscript, April 1974, 84 pp.
- Kesel, Philip G. and Francis J. Winninghamhoff, "The Fleet Numerical Weather Central Operational Primitive Equation Model", Monthly Weather Review, Vol. 100, No. 5, May 1972, pp. 360-373.
- Morenoff, E., P.G. Kesel and L.C. Clarke, "Horizontal Domain Partitioning of the Navy Atmospheric Primitive Equation Prediction Model," AFIPS Conference Proceedings Volume 41, Part I, December 5-7, 1972, Anaheim, California, pp. 393-405.

C. FNWC 5-Layer Global Model

The FNWC global primitive equation atmospheric prediction model has been proposed as a successor to the current hemispheric operational model. (See Section B.) Development of this model was begun by Winninghamoff (1971) and has been continued by Elias (1973), Mihok (1974) and Mihok and Kaitala (1976). Since this global model is an outgrowth of the operational hemispheric model, there are many similarities between the two models. The grid structure and finite difference techniques used are quite different, while most of the physical parameterizations other than the treatment of the boundary layer are identical.

MODEL DESCRIPTION

1.0 Variables

1.1 Independent

The independent variables are latitude, θ , and longitude, λ , of a spherical polar coordinate system in the horizontal, sigma in the vertical defined as

$$\sigma = \frac{p}{\pi} \quad [C.1]$$

where π is the local terrain pressure, and time, t .

1.2 Dependent

1.2.1 Prognostic

The prognostic variables are the terrain pressure, π , the temperature, T , the water vapor pressure, q , the latitudinal wind component, u , and the longitudinal wind component, v . A secondary prognostic variable is the precipitation, Pr , obtained from both the large scale precipitation algorithm and the cumulus parameterization.

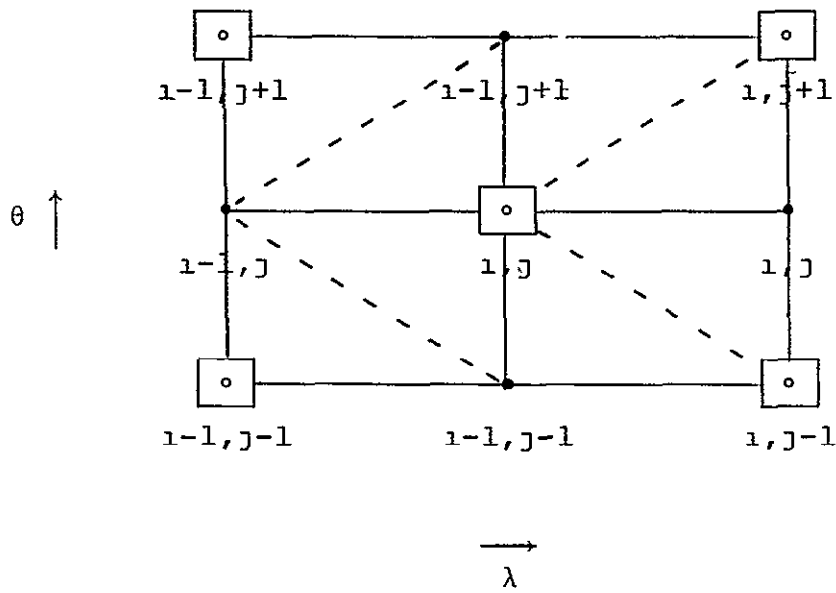
1.2.2 Diagnostic

The diagnostic variables are the geopotential, ϕ , and the vertical velocity, $w \equiv -\dot{\sigma}$.

2.0 Domain

2.1 Horizontal

The horizontal domain is a global latitude, longitude grid with θ and λ as the coordinates. The resolution is 5° between values of like variables giving a 71×72 grid with a grid distance of 556 km at the equator. The poles are considered as mass points and are treated separately. The variables are staggered in the horizontal as shown in Figure C-1 with velocity components of the wind carried at one set of points and mass variables at the other.



- \equiv Velocity Point (u, v)
- \equiv Mass Point (π, T, ϕ, q, w)

Figure C-1

Horizontal Grid Structure of the FNWC 5-Layer Global Model

2.2 Vertical

The vertical coordinate is sigma as defined by Equation [C.1]. Figure C-2 shows the model sigma surfaces and the placement of the variables in the vertical.

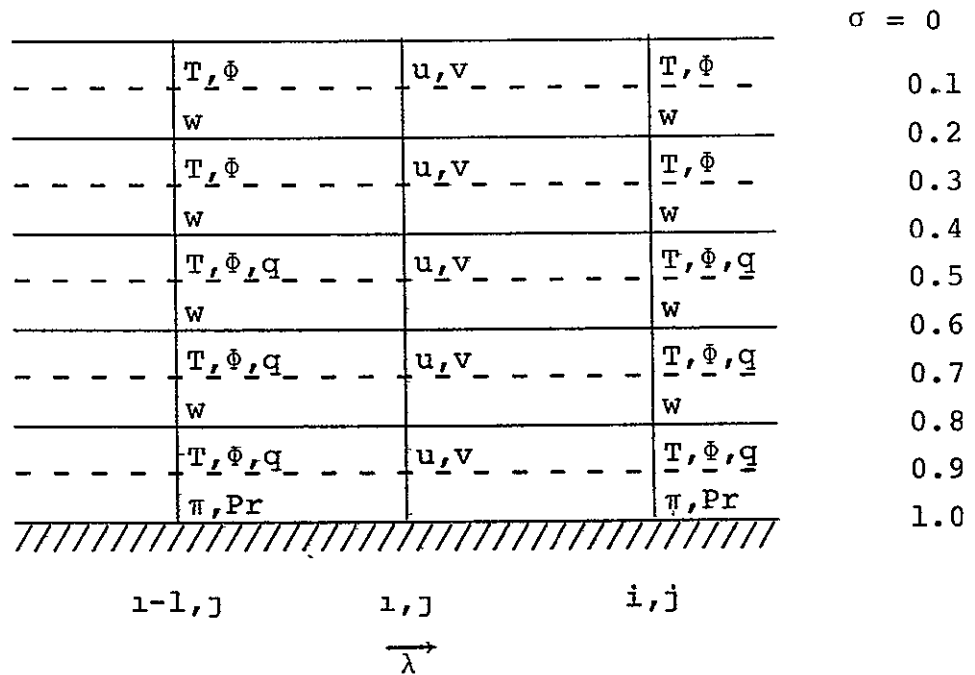


Figure C-2

Vertical Structure of the FNWC 5-Layer Global Model

2.3 Temporal

Two time levels of data are required (except during the first time step) since a centered time differencing scheme is used with Shuman's pressure gradient force averaging technique and Robert time filtering. A nine minute time step is used. There is no staggering of variables in time.

3.0 Equations

The governing partial differential equations written in flux form for a spherical polar coordinate system, θ and λ , in the horizontal and a sigma coordinate in the vertical are listed below.

Momentum equation in the latitudinal direction:

$$\begin{aligned} \frac{\partial(\pi u)}{\partial t} &= - \frac{1}{a \cos \theta} \left[\frac{\partial(uu\pi)}{\partial \lambda} + \frac{\partial(uv\pi \cos \theta)}{\partial \theta} \right] + \pi \frac{\partial(wu)}{\partial \sigma} \\ &+ \left(f + \frac{u \tan \theta}{a} \right) \pi v - \frac{1}{a \cos \theta} \left[\frac{\pi \partial \Phi}{\partial \lambda} + RT \frac{\partial \pi}{\partial \lambda} \right] \\ &+ F_x + D_m \end{aligned} \tag{C.2}$$

Momentum equation in the longitudinal direction:

$$\begin{aligned} \frac{\partial(\pi v)}{\partial t} &= - \frac{1}{a \cos \theta} \left[\frac{\partial(uv\pi)}{\partial \lambda} + \frac{\partial(vv\pi \cos \theta)}{\partial \theta} \right] + \pi \frac{\partial(wv)}{\partial \sigma} \\ &- \left(f + \frac{u \tan \theta}{a} \right) \pi u - \frac{1}{a} \left[\pi \frac{\partial \Phi}{\partial \theta} + RT \frac{\partial \pi}{\partial \theta} \right] \\ &+ F_y + D_m \end{aligned} \tag{C.3}$$

Thermodynamic energy equation:

$$\begin{aligned} \frac{\partial (\pi T)}{\partial t} &= - \frac{1}{a \cos \theta} \left[\frac{\partial (\pi u T)}{\partial \lambda} + \frac{\partial (\pi v T \cos \theta)}{\partial \theta} \right] + \pi \frac{\partial (w T)}{\partial \sigma} \\ &+ \frac{R T}{C_p \sigma} \left\{ -w \pi + \sigma \left[\frac{\partial \pi}{\partial t} + \frac{1}{a \cos \theta} \left(u \frac{\partial \pi}{\partial \lambda} + v \frac{\partial (\pi \cos \theta)}{\partial \theta} \right) \right] \right\} \\ &+ H \pi + D_T \end{aligned} \quad [C.4]$$

Moisture conservation equation:

$$\begin{aligned} \frac{\partial (\pi q)}{\partial t} &= - \frac{1}{a \cos \theta} \left[\frac{\partial (\pi u q)}{\partial \lambda} + \frac{\partial (\pi v q \cos \theta)}{\partial \theta} \right] + \pi \frac{\partial (w q)}{\partial \sigma} \\ &+ Q \pi + D_q \end{aligned} \quad [C.5]$$

Pressure tendency equation:

$$\frac{\partial \pi}{\partial t} = - \int_0^1 \frac{1}{a \cos \theta} \left[\frac{\partial (u \pi)}{\partial \lambda} + \frac{\partial (v \pi \cos \theta)}{\partial \theta} \right] d\sigma \quad [C.6]$$

Hydrostatic equation:

$$\frac{\partial \phi}{\partial \sigma} = - \frac{R T}{\sigma} \quad [C.7]$$

In the above equations:

- u = zonal wind component
- v = meridional wind component
- π = terrain pressure
- T = Temperature

R = gas constant for dry air
 C_p = specific heat of dry air at constant pressure
 q = vapor pressure
 w = $-\frac{d\sigma}{dt}$ = vertical velocity
 a = radius of the earth
 f = Coriolis parameter
 F_x, F_y = skin friction
 D_m = lateral diffusion of momentum
 D_T = lateral diffusion of heat
 D_q = lateral diffusion of moisture
 H = diabatic heating/cooling term
 Q = moisture source/sink term
 ϕ = gz = geopotential

4.0 Numerics

Finite difference methods are used to approximate the solution of the forecast equations.

4.1 Spacial Differencing

Centered, fourth-order differencing in the horizontal is used to more accurately compute the derivatives and reduce the phase error. Vertical derivatives are approximated by centered, second-order differences. Due to the staggering of variables in the horizontal, space averaging of variables is sometimes required in the finite difference approximations. This renders the difference scheme slightly dissipative and, hence, somewhat more stable than a non-space averaged scheme.

The polar calculations follow Arakawa in that the change of the variables defined at the poles (π , T and q) is a result of the meridional mass flux at all points on the latitude circle around the particular pole.

The lateral diffusion terms shown in the momentum, thermodynamic energy and moisture equations take the form of diffusion of the departures from the initial state. Thus, the term D_T is defined as:

$$D_T = \frac{K}{a \cos \theta \Delta x^2} \Delta^2 (\pi^0 T^0 - \pi^\tau T^\tau) \quad [C.8]$$

where K is the diffusion coefficient, Δ^2 represents the Laplacian operator, the superscript zero denotes the initial value and the superscript τ denotes the current time.

4.2 Temporal Differencing —

Centered time differencing with Shuman's pressure-gradient force time averaging is used to allow a longer time step of nine minutes to be used. This procedure is coupled with Robert time filtering of the solutions to help control computational noise.

The computation is started with an Euler-backward or Matsuno step.

The removal of the overspecification of the tendencies, caused by the decreasing grid size as one approaches the poles, is accomplished through the use of a modified Arakawa three point averaging scheme.

4.3 Boundary Conditions

The horizontal boundary conditions are periodicity in longitude and the poles are treated as mass points as explained in Section 4.1.

The vertical boundary conditions are $w \equiv 0$ at $\sigma=0$ and 1.

5.0 Processes and Effects

5.1 Dynamics

Terms representing the horizontal and vertical advection and convergence/divergence of heat, moisture and momentum are included as are terms representing the pressure gradient and Coriolis forces in the momentum equations. Adiabatic temperature changes are also modeled.

Orography that is consistent with reality and the grid resolution is included to add realism to the flows. The terrain gradients are limited and the terrain is smoothed.

The skin friction, F_x and F_y , is included in the lowest sigma layer and is calculated from the planetary boundary layer (PBL) parameterization devised by Kaitala. This PBL parameterization is based on the premise that the steady state, barotropic PBL is completely determined by a pair of external parameters: the surface Rossby number, and the stability parameter.

5.2 Heat Sources/Sinks

Both solar and terrestrial radiation are included in a manner similar to that of the Mintz and Arakawa model of the late sixties. Moisture is included only in the lower three sigma layers, and heating rates are evaluated in two gross layers only, from $\sigma = 1.0$ to 0.6 and from $\sigma = 0.6$ to 0.2 . Clouds are included at the $\sigma = 0.7$ level using a parameterization due to Smagorinsky.

Sensible heating in the PBL is evaluated for the lowest sigma layer, and a land-sea-ice discriminator is included. The ocean temperature is spatially varying, but held constant during the forecast.

Release of latent heat due to large scale precipitation is included in the moisture carrying layers.

A parameterization of cumulus ensembles (moist convective adjustment) based on the Arakawa method and modified somewhat by Kaitala redistributes heat and moisture in the vertical when the appropriate conditions prevail. A dry convective adjustment procedure is included to preclude hydrostatic instability.

5.3 Moisture Sources/Sinks

The large scale precipitation process removes supersaturated states from the model atmosphere and may result in evaporation in layers below the supersaturated layer.

The moist convective adjustment process can result in the evaporation/condensation of moisture in the lower layers.

Evaporation from the surface is evaluated as part of the PBL computations and included in the lowest sigma layer.

6.0 Inputs

The forecast model initial data is obtained from a global 2 1/2° objective analysis of the mass structure between 1000 mb and 100 mb. The analyses are performed using a technique called Fields by Information Blending (FIB) devised by Holl (1972). The 50 mb heights and temperatures are obtained through linear regression formulae from the 100 mb heights and temperatures. Dewpoint depression, sea level pressure and sea surface temperature analyses are also made using the FIB technique.

Winds (rotational component) are calculated on pressure surfaces from the stream function (ψ) obtained from the solution of the full balance equation in which the nonlinear terms are approximated geostrophically. The balance equation is solved first in the southern hemisphere while holding the pole and the equator plus one latitude circle to the north constant. This extra latitude circle has the same sign and magnitude of the Coriolis force as that of the latitude circle to the south. The process is then reversed for the northern

hemisphere. The winds at the equator are averages of the components at the latitude circles adjacent to the equator.

The fields on pressure surfaces are then interpolated (linearly in $\ln(p)$) to the model sigma surfaces.

7.0 Outputs

A normal output cycle is made every six forecast hours. The sea level pressure, precipitation and heights and temperatures at standard pressure levels from 1000 mb to 100 mb are output. The fields on pressure surfaces are produced by interpolation (or extrapolation algorithms below the terrain) from the sigma surface data. Various filters are used to render the output fields more visually pleasing.

8.0 Computer Information

The forecast model is programmed mostly in CDC Fortran Extended (a dialect of FTN IV) with a few routines in assembly language. The current computer systems used are a CDC 6500 and a CDC Cyber 175.

9.0 References

- Arakawa, A. and Y. Mintz, "The UCLA Atmospheric General Circulation Model", Notes distributed at UCLA workshop: 25 March - 4 April 1974, Department of Meteorology, University of California, Los Angeles, 1974.
- Holl, M.M. and B.R. Mendenhall, 1972, "Fields by Information Blending, Sea-Level Pressure Version", U.S. Navy Fleet Numerical Weather Central Technical Note No. 72-2, Monterey, CA, 66 pp.
- Kesel, P.G. and F.J. Winninghoff, "The Fleet Numerical Weather Central Operational Primitive Equation Model", Monthly Weather Review, Vol. 100, No. 5, May 1972, pp. 360-373.
- Mihok, W.F., "Global Weather Prediction Model Difference Schemes", Masters Thesis, Naval Postgraduate School, Monterey, CA, 1974, 58 pp.
- Mihok, W.F. and J.E. Kaitala, "U.S. Navy Fleet Numerical Weather Central Proposed Operational Five-Level Global Fourth-Order Primitive-Equation Model", paper presented at Sixth Conference on Weather Forecasting and Analysis: American Meteorological Society, 10-13 May 1976, Albany, N.Y.
- Winninghoff, F.J., "Restorative-Iterative Initialization for a Global Model", Naval Postgraduate School Report, NPS-51 Wu72031A, 1971, 12 pp.

D. GFDL 9-Layer Global Model

This Geophysical Fluid Dynamics Laboratory (GFDL) atmospheric general circulation model was developed for use in long range prediction and general circulation simulation experiments. The model is based on earlier versions developed at GFDL, but uses a different finite difference grid and approximations and contains improved parameterizations of the subgrid scale processes. What follows is a description of the model as of 1976 as described in GARP publication No. 14.

MODEL DESCRIPTION

1.0 Variables

1.1 Independent

The independent variables are the longitude, λ , and the latitude, ϕ ; sigma defined as

$$\sigma = \frac{p}{p_*} \quad [D.1]$$

where p_* is the surface pressure; and time, t .

1.2 Dependent

1.2.1 Prognostic

The prognostic variables are the longitudinal component, u , and the meridional component, v , of the wind; the temperature, T ; the surface pressure, p_* ; and the moisture mixing ratio, r . Secondary prognostic variables are the surface temperature over land, T_g , and the soil moisture, W .

1.2.2 Diagnostic

The diagnostic variables are the geopotential, ϕ , the vertical σ velocity, $\dot{\sigma} = \frac{d\sigma}{dt}$, and the vertical p velocity, ω .

2.0 Domain

2.1 Horizontal

The horizontal domain is a global latitude-longitude grid with λ and ϕ as coordinates. The variables are specified at the center of the latitude-longitude boxes and, thus, the poles are not grid points. There is no staggering of variables in the horizontal. Different versions of the model exist with varying horizontal resolution ranging from a low resolution version with

nineteen points between the equator and the poles (N19) and 64 points around a latitude circle to much finer resolution versions.

2.2 Vertical

The vertical coordinate is sigma as defined by Equation [D.1]. Figure D-1 shows the vertical structure of the model and the placement of variables in the vertical. Table D-1 gives the distribution of the sigma levels and their approximate height above sea level.

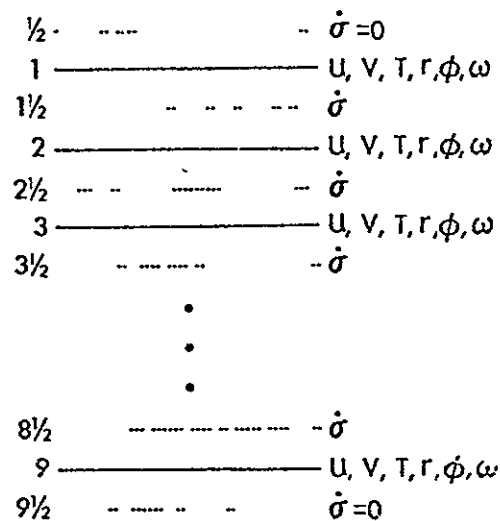


Figure D-1

Vertical Structure of the GFDL 9-Layer Global Model

Table D-1

Location of the σ Levels in the GFDL 9-Layer Model and Their Approximate Elevations Above the Surface Points at Sea Level. (p_* is assumed to be 1000 mb.)

Level	$\sigma=p/p_*$	Height (m)
0.5	0.00000000	∞
1.0	.01594441	27,900
1.5	.04334139	21,370
2.0	.07000000	18,330
2.5	.11305591	15,290
3.0	.16500000	12,890
3.5	.24081005	10,500
4.0	.31500000	8,680
4.5	.41204675	6,860
5.0	.50000000	5,430
5.5	.60672726	4,010
6.0	.68500000	3,060
6.5	.77337055	2,110
7.0	.83500000	1,490
7.5	.90154066	860
8.0	.94000000	520
8.5	.98010000	170
9.0	.99000000	80
9.5	1.00000000	0

2.3 Temporal

Two time levels of data are required (except during the startup step) since a centered time differencing scheme is used with a ten minute time step for the N19 version of the model. There is no staggering of variables in time.

3.0 Governing Equations

The governing partial differential equations written in flux form and spherical polar coordinates with a vertical coordinate sigma are listed below:

Wind component in the latitudinal direction:

$$\begin{aligned} \frac{\partial}{\partial t} (p_* u) = & - \frac{\partial (p_* u u)}{a \cos \phi \partial \lambda} - \frac{\partial (p_* \cos \phi u v)}{a \cos \phi \partial \phi} - \frac{\partial (\dot{\sigma} p_* u)}{\partial \sigma} \\ & + \left(f + \frac{u \tan \phi}{a} \right) p_* v - p_* \left(\frac{\partial \phi}{a \cos \phi \partial \lambda} \right) p + H^F \lambda + v^F \phi \end{aligned} \quad [D.2]$$

Wind component in the meridional direction:

$$\begin{aligned} \frac{\partial}{\partial t} (p_* v) = & - \frac{\partial (p_* u v)}{a \cos \phi \partial \lambda} - \frac{\partial (p_* \cos \phi v v)}{a \cos \phi \partial \phi} - \frac{\partial (\dot{\sigma} p_* v)}{\partial \sigma} \\ & - \left(f + \frac{u \tan \phi}{a} \right) p_* u - p_* \left(\frac{\partial \phi}{a \partial \phi} \right) p + H^F \lambda + v^F \phi \end{aligned} \quad [D.3]$$

Temperature equation:

$$\begin{aligned} \frac{\partial}{\partial t} (p_* T) = & - \frac{\partial (p_* T u)}{a \cos \phi \partial \lambda} - \frac{\partial (p_* \cos \phi T v)}{a \cos \phi \partial \phi} - \frac{\partial (\dot{\sigma} p_* T)}{\partial \sigma} \\ & + \frac{RT\omega}{C_p \sigma} + \frac{p_* Q}{C_p} + H^F T + v^F T \end{aligned} \quad [D.4]$$

Pressure tendency equation:

$$\frac{\partial p_*}{\partial t} = - \int_0^1 \left[\frac{\partial(p_* u)}{a \cos \phi \partial \lambda} + \frac{\partial(p_* v \cos \phi)}{a \cos \phi \partial \phi} \right] d\sigma \quad [D.5]$$

Moisture equation:

$$\begin{aligned} \frac{\partial(p_* r)}{\partial t} = & - \frac{\partial(p_* r u)}{a \cos \phi \partial \lambda} - \frac{\partial(p_* \cos \phi r v)}{a \cos \phi \partial \phi} - \frac{\partial(\dot{\sigma} p_* r)}{\partial \sigma} \\ & - C + H^F r + v^F r \end{aligned} \quad [D.6]$$

Hydrostatic equation:

$$\frac{\partial \phi}{\partial \sigma} = - \frac{RT}{\sigma} \quad [D.7]$$

Vertical velocity (p) equation:

$$\omega = p_* \dot{\sigma} + \sigma \left[\frac{\partial p_*}{\partial t} + u \frac{\partial p_*}{a \cos \phi \partial \lambda} + v \frac{\partial p_*}{a \partial \phi} \right] \quad [D.8]$$

In the above equations,

u = zonal wind component

v = meridional wind component

T = temperature

r = moisture mixing ratio

p_* = surface pressure

Φ = gz = geopotential

f = Coriolis parameter

$\dot{\sigma} = \frac{d\sigma}{dt}$ = vertical velocity (σ)

ω = vertical velocity (p)

Q = diabatic heating term

C = moisture source/sink term

C_p = specific heat of air at constant pressure

F = frictional force terms due to subgrid scale mixing
in the horizontal and vertical directions

The subscript p attached to the pressure gradient terms
indicates differentiation on an isobaric surface.

4.0 Numerics

Finite difference methods are used to approximate the
solution of the atmospheric model equations.

4.1 Spacial Differencing

The spacial finite differencing is based on the concept
of the "box method" proposed by Bryan and is essentially
similar to the energy conserving system suggested earlier
by Lilly. This method basically consists of differencing
quantities that have been averaged over one grid interval
and is second-order.

The pressure gradient force terms in the momentum equations are evaluated on locally synthesized pressure surfaces to reduce the truncation error that arises from differencing these terms on sigma surfaces over terrain of varying height.

Horizontal mixing of momentum, heat and moisture is based on the deformation scheme of Smagorinsky with the characteristic scale of subgrid eddies defined as the mean of the meridional and Fourier filtered latitudinal grid distance.

4.2 Temporal Differencing

Centered time differencing is used with a time step of ten minutes for the N19 version of the model.

The overspecification of tendencies due to the poleward convergence of the meridians is removed through Fourier filtering of all of the prognostic variables at each time step. The meridional component of the divergence operator is also Fourier filtered.

The minimum wavelength allowed is specified by

$$L_{\text{MIN}} = \frac{2\pi a \cos \phi_c}{(N/2)} \quad [\text{D.9}]$$

where ϕ_c is the equatorward boundary of the filtered region and N is the number of grid points on a latitude circle.

($\phi_c = 45^\circ$ and $N = 64$ for the N19 version of the model.)

This minimum wavelength is obtained by limiting the maximum wave number at latitude $\phi > \phi_c$ to

$$K_{\text{MAX}} = \frac{2\pi a \cos \phi}{L_{\text{MIN}}} = \frac{N \cos \phi}{2 \cos \phi_c} \quad [\text{D.10}]$$

In the case of the vector variables u and v , the components are transformed to a polar stereographic projection before the Fourier filtering is performed.

4.3 Boundary Conditions

The horizontal boundary condition is periodicity in longitude and the poles are not grid points. The vertical boundary conditions are that $\dot{\sigma} \equiv 0$ at $\sigma = 1$ and 0 .

5.0 Processes and Effects

5.1 Dynamics

Terms representing the horizontal and vertical advection of heat, moisture and momentum are included as are terms representing the pressure gradient and Coriolis forces in the momentum equations and a term representing adiabatic heating/cooling in the thermodynamic equation.

Orography that is consistent with reality and the grid resolution is included to add realism to the model simulations.

Surface stress which is dependent on the surface wind and a terrain height dependent drag coefficient is computed. This surface stress constitutes the lower boundary condition for the computation of the Reynolds stress from vertical mixing.

5.2 Heat Sources/Sinks

Sensible heating in the lowest sigma layer is evaluated using a formulation for the heat flux at the surface of the earth that is similar to that used for the surface stress. The ground temperature over the continents is predicted from the net surface heating or cooling. The ocean temperature is spatially varying, but held constant during the simulation.

Subgrid scale vertical mixing of heat is included in the uppermost eight layers.

Solar and terrestrial radiation effects are included in the manner described by Manabe and Strickler and Manabe and Wetherald and used in earlier GFDL models (Holloway, et al., 1971). The diurnal variation of the solar radiation is eliminated by the use of an effective mean zenith angle for each latitude. High, middle and low clouds are considered.

Release of latent heat due to large scale precipitation is included.

A moist convective adjustment procedure is included which has the net effects of stabilizing the lapse rate,

condensing water vapor, releasing the heat of condensation and transferring heat from lower to upper layers.

5.3 Moisture Sources/Sinks

The large scale precipitation algorithm removes supersaturated states from the model atmosphere which results in precipitation.

The moist convection process can result in the condensation of moisture which also contributes to the precipitation.

Evaporation from the surface (land or ocean) is evaluated using a formulation for the moisture flux that is similar to that used for the surface stress.

Subgrid scale vertical mixing of moisture is included in the uppermost eight layers.

6.0 Inputs

The GFDL atmospheric general circulation model was developed for use in long range prediction and general circulation simulation experiments. Thus, data inputs are either self generated by going through a spin-up period for general circulation experiments or obtained from analyses of the atmosphere at a particular time for prediction experiments. These analyses, obtained from

various sources, are then interpolated to the model grid to obtain initial data for the forecast.

7.0 Outputs

An output cycle may be specified at any desired interval and produces the sea level pressure, heights and temperatures at standard levels, and numerous other forecast and diagnostic quantities. The fields on pressure surfaces are produced by interpolation from the sigma surface data.

8.0 Computer Information

The atmospheric general circulation model is programmed in Fortran IV for the Texas Instrument ASC Computer System.

9.0 References

Joint Organizing Committee - GARP, "Modelling for the First GARP Global Experiment," GARP Publication Series No. 14, June 1974, Chapter 2, pp. 7-26.

Holloway, J.L.Jr. and S. Manabe, "Simulation of Climate by a Global General Circulation Model," Monthly Weather Review, Vol. 99, No. 5, May 1971, pp. 335-370.

Holloway, J.L.Jr., M.J. Spelman and S. Manabe, "Latitude-Longitude Grid Suitable for Numerical Time Integration of a Global Atmospheric Model," Monthly Weather Review, Vol. 101, No. 1, January 1973, pp. 69-78.

E. GFDL 18-Layer Global Model

The 18-layer Geophysical Fluid Dynamics Laboratory (GFDL) atmospheric general circulation model was developed for use in long range prediction and general circulation experiments. This model is a predecessor of the 9-layer model described in Section D and the governing equations and many of the parameterizations are identical. Thus, reference is made to Section D where appropriate rather than repeat the material here. Of particular interest in this model is the finite difference grid that is used - the modified Kurihara grid.

MODEL DESCRIPTION

1.0 Variables

1.1 Independent

The independent variables are the longitude, λ , and the latitude, ϕ ; sigma in the vertical defined as

$$\sigma = \frac{p}{p_*} \quad [E.1]$$

where p_* is the surface pressure; and time, t .

1.2 Dependent

1.2.1 Prognostic

The prognostic variables are the longitudinal component, u , and the meridional component, v , of the wind; the temperature, T ; the surface pressure, p_* ; and the moisture mixing ratio, q . Secondary prognostic variables are the surface temperature over land and the precipitation.

1.2.2 Diagnostic

The diagnostic variables are the geopotential, ϕ , the vertical σ velocity, $\dot{\sigma} = \frac{d\sigma}{dt}$, and the vertical p velocity, ω .

2.0 Domain

2.1 Horizontal

The horizontal grid is a global latitude-longitude grid with λ and ϕ as coordinates. Grid points are placed on the globe according to a scheme known as the modified Kurihara grid. Figure E-1 shows a portion of a modified Kurihara grid which has nineteen grid points between the equator and a pole. (There are 48 points between a pole and the equator in this model giving rise to the denotation of N48.) Variables are placed at the center of the grid boxes and, thus, the poles are not grid points. There is no staggering of variables in the horizontal.

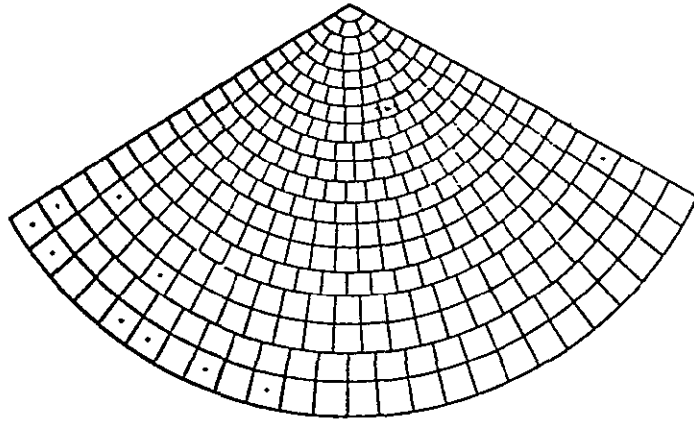


Figure E-1

Polar Stereographic Projection of a Portion of a
Modified Kurihara Grid

2.2 Vertical

The vertical coordinate is sigma as defined by Equation [E-1]. Figure E-2 shows the vertical structure of the model and the placement of the sigma surfaces and variables in the vertical.

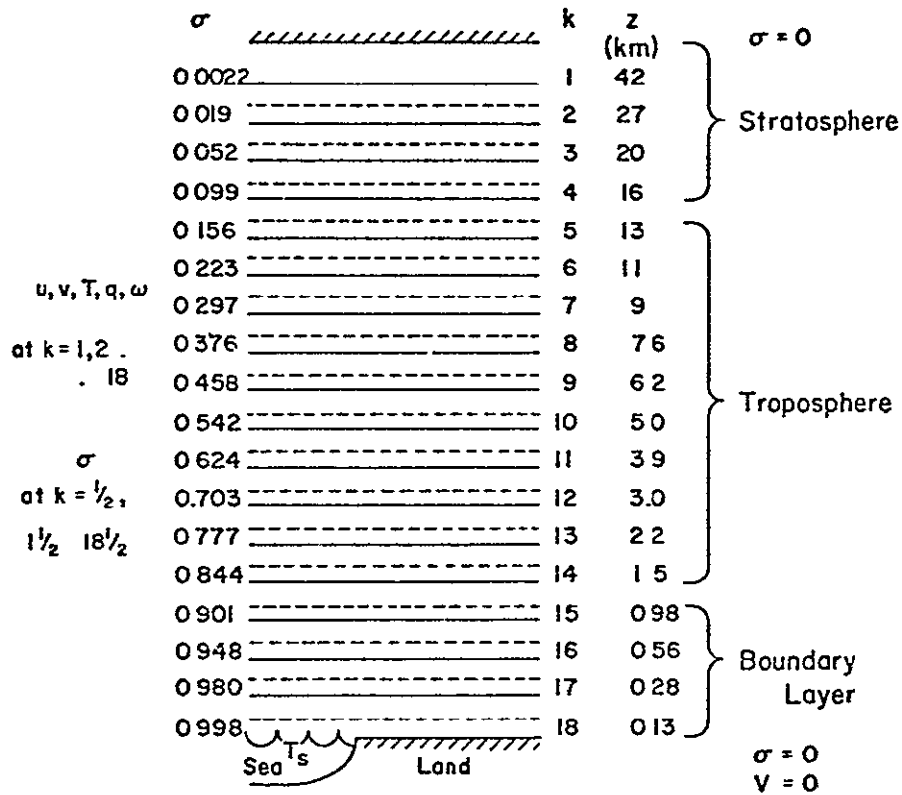


Figure E-2

Vertical Structure of the GFDL 18-Layer Global Model

2.3 Temporal

Two time levels of data are required (except during the startup step) since a centered time differencing scheme is used along with periodic Matsuno time steps. There is no staggering of variables in time.

3.0 Governing Equations

Refer to Section D-3.0.

4.0 Numerics

Finite difference methods are used to approximate the solution of the atmospheric model equations.

4.1 Spacial Differencing

The spacial finite differencing is based on the concept of the "box method" proposed by Bryan. In the modified Kurihara grid each box is surrounded by six other boxes as shown in Figure E-3 and all variables are defined at the centers of the boxes. The horizontal flux

$$N(y) = \frac{\partial (p_* u y)}{a \cos \phi \partial \lambda} + \frac{\partial (p_* v \cos \phi y)}{a \cos \phi \partial \phi} \quad [E.2]$$

is approximated by the finite difference operator

$$N(y) \doteq \sum_{\ell=1}^6 \left[\frac{(P_* \bar{V})_0 + (P_* \bar{V})_{\ell}}{2} \frac{y_0 + y_{\ell}}{2} w_{\ell} \right] \quad [E.3]$$

where ℓ is the index for the surrounding boxes, \bar{V} is the horizontal flow vector, w is the box weight and the summation is made for the surrounding boxes. Other terms are approximated in a similar manner.

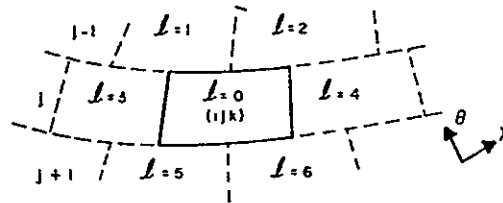


Figure E-3

Modified Kurihara Grid Box Indexing Scheme

The pressure gradient force terms in the momentum equations are evaluated on locally synthesized pressure surfaces to reduce the truncation error that arises from differencing these terms on sigma surfaces over terrain of varying height.

Horizontal mixing of momentum, heat and moisture is based on the deformation formulation of nonlinear viscosity of Smagorinsky.

4.2 Temporal Differencing

Centered time differencing is used along with periodic Matsuno time steps for control of computational noise.

The overspecification of tendencies due to the poleward convergence of the meridians is removed either through a spectral filtering technique or weighted averaging at high latitudes (the six rows nearest each pole).

4.3 Boundary Conditions

The horizontal boundary condition is periodicity in longitude and the poles are not grid points. The vertical boundary conditions are that $\dot{\sigma} \equiv 0$ at $\sigma = 1$ and 0 .

5.0 Processes and Effects

Refer to Section D-5.0.

6.0 Inputs

The 18-layer GFDL atmospheric prediction model was developed for use in long range prediction and general circulation simulation experiments. Thus, data inputs are either self generated by going through a spin-up period for general circulation experiments or obtained from analyses of the atmosphere at a particular time

for prediction experiments. These analyses are then interpolated to the model grid to obtain initial data for the forecast.

7.0 Outputs

An output cycle may be specified at any desired interval and produces the sea level pressure, heights and temperatures at standard levels, and numerous other forecast and diagnostic quantities. The fields on pressure surfaces are produced by interpolation from the sigma surface data.

8.0 Computer Information

The atmospheric general circulation model is programmed in Fortran IV for the Texas Instruments ASC Computer System.

9.0 References

- Joint Organizing Committee - GARP, "Modelling for the First GARP Global Experiment," GARP Publication Series No. 14, June 1974, Chapter 3, pp. 27-41.
- Miyakoda, K., R.W. Moyer, H. Stambler, R.H. Clarke and R.F. Strickler, "A Prediction Experiment with a Global Model Made in the Kurihara Grid," Journal of Meteorological Society of Japan, Vol. 49, 1971, pp. 521-536.

F. GISS 9-Layer Global Model

The GISS global atmospheric prediction model was developed as a medium-range forecast model for use in observing system simulation experiments, asynoptic data assimilation studies and experimental long-range forecasting (Sommerville, et al., 1974). The GISS model shares the overall structure of the UCLA three-level model (Arakawa, 1972) and retains the sigma coordinate formulation of the governing equations, the Arakawa numerical method with advective quasi-conservation of quadratic quantities and much of the UCLA representation of physical processes occurring at and near the lower boundary of the atmosphere. The GISS model differs from the UCLA model in having a finer vertical resolution (nine levels) and in its treatment of four areas of physical processes: moist convection, turbulent subgrid-scale processes, solar radiation and terrestrial radiation.

MODEL DESCRIPTION

1.0 Variables

1.1 Independent

The independent variables are λ and ϕ of a spherical polar coordinate system in the horizontal; sigma in the vertical defined as

$$\sigma = \frac{P - P_t}{P_s - P_t} \quad [F.1]$$

where P_t is the pressure at the top of the model atmosphere and P_s is the pressure at the bottom of the model atmosphere; and time, t .

1.2 Dependent

1.2.1 Prognostic

The prognostic variables are the pressure, $\pi = P_s - P_t$, the temperature, T , the latitudinal wind component, u , and the longitudinal wind component, v , and the specific humidity, q . A secondary prognostic variable is the precipitation obtained from large scale precipitation and the moist convection process.

1.2.2 Diagnostic

The diagnostic variables are the geopotential, Φ , and the vertical velocity, $\dot{\sigma} = \frac{d\sigma}{dt}$.

2.0 Domain

2.1 Horizontal

The horizontal domain is a global latitude, longitude grid with λ and ϕ as the coordinates and the grid resolution

is 4° in latitude and 5° in longitude. The poles are considered as mass points and are treated separately. The variables are distributed in the horizontal according to Arakawa's Scheme B as shown in Figure F-1.

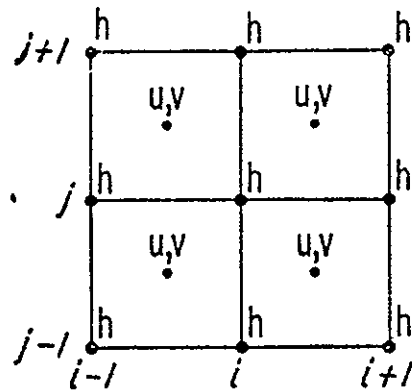


Figure F-1

Horizontal Grid Structure of the GISS 9-Level Global Model

2.2 Vertical

The vertical coordinate is sigma as defined by Equation [F.1]. Figure F-2 shows the model sigma surfaces and the placement of the variables in the vertical. The vertical levels are equally spaced in sigma.

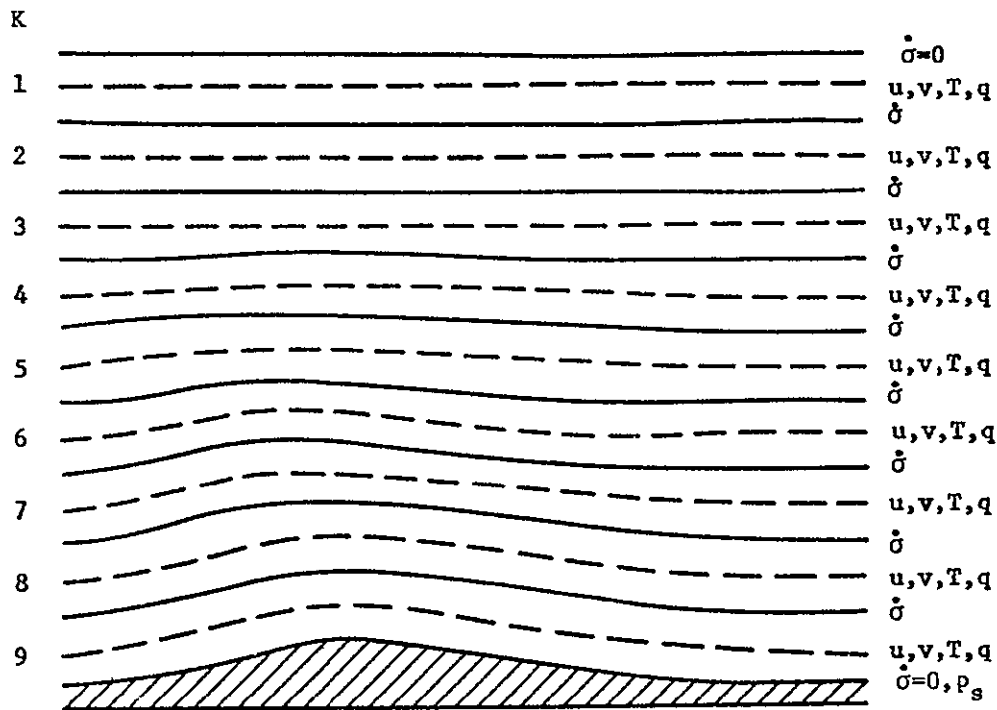


Figure F-2

Vertical Structure of the GISS 9-Level Global Model

2.3 Temporal

One time level of data is required since either the Time Averaged Space Uncentered (TASU) - Matsuno or regular Matsuno time steps are used. Each simulated half-hour consists of ten minutes of TASU - Matsuno steps and twenty minutes of regular Matsuno steps with a time step of five minutes. There is no staggering of variables in time.

3.0 Governing Equations

The governing partial differential equations written in flux form with a sigma coordinate in the vertical are listed below.

Equation of motion:

$$\frac{d\bar{V}}{dt} + f\bar{k}\bar{x}\bar{V} + \nabla\phi + \sigma\alpha\nabla\pi = \bar{F} \quad [\text{F.2}]$$

Pressure tendency equation:

$$\frac{\partial\pi}{\partial t} = -\int_0^1 \nabla \cdot (\pi\bar{V}) d\sigma \quad [\text{F.3}]$$

First law of thermodynamics:

$$\frac{d\theta}{dt} = \frac{Q}{C_p} \frac{\theta}{T} \quad [\text{F.4}]$$

Water vapor equation:

$$\frac{dq}{dt} = -C + E \quad [\text{F.5}]$$

Equation of state:

$$p\alpha = RT \quad [\text{F.6}]$$

Hydrostatic equation:

$$\frac{\partial \phi}{\partial \sigma} = -\alpha \pi \quad [\text{F.7}]$$

In the above equations:

- \bar{V} = horizontal velocity
- f = Coriolis parameter
- \bar{K} = vertical unit vector
- ∇ = two dimensional gradient operator
- α = specific volume
- π = $P_s - P_t$
- \bar{F} = horizontal frictional force
- R = gas constant
- T = temperature
- θ = potential temperature
- C_p = specific heat of dry air at constant pressure
- Q = heating rate per unit mass
- ϕ = gz = geopotential
- q = water vapor mixing ratio
- C = rate of condensation
- E = rate of evaporation

4.0 Numerics

Finite difference methods are used to approximate the solution of the forecast equations.

4.1 Spacial Differencing

The horizontal differencing follows that of Arakawa (1972). The distribution of variables on the horizontal grid corresponds to his Scheme B as shown in Figure F-1. The space differencing of the nonlinear advective terms in the equation of motion is constructed so as to maintain a constraint analogous to the conservation of mean square vorticity. The TASU-Matsuno time steps use uncentered differencing while the Matsuno time steps use centered differencing.

The polar calculations follow Arakawa in which the change of the variables defined at the poles (π , T and q) is a result of the meridional flux at all points on the latitude circle around the particular pole.

4.2 Temporal Differencing

Time differencing proceeds in half-hour cycles using a five minute time step. The first two steps of a cycle are TASU-Matsuno and the last four are regular Matsuno steps

(Arakawa, 1972). For computational economy, physical processes other than advection are calculated every half hour of simulated time, except for solar and terrestrial radiation calculations which are performed every two hours.

To avoid reducing the time step due to the convergence of the grid near the poles, the zonal mass flux and zonal pressure force are smoothed longitudinally using the three point smoothing technique described by Gates et al. (1971).

4.3 Boundary Conditions

The horizontal boundary conditions are periodicity in longitude and the poles are treated as mass points as explained in Section 4.1.

The vertical boundary conditions are $\dot{\sigma} \equiv 0$ at $\sigma = 0$ and 1, and the upper pressure P_t is taken to be 10 mb.

5.0 Processes and Effects

5.1 Dynamics

Terms representing the horizontal and vertical advection and convergence/divergence of heat, moisture and momentum are included as are terms representing the pressure gradient and

Coriolis forces in the equation of motion. Adiabatic temperature changes are also modeled.

Orography that is consistent with reality and the grid resolution is included to add realism to the flows.

The surface stress is parameterized by drag laws with the drag coefficient being a function of wind speed, type of surface and surface height (to simulate mountain drag). The surface velocity is estimated by extrapolating the velocities in the lowest two layers to the lower boundary.

5.2 Heat Sources/Sinks

Sensible heating in the boundary layer (lowest sigma layer) is evaluated by the method of Arakawa (1972) with the diffusivity given by Deardorff used to evaluate the thermal flux. The ground temperature (land, ice or snow) is predicted from the net surface heating or cooling. The ocean temperature is spatially varying, but held constant during the forecast.

Subgrid scale vertical diffusion of heat with a constant diffusivity is included in the upper eight sigma layers.

Solar and terrestrial radiation effects are included as fairly detailed parameterizations (Sommerville, et al., 1974.) Cloudiness effects are considered at all sigma levels.

Release of latent heat due to large scale precipitation is also included.

A parameterization of cumulus ensembles (moist convection) based on the Arakawa (1972) method redistributes heat and moisture in the vertical. The lower six model layers are "strapped" into three layers analogous to the UCLA 3-layer model. A dry convective adjustment procedure is included to preclude hydrostatic instability.

5.3 Moisture Sources/Sinks

The large scale precipitation algorithm removes supersaturated states from the model atmosphere and may result in evaporation in layers below the saturated layer.

The moist convection process can result in the evaporation/condensation of moisture in the lower six layers.

Evaporation/condensation from the surface into the lowest sigma layer is evaluated as part of the Arakawa type boundary layer computations. Subgrid scale vertical diffusion of moisture with a constant diffusivity is included in the upper eight sigma layers.

6.0 Inputs

The GISS model while generally used as a forecast model, has also been tested as a climate simulation model

(long term January). Thus, data inputs are either self generated by going through a spin-up period for climate simulation or obtained from analyses of the atmosphere at a particular time. These analyses, obtained from various sources, are then interpolated to the model grid and no further balancing or smoothing procedures are employed.

7.0 Outputs

An output cycle may be specified at any desired interval and produces the sea level pressure, heights and temperatures at standard levels, and numerous other forecast and diagnostic quantities. The fields on pressure surfaces are produced by interpolation from the sigma surface data.

8.0 Computer Information

The forecast model is programmed in Fortran IV (Level H Compiler) for the IBM 360/95 Computer System. The code is quite modular and the execution time is 70 minutes of CPU time per simulated model day.

9.0 References

Arakawa, A., "Design of the UCLA General Circulation Model," Technical Report No. 7, 1 July 1972, Department of Meteorology, University of California at Los Angeles, 116 pp.

Gates, W.L., E.S. Batten, A.B. Kahle and A.B. Nelson,
"A Documentation of the Mintz-Arakawa Two-Level
Atmospheric General Circulation Model," Report
R-877-ARPA, RAND Corporation, December, 1971, 408 pp.

Joint Organizing Committee - GARP, "Modelling for the
First GARP Global Experiment," GARP Publication
Series No. 14, June 1974, Chapter 5, pp. 46-60.

Sommerville, R.C.J., P.H. Stone, M. Halem, J.E. Hansen,
J.S. Hogan, L.M. Druyan, G. Russell, A.A. Lacis,
W.J. Quirk and J. Tenenbaum, "The GISS Model of
the Global Atmosphere," Journal of the Atmospheric
Sciences, Vol. 31, January 1974, pp. 84-117.

G. NCAR Multi-Layer Second-Generation Global Model

Development of the NCAR second-generation model was begun in 1968 as a rewrite of the original six layer, 5° global model in order to obtain efficient programming with some degree of modularity. Various changes in the physical processes were also incorporated at the time. Over the years, this model has become a set of models with various resolutions and physical processes. The basic versions may be categorized as:

- A six layer (tropospheric), 5° model
- A twelve layer (stratospheric), 5° model
- A six layer (tropospheric), 2 1/2° high resolution model.

Thus, by necessity, the description that follows is somewhat vague concerning the exact physical processes contained in a given model version since any particular version has mutated over the years.

MODEL DESCRIPTION

1.0 Variables

1.1 Independent

The independent variables are the longitude, λ , the latitude, ϕ , the geometric height, Z , and time, t .

1.2 Dependent

1.2.1 Prognostic

The prognostic variables are the pressure, p , at the various levels, the longitudinal component, u , and the meridional component, v , of the wind, and the specific humidity, q . Secondary prognostic variables are the ground temperature, T_g , and the soil moisture in certain versions.

1.2.2 Diagnostic

The main diagnostic variables are density, ρ , temperature, T , and the vertical velocity, w .

2.0 Domain

2.1 Horizontal

The horizontal domain is a global latitude, longitude grid with λ and ϕ as the coordinates. The resolution is either 5° or $2\ 1/2^\circ$ giving a 72×37 grid or 144×73 grid, respectively. The variables are staggered in space and time as shown in Figure G-1. The poles are treated separately and are considered as mass points for pressure.

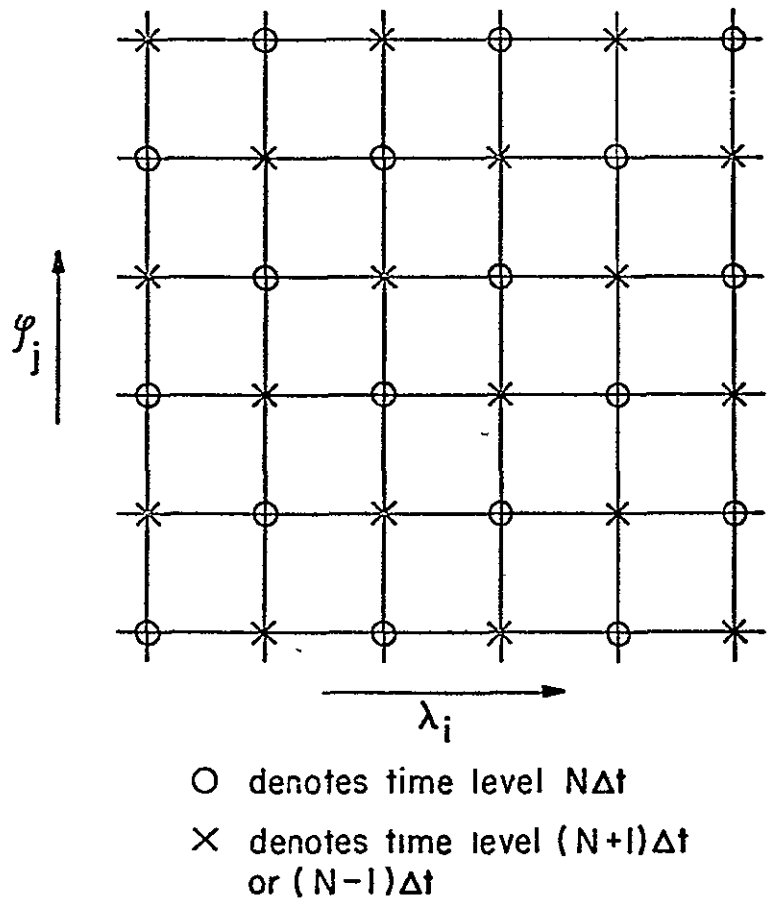


Figure G-1

Horizontal Staggering of Variables in Space and Time for the Second-Generation NCAR Model.

2.2 Vertical

The vertical coordinate is geometric height, Z . The vertical grid increment is 3 Km giving a model atmosphere top of 18 Km for the six layer (tropospheric) version and 36 Km for the twelve layer (stratospheric) version. Figure G-2 shows the vertical grid and the placement of variables in the vertical for the six layer tropospheric version.

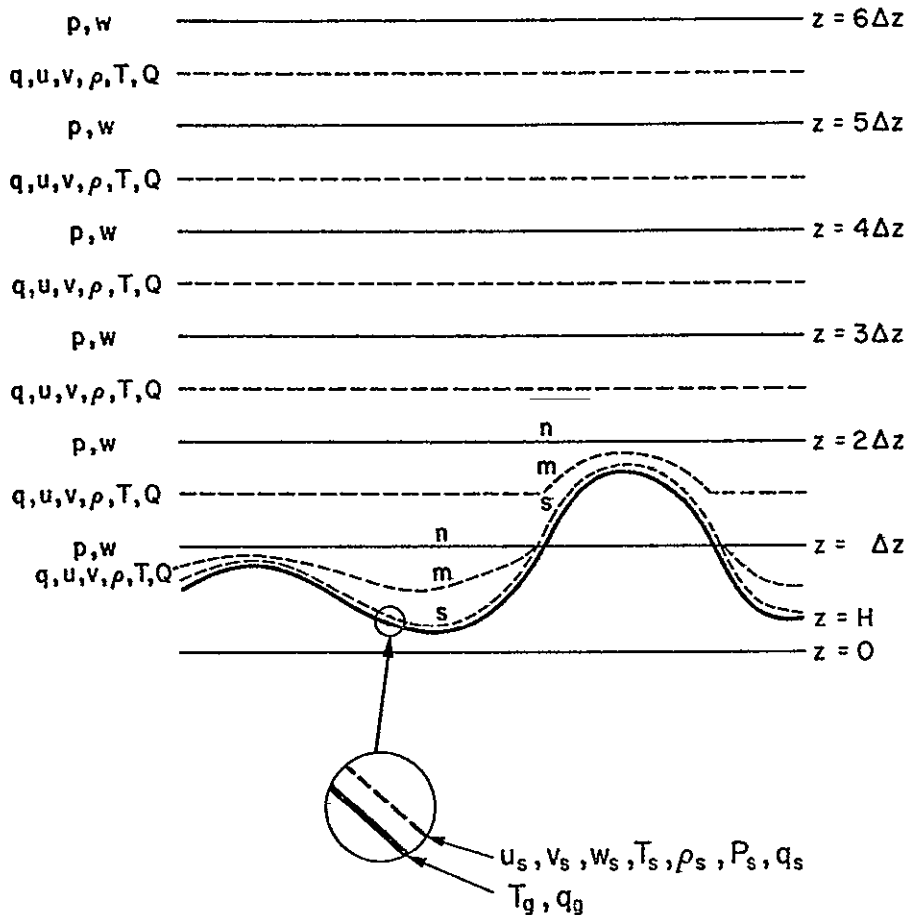


Figure G-2

Vertical Grid and Placement of Variables for the Tropospheric Second-Generation NCAR Model.

2.3 Temporal

Due to the staggering of the variables in space and time as shown in Figure G-1, only one copy of the history variables is required for the centered time difference scheme. A time step of six minutes is used with the 5° versions and a time step of three minutes is used with the 2 1/2° version.

3.0 Governing Equations

The governing partial differential equations written in spherical polar coordinates in the horizontal and geometric height in the vertical are listed below.

Momentum equation in the longitudinal direction:

$$\begin{aligned} \frac{\partial(\rho u)}{\partial t} = & - \frac{1}{a \cos \phi} \left[\frac{\partial(\rho u u)}{\partial \lambda} + \frac{\partial(u v \rho \cos \phi)}{\partial \phi} \right] - \frac{\partial(\rho w u)}{\partial z} \\ & + \left(f + \frac{u \tan \phi}{a} \right) \rho v - \frac{1}{a \cos \phi} \frac{\partial p}{\partial \lambda} + F_{\lambda} \end{aligned} \quad [G.1]$$

Momentum equation in the latitudinal direction:

$$\begin{aligned} \frac{\partial(\rho v)}{\partial t} = & - \frac{1}{a \cos \phi} \left[\frac{\partial(\rho u v)}{\partial \lambda} + \frac{\partial(v v \rho \cos \phi)}{\partial \phi} \right] - \frac{\partial(\rho w v)}{\partial z} \\ & - \left(f + \frac{u \tan \phi}{a} \right) \rho u - \frac{1}{a} \frac{\partial p}{\partial \phi} + F_{\phi} \end{aligned} \quad [G.2]$$

Moisture Conservation equation:

$$\frac{\partial(\rho q)}{\partial t} = -\frac{1}{a \cos \phi} \left[\frac{\partial(\rho u q)}{\partial \lambda} + \frac{\partial(\rho v q \cos \phi)}{\partial \phi} \right] - \frac{\partial(\rho w q)}{\partial Z} + M + \rho E \quad [G.3]$$

Pressure tendency equation:

$$\frac{\partial p}{\partial t} = B + g \rho w - g \int_Z^{Z_T} \frac{1}{a \cos \phi} \left[\frac{\partial(\rho u)}{\partial \lambda} + \frac{\partial(\rho v \cos \phi)}{\partial \phi} \right] dz \quad [G.4]$$

$B = \frac{\partial p}{\partial t}$ at $Z = Z_T$ and it is assumed that $w = 0$ at $Z = Z_T$ and thus,

$$B = \frac{w_s - \int_H^{Z_T} \left\{ \frac{J}{\gamma p} - \frac{Q}{C_p T} + \frac{1}{a \cos \phi} \left[\frac{\partial u}{\partial \lambda} + \frac{\partial(v \cos \phi)}{\partial \phi} \right] \right\} dz}{\frac{1}{\gamma} \int_H^{Z_T} \frac{dz}{p}} \quad [G.5]$$

where

$$J = \frac{u}{a \cos \phi} \frac{\partial p}{\partial \lambda} + \frac{v}{a} \frac{\partial p}{\partial \phi} - g \int_Z^{Z_T} \frac{1}{a \cos \phi} \left[\frac{\partial(\rho u)}{\partial \lambda} + \frac{\partial(\rho v \cos \phi)}{\partial \phi} \right] dz \quad [G.6]$$

and $w_s = V_s \cdot \nabla H$ at $Z = H$.

Density is evaluated using the hydrostatic equation:

$$\frac{\partial p}{\partial Z} = -\rho g \quad [G.7]$$

Temperature is computed using

$$T = -\frac{g}{R \frac{\partial}{\partial Z} (\ln p)} \quad [G.8]$$

Vertical velocity is evaluated using Richardson's equation:

$$w = w_s - \int_H^Z \left\{ \frac{1}{a \cos \phi} \left[\frac{\partial u}{\partial \lambda} + \frac{\partial (v \cos \phi)}{\partial \phi} \right] + \frac{B+J}{\gamma p} - \frac{Q}{C_p T} \right\} dz \quad [G.9]$$

In the above equations,

- u = zonal wind component
- v = meridional wind component
- p = pressure
- q = ρ_w / ρ = specific humidity
- ρ = density of air
- ρ_w = density of water vapor
- H = terrain height
- T = temperature
- w = vertical velocity
- Q = rate of heating per unit mass
- F_λ, F_ϕ = longitudinal and latitudinal components of frictional force per unit volume
- M = condensation rate of water vapor per unit volume
- E = rate of change of water vapor per unit mass due to the vertical and horizontal diffusion of water vapor
- a = radius of the earth
- g = acceleration due to gravity
- f = Coriolis parameter
- R = gas constant for dry air
- C_p = specific heat for dry air at constant pressure
- C_v = specific heat for dry air at constant volume
- γ = C_p / C_v

4.0 Numerics

Finite difference methods are used to approximate the solution of the primitive equations.

4.1 Spacial Differencing

Second-order centered differencing is used to calculate the horizontal derivatives and vertical derivatives except near the surface where first-order approximations are used.

Grid points are dropped near the poles to maintain a nearly constant geographical distance between mesh points for linear stability. Table G-1 defines the number of grid points per latitude circle of the 5° model. The points are placed on the latitude circles such that there is a point at $\lambda = -\pi$ (180°W) and the points on each line are equidistant (see Figure G-3). When neighbors on the latitude circles $\Delta\phi$ above and below a point are needed they are linearly interpolated from the nearest two points on the appropriate circle at the appropriate level in time. This procedure, of course, renders the finite differencing first-order near the poles.

At grid points neighboring terrain which penetrates some ΔZ level, the second-order differencing scheme must be modified somewhat. Rather than use special difference formulas at these points, virtual points are created by

extrapolation through the midpoint of the difference stencil. This allows the use of the second-order difference formulas, but since the virtual points were created by linear extrapolation, the computation becomes first-order near the blocking terrain.

The poles are treated as mass points for pressure in the computation with the polar pressures being defined as the average of the pressures on the latitude circle surrounding the pole.

The horizontal eddy viscosity terms are based on either the deformation formulation of Smagorinsky or the divergence of the vorticity as formulated by Leith according to the particular model version. In both cases time levels are mixed, thereby avoiding grid separation which is a characteristic of centered time differencing.

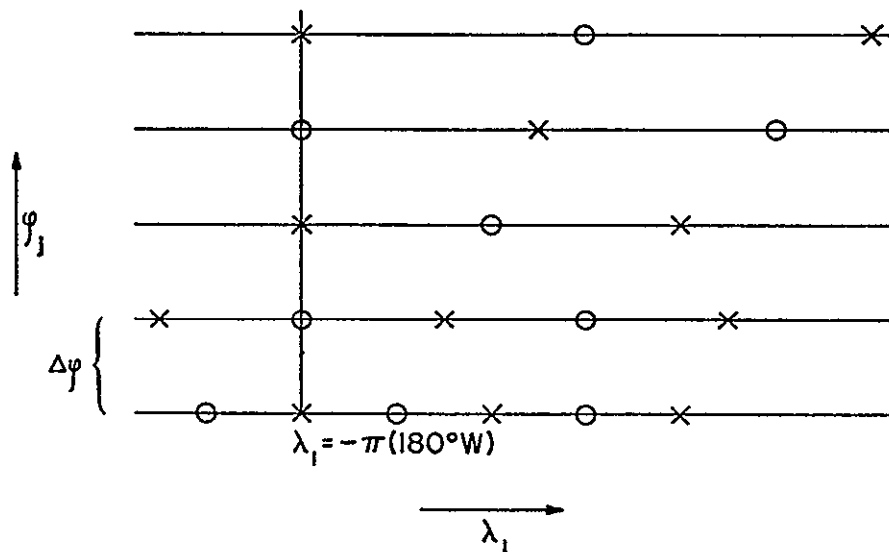


Figure G-3

Grid Near The Poles for the NCAR Second-Generation Model.

Table G-1

Number of Grid Points as a Function of Latitude
for NCAR Second-Generation Model.

<u>Latitude</u>	<u>NPTS (ϕ_j)</u>
90N	1
85	12
80	24
75	36
70	48
65	60
60N	72
.	.
.	.
.	.
0	72
.	.
.	.
.	.
60S	72
65	60
70	48
75	36
80	24
85	12
90S	1

4.2 Temporal Differencing

Centered time differencing is used with either a six or three minute time step for the 5° and $2\ 1/2^\circ$ models, respectively.

A non-linear pressure smoother is applied on every time step which mixes the time levels for additional computational stability.

A characteristic of the second-generation model which is due to the interpolation schemes used near the poles and around domains blocked by the orography, is an increase in the globally averaged value of surface pressure with time. Therefore, a procedure is invoked to maintain the globally averaged value of surface pressure at each time step.

4.3 Boundary conditions

The horizontal boundary conditions are periodicity in longitude and the poles are treated as mass points for pressure as explained in Section 4.1.

The vertical boundary conditions are $w \equiv 0$ at $Z = Z_T$ and $w = w_s = V_s \cdot \nabla H$ at $Z = H$.

5.0 Processes and Effects

5.1 Dynamics

Terms representing the horizontal and vertical advection and convergence/divergence of momentum and moisture are

included as are terms representing the pressure gradient and Coriolis forces in the momentum equations. The horizontal and vertical diffusion of water vapor is included in the moisture equation, and eddy diffusion of heat is included in the pressure equation.

Orography that is consistent with reality and the grid resolution of the particular version of the model is included to add realism to the flows.

The frictional force includes horizontal and vertical (Deardorff) diffusion of momentum. Various formulations have been used for the horizontal diffusion including the deformation of Smagorinsky and Leith's divergence of vorticity procedures.

5.2 Heat Sources/Sinks

Both solar and terrestrial radiation are included according to the formulation of Sasamori. Clouds are included at two levels (3 Km and 9 Km) in the tropospheric version. The stratospheric version includes heating due to ozone absorption of solar energy and numerous levels of cloudiness.

The release of latent heat due to the condensation of water vapor is included as part of the precipitation algorithm.

Heating/cooling due to eddy diffusion in both the horizontal and vertical (Deardorff) is included.

A surface energy balance equation is used to determine T_g over land areas.

A dry convective adjustment procedure is included to preclude hydrostatic instability.

The high resolution model (2 1/2°) includes elaborate parameterization schemes which include a convective parameterization (Krishnamurti and Moxim).

5.3 Moisture Sources/Sinks

The precipitation algorithm removes supersaturated states with upward vertical motion from the model atmosphere as precipitation.

Evaporation or condensation is included in the Ekman layer (Deardorff) as is the horizontal diffusion of water vapor.

The high resolution model (2 1/2°) includes elaborate parameterization schemes for convective parameterization (Krishnamurti and Moxim) and a predictive equation for snow cover and soil moisture.

6.0 Inputs

The models are run in two basic modes:

- a) The "GCM mode" in which data is self generated by going through a spin-up period which starts with an isothermal atmosphere at rest to obtain climate simulations,
- b) the "real data mode" in which analyzed data sets

(either subjective or objective analyses) obtained from various sources are used to make short and mid-range forecasts.

7.0 Outputs

An output cycle for the models consists of dumping the current integration state onto a history tape at regular intervals of model time. A large, sophisticated processor program then processes these history tapes to produce a wide variety of output fields which are under the control of the user. Numerous other processor programs which produce quantities such as climate statistics, etc. exist to process the history tapes .

8.0 Computer Information

The models are programmed in NCAR Fortran (a dialect of FTN IV) for the CDC 7600 using the NCAR Operating System. Running times in CPU hr/day for the various versions are listed below:

6 layer, 5°	0.2 hr.
12 layer, 5°	0.4 hr.
6 layer, 2.5°	1.6 hr.

9.0 References

- GCM Steering Committee, NCAR, "Development and Use of the NCAR GCM," NCAR-TN/STR-101, National Center for Atmospheric Research, Boulder, Colorado, September 1975, 177 pp.
- Joint Organizing Committee - GARP, "Modelling for the First GARP Global Experiment," GARP Publication Series No. 14, June 1974, Chapter 6, pp. 61-78.
- Olliger, J.E., R.E. Wellck, A. Kasahara and W.M. Washington, "Description of NCAR Global Circulation Model," NCAR-TN/STR-56, National Center for Atmospheric Research, Boulder, Colorado, May 1970, 94 pp.

H. NCAR Multi-Layer Limited Area Model

The NCAR limited-area model (LAM) was developed for numerical weather prediction studies on a very fine scale. This model is a version of the second-generation model described in Section G and contains physical parameterizations identical to the low resolution (5°) model. Thus, in the description that follows, reference is made to Section G where appropriate rather than repeating the material in this section.

MODEL DESCRIPTION

1.0 Variables

1.1 Independent

The independent variables are the longitude, λ , the latitude, ϕ , the geometric height, Z , and the time, t .

1.2 Dependent

1.2.1 Prognostic

The prognostic variables are the pressure, p , at the various levels, the longitudinal component, u , and the meridional component, v , of the wind, and the specific humidity, q . A secondary prognostic variable is the ground temperature, T_g .

1.2.2 Diagnostic

The main diagnostic variables are density, ρ , temperature, T , and the vertical velocity, w .

2.0 Domain

2.1 Horizontal

The horizontal domain is a limited area of the globe which depends on the horizontal resolution chosen (5° to $5/8^\circ$ grid increments). Typical fine scale ($5/8^\circ$ grid increment) forecasts are made for regions encompassing 90° of longitude and 55° of latitude. Figure G-1 in Section G shows the placement of variables in the horizontal.

2.2 Vertical

The vertical coordinate is geometric height, Z . The vertical resolution is variable from six to twenty-four layers with various vertical grid increments. Figure G-2 in Section G shows the placement of the variables in the vertical.

2.3 Temporal

The staggering of variables in space and time is shown in Figure G-1 of Section G. The time step used depends on the horizontal resolution, ranging from six minutes for 5° resolution to three-quarters of a minute for $5/8^\circ$ resolution.

3.0 Governing Equations

Refer to Section G-3.0.

4.0 Numerics

Finite difference methods are used to approximate the solution of the primitive equations.

4.1 Spatial Differencing

A discussion of the spatial differencing techniques and the dropping of grid points near the poles is given in Section G-4.1. The areas near the poles (north or south of 60°) are not allowed in the LAM domain due to the problem arising from the linear interpolation required to obtain inflow boundary values from the global forecast.

Increased diffusion is used near the edges of the LAM to suppress computational noise arising from the boundary calculations. The diffusion coefficient is increased by a factor of four in the 5° band along the boundary and by a factor of two in the adjacent 5° band.

4.2 Temporal Differencing

A discussion of the temporal differencing is given in Section G-4.2. No correction to the surface pressure is made in the LAM during the integration.

4.3 Boundary Conditions

The vertical boundary conditions are $w \equiv 0$ at $Z = Z_T$ and $w = w_s = V_s \cdot \nabla H$ at $Z=H$.

The horizontal boundary values are determined from 5° global forecast values for the inflow boundary points and by Lagrangian extrapolation of the LAM interior point values for the outflow boundary points. The decision as to which boundary points are inflow points is based on the winds obtained from the 5° global forecast. If the winds are directed into the LAM domain, then the boundary point is an inflow point and the LAM prognostic variables are determined from the corresponding global values by linear space-time interpolation. If the global winds on the LAM boundary are directed out of the LAM domain, then the point is an outflow point and the LAM prognostic variables are determined by an extrapolation from the LAM interior to the boundary. The extrapolation is simply the horizontal advection of LAM variables by the global wind.

5.0 Processes and Effects

Refer to Section G-5.0.

6.0 Inputs

Input to the LAM consists of an initial state obtained from either a general circulation model simulation computation

or through an analysis of real data. Also required are computed values for the boundary points generated by the global model for the "forecast" period. The "global" winds are used to determine whether the boundary points are inflow or outflow points. The inflow points are then determined from the global values by linear space-time interpolation and the outflow points by Lagrangian extrapolation from the LAM interior.

7.0 Outputs

An output cycle for the model consists of dumping the current integration cycle onto a history tape at regular intervals of model time. A large, sophisticated processor program then processes these history tapes to produce a wide variety of output fields which are under the control of the user.

8.0 Computer Information

The LAM is programmed in NCAR Fortran (a dialect of FTN IV) for the CDC 7600 using the NCAR Operating System. Running times in CPU hr/day for various versions are listed below (ranges are given since running time depends on the size of the forecast domain).

6 layer, 1.25°	1.0 - 2.0 hr.
12 layer, 1.25°	2.0 - 4.0 hr.
24 layer, 1.25°	4.0 - 8.0 hr.
24 layer, 0.625°	32.0 - 64.0 hr.

9.0 References

- GCM Steering Committee, NCAR, "Development and Use of the NCAR GCM", NCAR-TN/STR-101, National Center for Atmospheric Research, Boulder, Colorado, September 1976, 177 pp.
- Joint Organizing Committee - GARP, "Modelling for the First GARP Global Experiment", GARP Publication Series No. 14, June 1974, Chapter 6, pp. 61-78.
- Olinger, J.E., R.E. Wellock, A. Kasahara and W.M. Washington, "Description of NCAR Global Circulation Model", NCAR-TN/STR-56, National Center for Atmospheric Research, Boulder, Colorado, May 1970, 94 pp.
- Williamson, D.L. and G.L. Browning, "Formulation of the Lateral Boundary Conditions for the NCAR Limited-Area Model", Journal of Applied Meteorology, Vol. 13, February 1974, pp. 8-16.

I. NCAR Multi-Layer Third-Generation Global Model

Development of the NCAR third-generation model was begun in 1972 to obtain an improved and more flexible model. The procedure of dropping points near the poles and of mountain blocking of layers in the second-generation model resulted in first-order difference approximations in these regions. Williamson and Browning (1973) showed that substantial improvement could be made by restoring the skipped gridpoints and removing computationally unstable modes by Fourier filtering. Fourth-order differencing is also included to reduce truncation errors. The model uses a new vertical coordinate, transformed height, developed by Kasahara (1974). Both the horizontal and vertical resolution is variable.

The physical processes are essentially the same as in the second-generation model. However, solar and infrared radiation calculations are improved and cloudiness can be included at all levels. A new boundary layer treatment is being developed.

MODEL DESCRIPTION

1.0 Variables

1.1 Independent

The independent variables are the longitude, λ , the latitude, ϕ ; the transformed geometric height, \tilde{z} , given by

$$\tilde{z} = \frac{z_T - z}{z_T - H} \quad [I.1]$$

where z_T is the height of the model top and H is the terrain height; and time, t .

1.2 Dependent

1.2.1 Prognostic

The prognostic variables are the pressure, p , at the various levels, the longitudinal component, u , and the meridional component, v , of the wind, and the specific humidity, q . A secondary prognostic variable is the ground temperature, T_g .

1.2.2 Diagnostic

The main diagnostic variables are density, ρ , temperature, T , and the vertical velocity, $w = \frac{d\tilde{z}}{dt}$.

2.0 Domain

2.1 Horizontal

The horizontal domain is a global latitude, longitude grid with ϕ and λ as the coordinates. The resolution is either 5.6° or 2.8° giving a 64×33 or 128×65 grid, respectively. The poles are treated separately to maintain the fourth-order accuracy of the finite difference approximations. There is no staggering of variables in the horizontal.

2.2 Vertical

The vertical coordinate is transformed geometric height, \tilde{z} . Figure I-1 shows the vertical grid and the placement of variables in the vertical.

2.3 Temporal

A centered difference scheme is used with a time step of either five or two and one-half for the 5.6° and 2.8° grids, respectively. Fourier filtering of the prognostic variables at each time step is performed to remove the computationally unstable modes caused by the convergence of the grid near the poles.

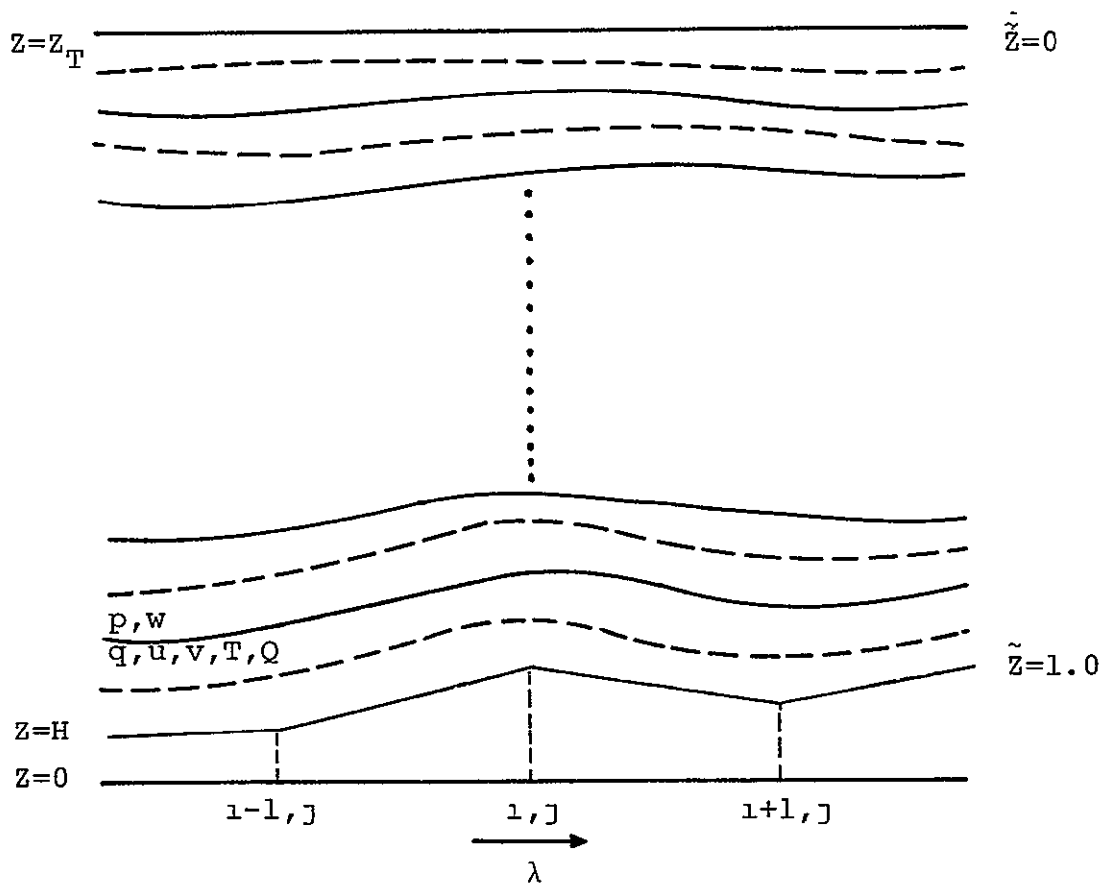


Figure I-1

Vertical Grid and Placement of Variables for the Third-Generation NCAR Model.

3.0 Governing Equations

The governing partial differential equations written in spherical polar coordinates in the horizontal and transformed height in the vertical are listed below.

Longitudinal equation of motion:

$$\begin{aligned} \frac{\partial u}{\partial t} = & - \frac{1}{a \cos \phi} \left[\frac{\partial (uu)}{\partial \lambda} + \frac{\partial (uv \cos \phi)}{\partial \phi} \right] - \frac{\partial (wu)}{\partial \tilde{z}} \\ & + \left(f + \frac{u \tan \phi}{a} \right) v - \frac{1}{a \cos \phi} \left[\frac{\partial \phi}{\partial \lambda} + \frac{RT}{p} \frac{\partial p}{\partial \lambda} \right] + F_{\lambda} \end{aligned} \quad [1.2]$$

Latitudinal equation of motion:

$$\begin{aligned} \frac{\partial v}{\partial t} = & - \frac{1}{a \cos \phi} \left[\frac{\partial (uv)}{\partial \lambda} + \frac{\partial (vvcos\phi)}{\partial \phi} \right] - \frac{\partial (wv)}{\partial \tilde{z}} \\ & - \left(f + \frac{u \tan \phi}{a} \right) u - \frac{1}{a} \left[\frac{\partial \phi}{\partial \phi} + \frac{RT}{p} \frac{\partial p}{\partial \phi} \right] + F_{\phi} \end{aligned} \quad [1.3]$$

Moisture conservation equation:

$$\begin{aligned} \frac{\partial q}{\partial t} = & - \frac{1}{a \cos \phi} \left[\frac{\partial (uq)}{\partial \lambda} + \frac{\partial (vqc\cos\phi)}{\partial \phi} \right] - \frac{\partial (wq)}{\partial \tilde{z}} \\ & + \frac{1}{\rho} M + E \end{aligned} \quad [1.4]$$

Pressure tendency equation:

$$\frac{\partial p}{\partial t} = B - g\rho w (Z_T - H) + g\rho (Z_T - H) \int_{\tilde{z}}^0 \frac{1}{a \cos \phi} \left[\frac{\partial(\rho u)}{\partial \lambda} + \frac{\partial(\rho v \cos \phi)}{\partial \phi} \right] d\tilde{z} \quad [I.5]$$

$B = \frac{\partial p}{\partial t}$ at $\tilde{z} = 0$, and it is assumed that $w \equiv 0$ at $\tilde{z} = 0$,

and, thus,

$$B = \frac{w_s + (Z_T - H) \int_1^0 \left\{ \frac{J}{\gamma p} - \frac{Q}{C_p T} + \frac{1}{a \cos \phi} \left[\frac{\partial u}{\partial \lambda} + \frac{\partial(v \cos \phi)}{\partial \phi} \right] \right\} d\tilde{z}}{\frac{Z_T - H}{\gamma} \int_1^0 \frac{d\tilde{z}}{p}} \quad [I.6]$$

where

$$J = \frac{u}{a \cos \phi} \frac{\partial p}{\partial \lambda} + \frac{v}{a} \frac{\partial p}{\partial \phi} + g(Z_T - H) \int_{\tilde{z}}^0 \frac{1}{a \cos \phi} \left[\frac{\partial(\rho u)}{\partial \lambda} + \frac{\partial(\rho u \cos \phi)}{\partial \phi} \right] d\tilde{z} \quad [I.7]$$

and $w_s = -V_s \cdot \nabla(Z_T - H)$ at $\tilde{z} = 0$.

Density is evaluated using the hydrostatic equation:

$$\frac{\partial p}{\partial \tilde{z}} = g\rho (Z_T - H) \quad [I.8]$$

Temperature is computed using:

$$T = \frac{g}{R(Z_T - H) \frac{\partial}{\partial \tilde{z}} (\ln p)} \quad [I.9]$$

Vertical velocity is evaluated using Richardson's equation:

$$w = \frac{d\tilde{z}}{dt} = w_s - \int_1^{\tilde{z}} \left\{ \frac{1}{a \cos \phi} \left[\frac{\partial u}{\partial \lambda} + \frac{\partial (v \cos \phi)}{\partial \phi} \right] + \frac{B+J}{\gamma p} - \frac{Q}{C_p T} \right\} d\tilde{z} \quad [I.10]$$

In the above equations:

- u = zonal wind component
- v = meridional wind component
- p = pressure
- q = ρ_w / ρ = specific humidity
- ρ = density of air
- ρ_w = density of water vapor
- H = terrain height
- T = temperature
- w = $\frac{d\tilde{z}}{dt}$ = vertical velocity
- Q = rate of heating per unit mass
- F_λ, F_ϕ = longitudinal and latitudinal components of frictional force per unit volume
- M = condensation rate of water vapor per unit volume
- E = rate of change of water vapor per unit mass due to the vertical and horizontal diffusion of water vapor
- a = radius of the earth
- g = acceleration due to gravity
- f = Coriolis parameter
- R = gas constant for dry air
- Φ = gz = geopotential

C_p = specific heat for dry air at constant pressure

C_v = specific heat for dry air at constant volume

γ = C_p/C_v

4.0 Numerics

Finite difference methods are used to approximate the solution of the primitive equations.

4.1 Spacial Differencing

Fourth-order centered differences are used to calculate horizontal derivatives and second-order centered differences are used to calculate vertical derivatives. An option exists in the model to use second-order differencing in the horizontal.

The poles are handled separately to maintain the fourth-order difference approximations by transforming to polar stereographic coordinates to perform the pole calculations.

Various horizontal diffusion terms are available. These include a spectral chopping technique in both the latitudinal and longitudinal directions in which all waves smaller than $4\Delta x$ are set to zero at a specified time interval, and a combination method which consists of fourth-order smoothing in latitude and spectral chopping in longitude.

4.2 Temporal Differencing

Centered time differencing is used with either a five or two and one-half minute time step for the 5.6° and 2.8° models, respectively.

The elimination of computationally unstable modes near the poles due to the convergence of the grid is accomplished by Fourier filtering the prognostic variables every time step.

4.3 Boundary Conditions

The horizontal boundary conditions are periodicity in longitude and the poles are handled separately to remove the coordinate system caused discontinuity and maintain fourth-order accuracy.

The vertical boundary conditions are $w \equiv 0$ at $\tilde{z} = 0$ and 1.

5.0 Processes and Effects

5.1 Dynamics

Terms representing the horizontal and vertical advection and convergence/divergence of momentum and moisture are included as are terms representing the pressure gradient and Coriolis forces in the momentum operations. The horizontal

and vertical diffusion of water vapor is included in the moisture equation, and eddy diffusion of heat is included in the pressure equation.

Orography that is consistent with reality and the grid resolution of the particular version of the model is included to add realism to the flows. Frictional forces are included.

5.2 Heat Sources/Sinks

Both solar and terrestrial radiation are included according to the formulation of Sasamori. Clouds may be included at all levels, but diagnostic cloudiness at two levels is currently used.

The release of latent heat due to the condensation of water vapor is included as part of the precipitation algorithm.

Heating/cooling due to eddy diffusion in both the horizontal and vertical (Deardorff) is included.

A surface energy balance equation is used to determine T_g over land areas.

A dry convective adjustment procedure is included to preclude hydrostatic instability.

5.3 Moisture Sources/Sinks

The precipitation algorithm removes supersaturated states with upward vertical motion from the model atmosphere as precipitation.

Evaporation or condensation is included in the boundary layer through the bulk transfer coefficient method (Deardorff). Horizontal diffusion of water vapor is also included. The ground is assumed saturated.

6.0 Inputs

The model is run in two basic modes:

a) The "GCM mode" in which data is self generated by going through a spin-up period which starts with an isothermal atmosphere at rest to obtain climate simulations.

b) The "real data mode" in which analyzed data sets (either subjective or objective analyses) obtained from various sources are used to make short and mid-range forecasts.

7.0 Outputs

An output cycle for the model consists of dumping the current integration state onto a history tape at regular intervals of model time. A large, sophisticated processor program then processes these history tapes to produce a wide variety of output fields which are under the control of the user. Numerous other processor programs which produce quantities such as climate statistics, etc. exist to process the history tapes.

8.0 Computer Information

The model is programmed in NCAR Fortran (a dialect of FTN IV) for the CDC 7600 using the NCAR Operating System. Running times in CPU hr/day for various versions are listed below:

6 layer, 5.6°	0.33
6 layer, 2.8°	2.8
24 layer, 5.6°	1.5

9.0 References

GCM Steering Committee, NCAR, "Development and Use of the NCAR GCM", NCAR-TN/STR-101, National Center for Atmospheric Research, Boulder, Colorado, September 1975, 177 pp.

Kasahara, Akira, "Various Vertical Coordinate Systems Used for Numerical Weather Prediction", Monthly Weather Review, Vol. 102, No. 7, July 1974, pp. 509-522.

Williamson, D.L. and G.L. Browning, "Comparison of Grids and Difference Approximations for Numerical Weather Prediction Over a Sphere", Journal of Applied Meteorology, Vol. 12, March 1973, pp. 264-274.

J. NMC 6-Layer Hemispheric Operational Model

The NMC operational atmospheric prediction model is currently executed twice daily to produce three day forecasts for the Northern Hemisphere. The model as described by Shuman and Hovermale (1968) was first put into operational use on 6 June 1966. Since that time numerous changes have been made to the model to improve the quality of the forecasts produced and to achieve a more efficient computation. The description that follows is, thus, a snapshot of the state of the prediction model as of mid 1976.

MODEL DESCRIPTION

1.0 Variables

1.1 Independent

The independent variables are x and y derived from a polar stereographic map projection in the horizontal; σ in the vertical defined as:

$$\sigma = \frac{P - P_U}{P_L - P_U} \quad [J.1]$$

where P_U is the pressure at a given quasi-horizontal surface above some point and P_L is the pressure at a surface below; and time, t .

1.2 Dependent

1.2.1 Prognostic

The prognostic variables are the x wind component, u ; the y wind component, v ; the potential temperature, θ ; the vertical pressure gradient, $\frac{\partial p}{\partial \sigma}$, at the three interfaces (between the planetary boundary layer and the troposphere, between the troposphere and the stratosphere, and between the stratosphere and the constant θ layer); and the specific humidity, q , in the planetary boundary layer and the troposphere. A secondary prognostic variable is the precipitable water, W .

1.2.2 Diagnostic

The diagnostic variables are the geopotential, Φ , and the vertical velocity, $\dot{\sigma} = \frac{d\sigma}{dt}$.

2.0 Domain

2.1 Horizontal

The horizontal domain is a polar stereographic projection (true at 60°N) of the Northern Hemisphere using x-y coordinates with map factor

$$m = \frac{1 + \sin 60^\circ}{1 + \sin \phi} \quad [\text{J.2}]$$

The grid resolution is 381 km at 60°N and the grid dimensions are 53 x 57 which covers virtually the entire Northern Hemisphere as shown in Figure J-1. (The standard octagon is also shown.) There is no staggering of variables in the horizontal.

2.2. Vertical

The vertical coordinate is sigma as defined by Equation [J-1]. Figure J-2 shows the vertical structure of the model with the four distinct sigma domains. The variables u , v , θ and q are carried at the midpoints of the various sigma layers and the variables ϕ , π and p are carried at the layer interfaces. The vertical velocity, $\dot{\sigma}$, is defined at layer interfaces, but at the center of a horizontal gridpoint square.

ORIGINAL PAGE IS
OF POOR QUALITY

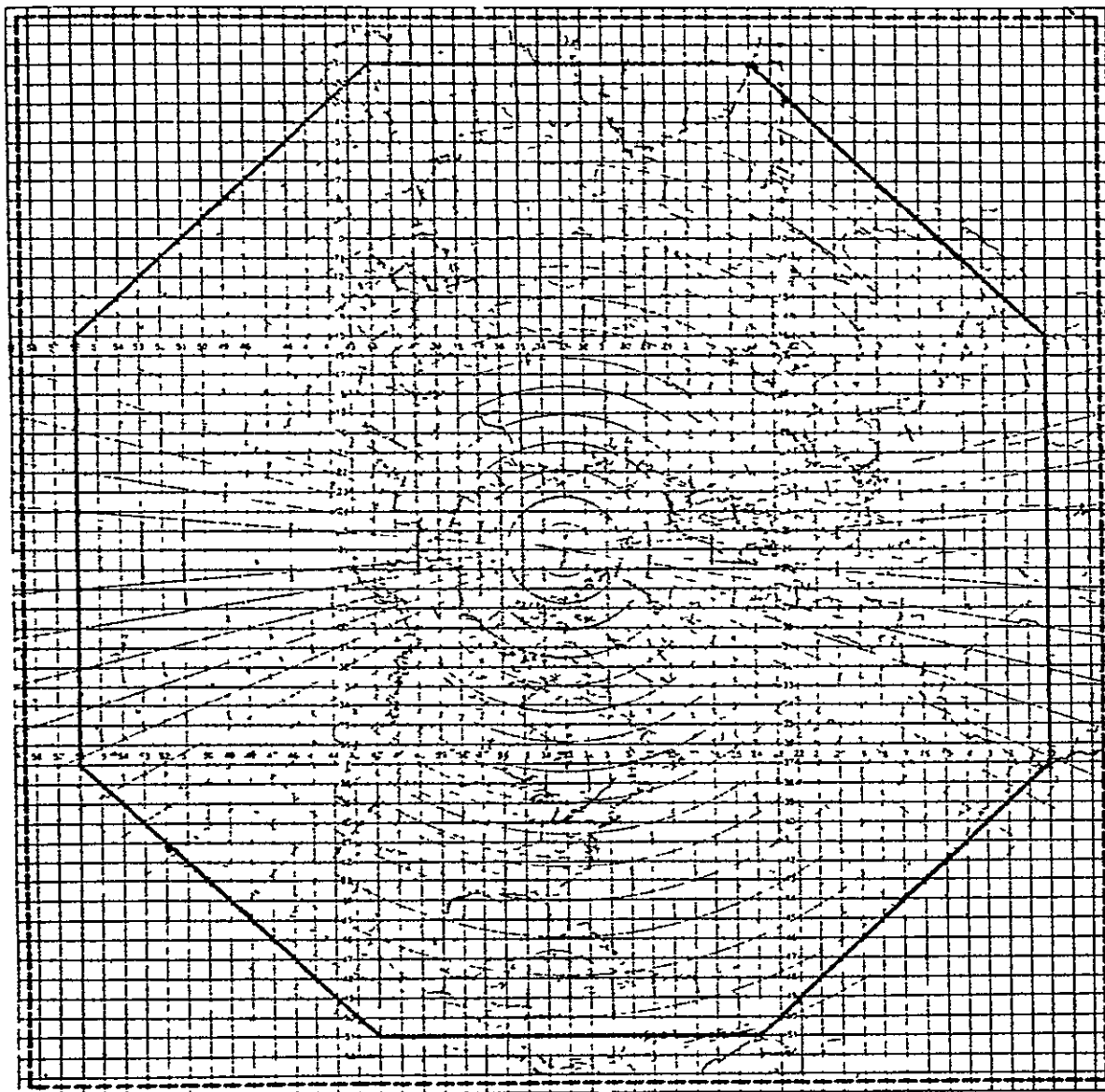


Figure J-1

NMC Northern Hemisphere Polar Stereographic Grid

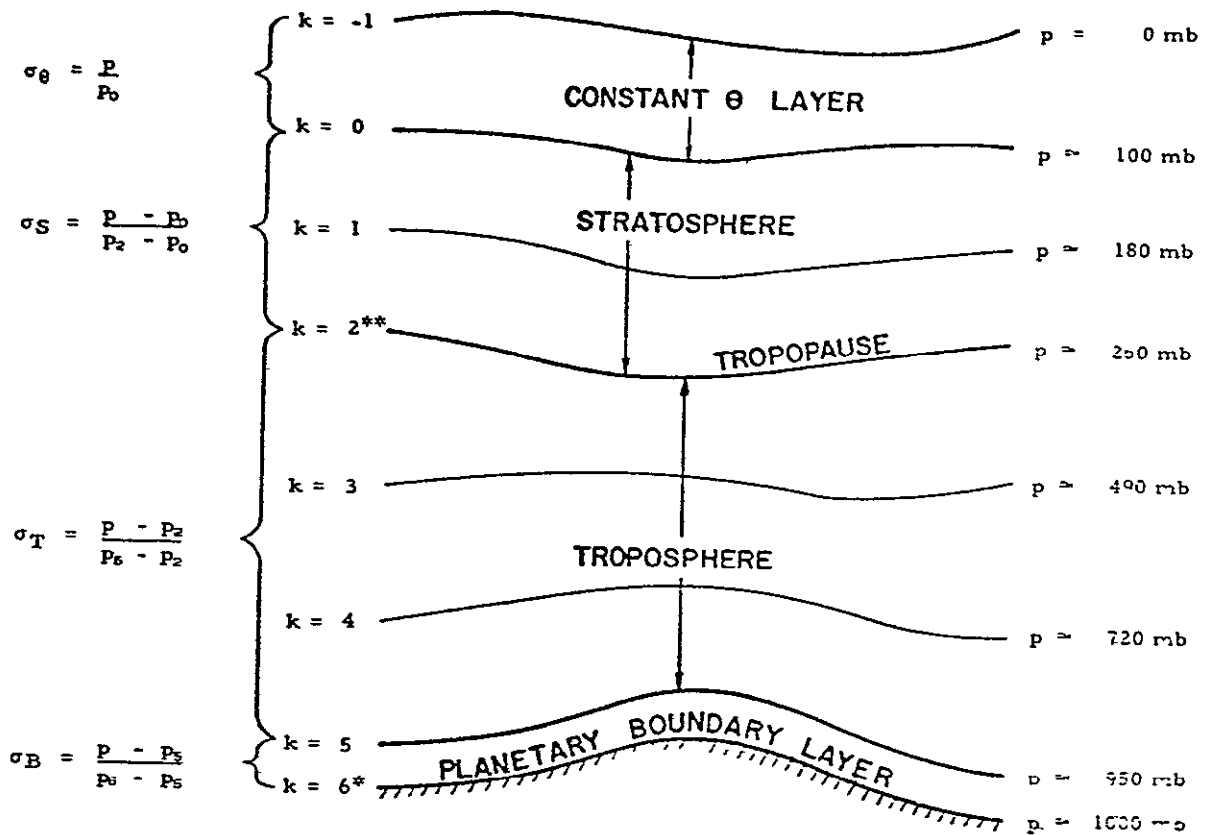


Figure J-2

Vertical Structure of the NMC Atmospheric Prediction Model

2.3 Temporal

Two time levels of data are required (except during the startup step) since a centered time differencing scheme is used with a twenty minute time step. There is no staggering of the variables in time.

3.0 Governing Equations

The governing partial differential equations written for an x-y map projection with map factor m and vertical coordinate σ are listed below.

Wind component in the x direction:

$$\begin{aligned} \frac{\partial u}{\partial t} = & -m \left[u \frac{\partial u}{\partial x} + v \frac{\partial u}{\partial y} \right] - m \left[\frac{\partial \Phi}{\partial x} + C_p \theta \frac{\partial \pi}{\partial x} \right] - \dot{\sigma} \frac{\partial u}{\partial \sigma} \\ & + v \left[f - v \frac{\partial m}{\partial x} + u \frac{\partial m}{\partial y} \right] + F_x + D_u \end{aligned} \quad [J.3]$$

Wind component in the y direction:

$$\begin{aligned} \frac{\partial v}{\partial t} = & -m \left[u \frac{\partial v}{\partial x} + v \frac{\partial v}{\partial y} \right] - m \left[\frac{\partial \Phi}{\partial y} + C_p \theta \frac{\partial \pi}{\partial y} \right] - \dot{\sigma} \frac{\partial v}{\partial \sigma} \\ & - u \left[f - v \frac{\partial m}{\partial x} + u \frac{\partial m}{\partial y} \right] + F_y + D_v \end{aligned} \quad [J.4]$$

Thermodynamic energy equation:

$$\frac{\partial \theta}{\partial t} = -m \left[u \frac{\partial \theta}{\partial x} + v \frac{\partial \theta}{\partial y} \right] - \dot{\sigma} \frac{\partial \theta}{\partial \sigma} + H \quad [J.5]$$

Pressure tendency equation:

$$\begin{aligned} \frac{\partial}{\partial t} \left(\frac{\partial P}{\partial \sigma} \right) = & -m \left[\frac{\partial}{\partial x} \left(\frac{\partial P}{\partial \sigma} u \right) + \frac{\partial}{\partial y} \left(\frac{\partial P}{\partial \sigma} v \right) \right] - \frac{\partial}{\partial \sigma} \left(\frac{\partial P}{\partial \sigma} \dot{\sigma} \right) \\ & + \frac{\partial P}{\partial \sigma} \left(u \frac{\partial m}{\partial x} + v \frac{\partial m}{\partial y} \right) \end{aligned} \quad [J.6]$$

Moisture equation:

$$\frac{\partial q}{\partial t} = -m \left[u \frac{\partial q}{\partial x} + v \frac{\partial q}{\partial y} \right] - \dot{\sigma} \frac{\partial q}{\partial \sigma} + C \quad [J.7]$$

Hydrostatic equation:

$$\frac{\partial \phi}{\partial \sigma} = -C_p \theta \frac{\partial \pi}{\partial \sigma} \quad [J.8]$$

Exner function:

$$\pi = \left(\frac{p}{1000} \right)^K \quad [J.9]$$

In the above equations,

- u = x direction wind component
- v = y direction wind component
- θ = potential temperature
- q = specific humidity
- ϕ = gz = geopotential
- p = pressure
- f = Coriolis parameter
- $\dot{\sigma}$ = $\frac{d\sigma}{dt}$ = vertical velocity
- F_x, F_y = stress components
- D_u, D_v = lateral diffusion terms
- H = diabatic heating/cooling term

C = condensation/evaporation term
 C_p = specific heat of dry air at constant pressure
 R = gas constant for dry air
 $\kappa = \frac{R}{C_p}$

4.0 Numerics

Finite difference methods are used to approximate the solution of the forecast model equations.

4.1 Spacial Differencing

Centered, second-order finite differencing is used to approximate the horizontal derivatives in the various sigma domains. A space averaging technique originated by Shuman (1968) is used in calculating the derivatives which results in defining the derivatives at the midpoint of a grid square through averaging and then averaging these values back to the grid points. This averaging technique makes the finite difference scheme somewhat dissipative and, hence, more stable.

The lateral diffusion terms included in the wind equations are of the form:

$$D_u = \nabla \cdot K \nabla u \quad [J.10]$$

where $K = 0$ for $\phi > 20^\circ\text{N}$, $K = 10^6 \text{ m}^2/\text{sec}$ for $\phi < 10^\circ\text{N}$
and $K = 5 \times 10^5 [1 + \sin\{(\phi_0 - \phi) \frac{90}{\Delta\phi}\}]$, $\phi_0 = 15^\circ$ and $\Delta\phi = 5^\circ$.

The vertical derivatives are approximated by second-order finite differences.

4.2 Temporal Differencing

Centered time differencing with pressure gradient force time averaging (Shuman, 1971) is used to obtain a time step of twenty minutes. The computation is started with an Euler backward or Matsuno time step.

A light time smoothing of the wind and moisture fields is also performed.

As a further control of the tropical region, the tendencies of all variables are truncated south of 20°N . North of 20°N , the full tendency is used and south of 10°N one-half of the tendency is used. These two zones are blended using a latitudinally dependent function such that three-quarters of the tendency is used at 15°N .

4.3 Boundary Conditions

The horizontal boundary conditions consist of insulated, slippery walls placed on the grid as shown in Figure J-1. That is, no heat or momentum flow is permitted through the wall, but a parallel flow is permitted along the wall.

The vertical boundary condition that $\dot{\sigma} = 0$ for a material surface is specified at the top of the model, the boundary surface between the topmost computational layer and the stratosphere, the tropopause; and the earth's surface. As a consequence of the above approach, no mass exchange takes place among the isentropic, stratospheric and tropospheric domains. However, mass exchange can take place between the boundary layer and the troposphere.

5.0 Processes and Effects

5.1 Dynamics

Terms representing the horizontal and vertical advection and convergence/divergence of heat and momentum are included as are terms representing the pressure gradient and Coriolis forces in the momentum equations.

Orography that is consistent with reality and the grid resolution is included to add realism to the flows.

Horizontal stress is applied at the lowest level to simulate vertical momentum transport at the surface.

5.2 Heat Sources/Sinks

Both solar and terrestrial radiation are included. Since moisture is carried in the lower three layers only,

solar heating is evaluated in these layers. Cloudiness effects are considered in both the solar and terrestrial heating computations.

Sensible heating is evaluated in the planetary boundary layer and a land-sea-ice discriminator is included. The ocean temperature is spatially varying, but held constant during the forecast.

Release of latent heat due to large scale precipitation is included in the moisture bearing layers.

A moist convective adjustment procedure is used to simulate sub-grid scale convective processes. Dry convective adjustment to maintain hydrostatic stability occurs as a limiting case of the moist convective adjustment.

5.3 Moisture Sources/Sinks —

Evaporation into the planetary boundary layer from the oceans is considered as a possible source of moisture.

The moist convective adjustment procedure may redistribute moisture in the moisture carrying layers.

The large scale precipitation algorithm acts as a moisture sink for precipitating layers. There is no absorption of precipitation in layers below precipitating layers.

6.0 Inputs

The forecast model initial data is obtained from Cressman type hemispheric analyses of the mass structure (temperature and geopotentials) between 1000 mb and 100 mb, the sea level pressure, and the sea surface temperature. Analyses of the winds on the standard pressure surfaces are also made.

The analyzed fields on pressure surfaces are then interpolated (linearly in $\ln p$) to obtain data on the model sigma surfaces.

7.0 Outputs

Temperatures, geopotential heights and winds on the mandatory pressure surfaces are produced by interpolation from the model sigma surfaces during an output cycle. Averaging of the output fields over time intervals surrounding the output time and filtering is used to render the output fields more visually pleasing. Precipitation fields are also produced during an output cycle.

8.0 Computer Information

The forecast model is run on the NOAA IBM 360/195

Computer System and is normally executed twice daily. The model is largely programmed in Fortran (Level H Compiler) with some specialized routines in assembly language and is fairly modular.

9.0 References

Shuman, F.G., "Resuscitation of an Integration Procedure", National Meteorological Center Office Note 54, 1971, 15 pp.

Shuman, F.G. and J.B. Hovermale, "An Operational Six-Layer Primitive Equation Model", Journal of Applied Meteorology, Vol. 7, No. 4, August 1968, pp. 525-547.

"PE Modifications Associated with 20 Minute Time-Step", Technical Procedures Bulletin No. 76, National Weather Service, June 27, 1972, 3 pp.

K. NMC 6-Layer Limited Area Operational Model

The NMC operational limited area, half-mesh model (LFM) is used in conjunction with the hemispheric model to obtain more detailed 48 hour forecasts over the North American Region. Boundary conditions for the LFM are obtained from the hemispheric model. The LFM is a modified version of the hemispheric model described in Section J. Thus, in the description that follows, reference is made to Section J where appropriate rather than repeating the material in this section.

MODEL DESCRIPTION

1.0 Variables

1.1 Independent

The independent variables are x and y derived from a polar stereographic map projection in the horizontal; σ in the vertical defined as

$$\sigma = \frac{P - P_U}{P_L - P_U} \quad [K.1]$$

where P_U is the pressure at a given quasi-horizontal surface above some point and P_L is the pressure at a surface below; and time, t .

1.2 Dependent

1.2.1 Prognostic

The prognostic variables are the x wind component, u ; the y wind component, v ; the potential temperature, θ ; the vertical pressure gradient, $\frac{\partial p}{\partial \sigma}$, at the three interfaces (between the planetary boundary layer and the troposphere, between the troposphere and the stratosphere, and between the stratosphere and the constant θ layer); and the specific humidity, q , in the planetary boundary layer and the troposphere. A secondary prognostic variable is the precipitable water, W .

1.2.2 Diagnostic

The diagnostic variables are the geopotential, ϕ , and the vertical velocity, $\dot{\sigma} = \frac{d\sigma}{dt}$.

2.0 Domain

2.1 Horizontal

The horizontal domain is a polar stereographic projection (true at 60°N) of part of the Northern Hemisphere using x-y coordinates with map factor

$$m = \frac{1 + \sin 60^\circ}{1 + \sin \phi} \quad [\text{K.2}]$$

The grid resolution is 190.5 km at 60°N and the LFM grid covers the North American region. (See Figure J-1.) There is no staggering of variables in the horizontal.

2.2 Vertical

The vertical coordinate is sigma as defined by Equation [K.1]. Figure J-2 in Section J shows the vertical structure of the model with the four distinct sigma domains. The variables u , v , θ and q are carried at the midpoints of the various sigma layers and the variables ϕ , π and p are carried at the layer interfaces. The vertical velocity, $\dot{\sigma}$, is defined at layer interfaces, but at the center of a horizontal gridpoint square.

2.3 Temporal

Two time levels of data are required (except during the startup step) since a centered time differencing scheme is used with a six minute time step. There is no staggering of the variables in time.

3.0 Governing Equations

Refer to Section J-3.0.

4.0 Numerics

Finite difference methods are used to approximate the solution of the forecast model equations.

4.1 Spacial Differencing

Centered, second-order finite differencing is used to approximate the horizontal derivatives in the various sigma domains. A space averaging technique originated by Shuman (1968) is used in calculating the derivatives which results in defining the derivatives at the midpoint of a grid square through averaging and then averaging these values back to the grid points. This averaging technique makes the finite difference scheme somewhat dissipative and, hence, more stable.

The vertical derivatives are also approximated by second-order finite differences.

4.2 Temporal Differencing

Centered time differencing is used with a time step of six minutes.

Two types of smoothers are used to control computational noise--spacial and temporal. A spacial smoother consisting of a twenty-five point operator is used at all points two or more grid intervals from the boundaries and a nine point operator is used at points one grid interval from the boundaries. The one-dimensional version of the

twenty-five point operator is given by:

$$\begin{aligned} \bar{u}_1 = & (1 - 6\beta^2)u_1 + 4\beta^2(u_{1-1} + u_{1+1}) \\ & -\beta^2(u_{1-2} + u_{1+2}) \end{aligned} \quad [K.3]$$

A value of $\beta = 0.1$ is currently used in the smoothing operator which is applied to all fields except precipitable water.

Robert time filtering is applied to all the fields--precipitable water, winds, $\frac{\partial p}{\partial \sigma}$ and θ .

4.3 Boundary Conditions

The LFM horizontal boundary conditions are obtained from the hemispheric six-layer model six-hourly output fields. The tendencies on and near the boundaries consist of a blend of the LFM and coarse mesh tendencies given by:

$$\begin{aligned} X_{n+1}(I) = & X_{n-1}(I) + W(I) \left. \frac{\partial X^m}{\partial t} \right|_I 2\Delta t \\ & + [1 - W(I)] \left. \frac{\partial X^{\ell s}}{\partial t} \right|_I 2\Delta t \end{aligned} \quad [K.4]$$

where X is the predicted variable, the subscript m denotes the LFM tendency and the subscript ℓs denotes the large-scale model tendency. The weighting factor $W(I)$ is given by:

W(I) = 0 for I = boundary points
= 0.33 for I = boundary points - 1 grid length
= 0.67 for I = boundary points - 2 grid length
= 1.00 for I = all other interior points

The coarse mesh model tendencies are calculated from six-hourly history fields biquadratically interpolated in space to the LFM grid points. (See Perkey and Kreitzberg, 1976.)

The vertical boundary conditions are identical to those of the coarse mesh model as described in Section J-4.3.

5.0 Processes and Effects

The various physical processes and effects are mostly described in Section J-5.0 since the LFM parameterizations differ only in detail from the six-layer hemispheric model.

6.0 Inputs

Initial data comes from a Cressman-type analysis on the LFM data points using raw data received during the one hour and forty-five minute time period after the synoptic time.

The mass structure variables are initialized from geopotentials analyzed on the ten mandatory pressure levels; temperature at the earth's surface and at the mandatory pressure levels with the exception of 1000 mb; and the

pressure and temperature of the analyzed "tropopause" surface. These data fields are then interpolated to the sigma surfaces.

Wind data is obtained from two sources, the coarse mesh twelve hour forecast winds on sigma surfaces, and the isobaric analysis of the winds interpolated to the sigma surfaces. A nondivergent wind is then calculated for each sigma layer which has the same relative vorticity as the interpolated analysis winds. Next, an irrotational wind is calculated which has the same divergence as the interpolated coarse-mesh forecast winds. The initial LFM wind is then taken to be the sum of the calculated nondivergent and irrotational wind components.

7.0 Outputs

Temperatures, geopotential heights and winds on the mandatory pressure surfaces are produced by interpolation and filtering from the model sigma surfaces during a six-hourly output cycle. Precipitation fields are also produced during an output cycle. Various other parameters are also produced during an output cycle (e.g., MOS forecasts and input to aviation winds forecasts).

8.0 Computer Information

The LFM forecast model is written in Fortran IV (Level H Compiler), except for some specialized I/O

routines, for the NOAA IBM 360/195 Computer System. The code is fairly modular and requires 520 k bytes of memory and 25 million bytes of mass storage. The execution time is three and one-half minutes of CPU time per twelve hours of forecast.

9.0 References

- Gerrity, J.P., "Drafts of Four Papers Describing the LFM Model Initialization and Physics - 1. Method for Initialization of σ Coordinate Heights and Potential Temperature, 2. The LFM Wind Initialization, 3. The Prediction of Precipitation - LFM Model, 4. Diabatic Effects of Radiative Energy - LFM Model", Regional Modeling Branch, Development Division, National Meteorological Center, August 1976.
- Gerrity, J.P. and J.E. Newell, "A Note on the LFM Time Integration," Office Note 129, Development Division, National Meteorological Center, July 1976, 9 pp.
- Perkey, D.J. and C.W. Kreitzberg, "A Time-Dependent Lateral Boundary Scheme for Limited-Area Primitive Equation Models", Monthly Weather Review, Vol. 104, June 1976, pp. 744-755.
- Shuman, F.G. and J.B. Hovermale, "An Operational Six-Layer Primitive Equation Model", Journal of Applied Meteorology, Vol. 7, No. 4, August 1968, pp. 525-547.

L. NMC 8-Layer Global Model

Initial development of the NMC 8-layer atmospheric prediction model was completed in 1972. This model is an extension of the earlier 6-layer hemispheric model (described in Section J) having increased vertical resolution and a latitude-longitude grid allowing either a global or hemispheric domain. While the original version of this model embodied much of the physics of the older 6-layer model, many additions and improvements have been made which are outlined in the following description.

MODEL DESCRIPTION

1.0 Variables

1.1 Independent

The independent variables are the longitude, λ , and the latitude, ϕ ; sigma defined as

$$\sigma = \frac{P - P_U}{P_L - P_U} \quad [L.1]$$

where P_U is the pressure at a given quasi-horizontal surface above some point and P_L is the pressure at a surface below; and time, t .

1.2 Dependent

1.2.1 Prognostic

The prognostic variables are the longitudinal component, u , and the meridional component, v , of the wind; the potential temperature, θ ; the vertical pressure gradient, $\frac{\partial p}{\partial \sigma}$ at the three interfaces (between the planetary boundary layer and the troposphere, between the troposphere and the stratosphere and between the stratosphere and the constant θ layer); and the specific humidity, q , in the planetary boundary layer and the troposphere. Secondary prognostic variables are the precipitable water, W , and the surface temperature, T_g .

1.2.2 Diagnostic

The diagnostic variables are the geopotential, ϕ , and the vertical velocity, $\dot{\sigma} = \frac{d\sigma}{dt}$.

2.0 Domain

2.1 Horizontal

The horizontal domain is a global (or hemispheric) latitude-longitude grid with λ and ϕ as the coordinates. The resolution is either $2\ 1/2^\circ$ or 2° (with 5° as a test version). The poles are treated separately as averages

of the forecast values one row removed from the pole. There is no staggering of variables in the horizontal.

2.2 Vertical

The vertical coordinate is sigma as defined by Equation [L.1]. Figure L-1 shows the vertical structure of the model with the four distinct sigma domains. The variables u , v , θ and q are carried at the midpoints of the various sigma layers and the variables ϕ , π and p are carried at the layer interfaces. The vertical velocity, $\dot{\sigma}$, is defined at layer interfaces, but at the center of a horizontal gridpoint square.

2.3 Temporal

Two time levels of data are required (except during the startup step) since a centered time differencing scheme is used with a ten minute (2.5°) or seven and one-half (2°) minute time step. There is no staggering of variables in time.

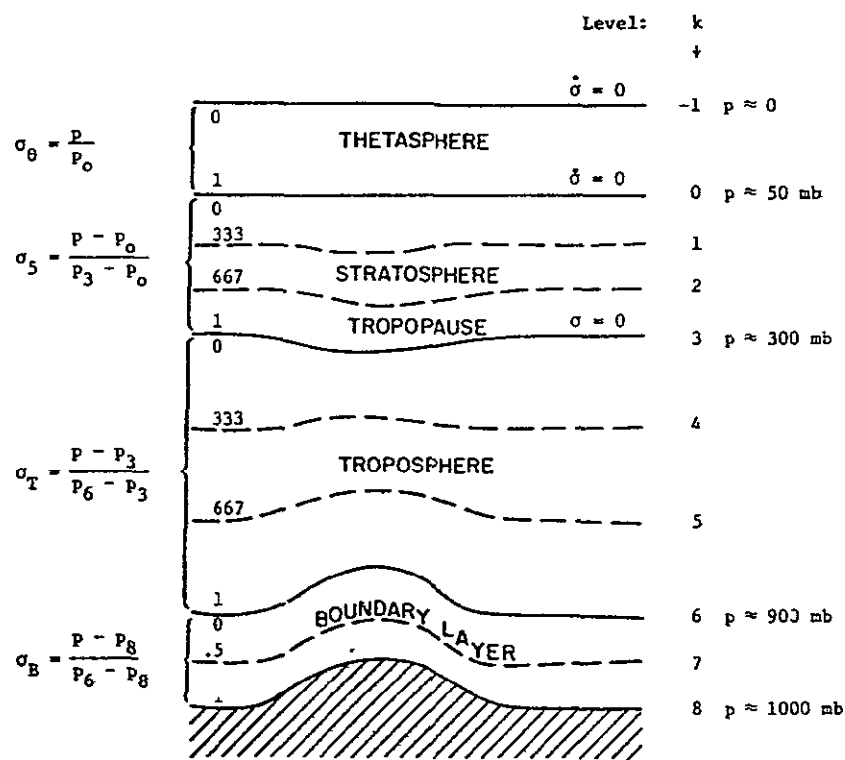


Figure L-1
Vertical Structure of the NMC 8-Layer Model

3.0 Governing Equations

The governing partial differential equations written in spherical polar coordinates and a vertical coordinate sigma are listed below:

Wind component in the latitudinal direction:

$$\begin{aligned} \frac{\partial u}{\partial t} = & -u \frac{\partial u}{\partial x} - v \frac{\partial u}{\partial y} - \dot{\sigma} \frac{\partial u}{\partial \sigma} + v \left(f + \frac{u \tan \phi}{a} \right) \\ & - \frac{\partial \Phi}{\partial x} - c_p \theta \frac{\partial \pi}{\partial x} + F_x \end{aligned} \quad [\text{L.2}]$$

Wind component in the meridional direction:

$$\begin{aligned} \frac{\partial v}{\partial t} = & -u \frac{\partial v}{\partial x} - v \frac{\partial v}{\partial y} - \dot{\sigma} \frac{\partial v}{\partial \sigma} - u \left(f + \frac{u \tan \phi}{a} \right) \\ & - \frac{\partial \Phi}{\partial y} - c_p \theta \frac{\partial \pi}{\partial y} + F_y \end{aligned} \quad [\text{L.3}]$$

Thermodynamic energy equation:

$$\frac{\partial \theta}{\partial t} = -u \frac{\partial \theta}{\partial x} - v \frac{\partial \theta}{\partial y} - \dot{\sigma} \frac{\partial \theta}{\partial \sigma} + H \quad [\text{L.4}]$$

Pressure tendency equation:

$$\frac{\partial}{\partial t} \left(\frac{\partial P}{\partial \sigma} \right) = - \frac{\partial}{\partial x} \left(\frac{\partial P}{\partial \sigma} u \right) - \frac{\partial}{\partial y} \left(\frac{\partial P}{\partial \sigma} v \right) - \frac{\partial}{\partial \sigma} \left(\frac{\partial P}{\partial \sigma} \dot{\sigma} \right) + \left(\frac{\partial P}{\partial \sigma} \right) \frac{v \tan \phi}{a} \quad [\text{L.5}]$$

Moisture equation:

$$\frac{\partial q}{\partial t} = -u \frac{\partial q}{\partial x} - v \frac{\partial q}{\partial y} - \dot{\sigma} \frac{\partial q}{\partial \sigma} + EP \quad [\text{L.6}]$$

Hydrostatic equation:

$$\frac{\partial \phi}{\partial \sigma} = -C_p \theta \frac{\partial \pi}{\partial \sigma} \quad [\text{L.7}]$$

Exner function:

$$\pi = \left(\frac{P}{1000} \right)^k \quad [\text{L.8}]$$

where

$$\frac{\partial}{\partial x} = \frac{\partial}{a \cos \phi \partial \lambda} \quad \text{and} \quad \frac{\partial}{\partial y} = \frac{\partial}{a \partial \phi} \quad [\text{L.9}]$$

In the above equations,

u = $a \cos\phi \frac{\partial\lambda}{\partial t}$ = zonal wind component

v = $a \frac{\partial\phi}{\partial t}$ = meridional wind component

θ = potential temperature

q = specific humidity

ϕ = gz = geopotential

p = pressure

f = Coriolis parameter

$\dot{\sigma}$ = $\frac{d\sigma}{dt}$ = vertical velocity

F_x, F_y = stress components

H = diabatic heating/cooling term

EP = evaporation and precipitation processes which alter q

C_p = specific heat of dry air at constant pressure

R = gas constant for dry air

κ = $\frac{R}{C_p}$

4.0 Numerics

Finite difference methods are used to approximate the solution of the forecast model equations.

4.1 Spacial Differencing

Centered, second-order finite differencing is used to approximate the horizontal derivatives in the various sigma

domains. A space averaging technique originated by Shuman (1968) is used in calculating the derivatives which results in defining the derivatives at the midpoint of a grid square through averaging and then averaging these values back to the grid points. This averaging technique makes the finite difference technique somewhat dissipative and, hence, more stable.

The vertical derivatives are approximated by second-order finite differences.

The values of the variables at the poles are obtained by averaging the variables one row equatorward and assigning this average to the pole value. The one vector wind at the pole is resolved into the u and v components appropriate to the meridian along which the pole is approached.

4.2. Temporal Differencing

Centered time differencing is used with a time step of either ten or seven and one-half minutes for the 2.5° and 2° versions, respectively. Robert time filtering with fairly heavy weighting (1/4, 1/2, 1/4) is used to maintain computational stability. The computation is started with a forward time step.

The overspecification of tendencies due to the poleward convergence of the meridians is handled by an averaging procedure. The tendency terms are averaged using a triangular

weighting function that expands longitudinally with increasing latitude. This weighting function is given by:

$$\begin{aligned}
 w &= 1 - \frac{x}{L \sec \phi_0} & x &= 1/2, 1 1/2, \dots L \sec \phi_0 \\
 &= 0 & x &\geq L \sec \phi_0
 \end{aligned}
 \tag{L.10}$$

where ϕ_0 is the latitude of the tendencies being averaged and $L = 1.5$.

4.3 Boundary Conditions

The horizontal boundary conditions consist of periodicity in longitude and the pole calculations as described above (Section 4.1) for the global versions of the model. The additional boundary condition of horizontal symmetry about the equator is used in the hemispheric versions.

The vertical boundary condition that $\dot{\sigma} = 0$ for a material surface is specified at the top of the model, the boundary surface between the topmost computational layer and the stratosphere, the tropopause; and the earth's surface. As a consequence of the above approach, no mass exchange takes place among the isentropic, stratospheric and tropospheric domains. However, mass exchange can take place between the boundary layer and the troposphere.

5.0 Processes and Effects

5.1 Dynamics

Terms representing the horizontal and vertical advection and convergence/divergence of heat and momentum are included as are terms representing the pressure gradient and Coriolis forces in the momentum equations.

Orography that is consistent with reality and the grid resolution is included to add realism to the flows.

Horizontal stress according to Shuman (1968) is applied at the lowest level to simulate vertical momentum transport at the surface.

5.2 Heat Sources/Sinks

Both solar and terrestrial radiation are included. Since moisture is carried in the lower five layers only, solar heating is evaluated in these layers. Cloudiness effects are considered in both the solar and terrestrial heating computations.

Sensible heating is evaluated in the planetary boundary layer and a land-sea-ice discriminator is included. The ocean temperature is spatially varying, but held constant during the forecast while the land temperature is predicted through an energy balance equation.

Release of latent heat due to large scale precipitation is included in the moisture bearing layers.

A moist convective adjustment procedure is used to simulate sub-grid scale convective processes. Dry convective adjustment to maintain hydrostatic stability occurs as a limiting case of the moist convective adjustment.

5.3 Moisture Sources/Sinks

Evaporation into the planetary boundary layer either from the oceans or over land is considered as a possible source of moisture.

The moist convective adjustment procedure may redistribute moisture in the moisture carrying layers.

The large scale precipitation algorithm acts as a moisture sink for precipitating layers. There is absorption of precipitation in layers below precipitating layers if they are not saturated.

6.0 Inputs

The forecast model initial data is obtained from Hough function analyses (Flattery, 1970). The end results of these analyses are heights, winds and temperatures at the mandatory levels up to 50 mb plus surface temperature (land and sea), tropopause pressure, snow/ice cover, and

relative humidity at mandatory levels up to 300 mb.

The analyzed fields on pressure surfaces are then interpolated (linearly in $\ln p$) to obtain initial data on the model sigma surfaces.

7.0 Outputs

Temperatures, geopotential heights and winds on the mandatory pressure surfaces are produced by interpolation from the model sigma surfaces during an output cycle. Various filters are used to render the fields more visually pleasing. Precipitation fields are also produced during an output cycle.

8.0 Computer Information

The forecast model is run on the NOAA IBM 360/195 Computer System. The model is largely programmed in Fortran IV (Level H Compiler) except for assembly language coding of high usage sections and some specialized I/O routines. The code is fairly modular and requires 750 k bytes and 950 k bytes of storage for the 2.5° and 2° versions, respectively. The mass storage requirement is approximately 50 million bytes. The execution time is ten CPU minutes per twelve hour forecast for both the 2.5° global and 2° hemispheric models.

9.0 References

- Flattery, T.W., "Spectral Models for Global Analysis and Forecasting," Automated Weather Support - Proceedings of the 6th AWS Technical Exchange Conference, U.S. Naval Academy, 21-24 September, 1970, Air Weather Service Technical Report 242, April 1971, pp. 42-54.
- Joint Organizing Committee - GARP, "Modelling for the First GARP Global Experiment," GARP Publication Series No. 14, June 1974, Chapter 7, pp. 79-93.
- Shuman, F.G. and J.B. Hovermale, "An Operational Six-Layer Primitive Equation Forecast Model," Journal of Applied Meteorology, Vol. 7, pp. 525-547.

M. UCLA 12-Layer Global Model

The UCLA Mintz-Arakawa atmospheric general circulation model was developed for numerical simulation experiments which study the mutual interactions of various physical processes in the atmosphere. This latest version of the Mintz-Arakawa model (Arakawa, et al., 1974) is based on earlier versions developed at UCLA, but contains greater vertical resolution extending to the stratopause, an improved finite difference formulation, and new parameterizations of the sub-grid scale processes. While not developed for use as a prediction model, numerous existing prediction models are based on earlier versions of this model and prediction models are being developed which are based on this latest version. What follows is a description of the nominal (twelve level) version as of mid-1976.

MODEL DESCRIPTION

1.0 Variables

1.1 Independent

The independent variables are λ and ϕ of a spherical polar coordinate system in the horizontal; sigma in the vertical defined in the troposphere as

$$\sigma = \frac{P - P_I}{P_S - P_I} \quad [M.1]$$

where $P_I = 100$ mb and P_S is the pressure at terrain level, and above 100 mb as

$$\sigma = \frac{P - P_I}{P_I - P_T} \quad [M.2]$$

where $P_T = 1$ mb; and time, t .

1.2 Dependent

1.2.1 Prognostic

The prognostic variables are the pressure, π_L , the horizontal velocity, \bar{V} , the temperature, T , and the water vapor, q . Secondary prognostic variables are the ground temperature, the ground water storage, the mass of snow on the ground, the amount of atmospheric ozone, the planetary boundary layer depth, and the magnitudes of the temperature and moisture discontinuities at the top of the boundary layer.

1.2.2 Diagnostic

The diagnostic variables are the geopotential, Φ , and the vertical velocity, $\dot{\sigma} = \frac{d\sigma}{dt}$.

2.0 Domain

2.1 Horizontal

The horizontal domain is a global latitude, longitude grid with λ and ϕ as the coordinates and the grid resolution

is 4° in latitude and 5° in longitude. The poles are considered as mass points and are treated separately. The variables are distributed in the horizontal according to Arakawa's Scheme C as shown in Figure M-1.

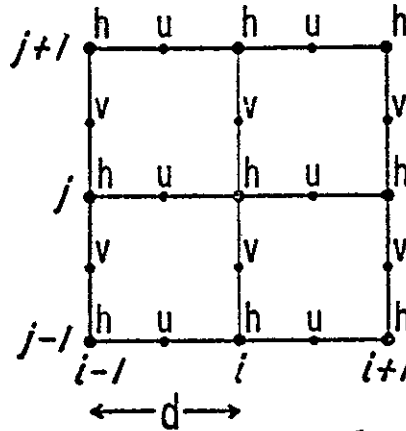


Figure M-1

Horizontal Grid Structure of the UCLA 12-Level Global Model

2.2 Vertical

The vertical coordinate is sigma as defined by Equations [M.1] and [M.2]. Figure M-2 shows the hybrid vertical coordinate system of the model consisting of five sigma layers in the troposphere and seven constant pressure surfaces in the stratosphere. The lowest four layers have equal depth in pressure, and the uppermost seven layers have equal depth in the logarithm of pressure.

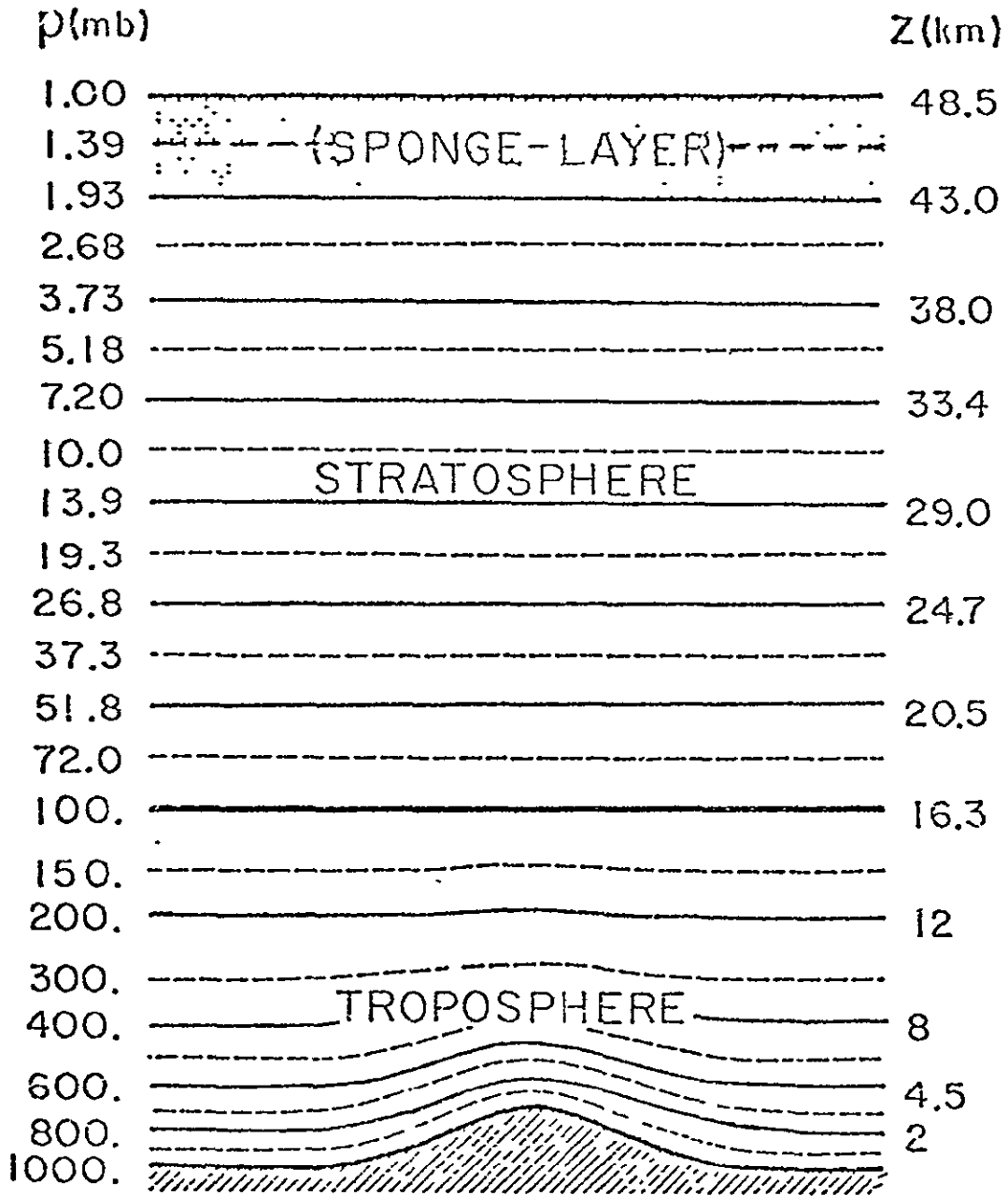


Figure M-2

Vertical Structure of the UCLA 12-Level Global Model

2.3 Temporal

Two time levels of data are required since a combination of centered and Matsuno time steps is used. A computational cycle consists of five six minute time steps with four centered steps followed by a Matsuno time step. There is no staggering of variables in time.

3.0 Governing Equations

The governing partial differential equations written in flux form with a sigma coordinate in the vertical are listed below.

Equation of motion:

$$\pi \frac{d\bar{V}}{dt} + f\bar{k}x\pi\bar{V} + \nabla(\pi\Phi) - \frac{\partial(\Phi\sigma)}{\partial\sigma}\nabla\pi = \pi\bar{F} \quad [M.3]$$

Pressure tendency equation:

$$\frac{\partial\pi_L}{\partial t} = -\int_1^1 \nabla \cdot (\pi\bar{V}) d\sigma \quad [M.4]$$

First law of thermodynamics:

$$\frac{\partial}{\partial t} (\pi \ln \theta) + \nabla \cdot (\pi \bar{V} \ln \theta) + \frac{\partial}{\partial \sigma} (\pi \dot{\sigma} \ln \theta) = \frac{Q}{C_p T} \quad [M.5]$$

Water vapor equation:

$$\frac{\partial}{\partial t} (\pi q) + \nabla \cdot (\pi \bar{V} q) + \frac{\partial}{\partial \sigma} (\pi \dot{\sigma} q) = \pi (-C+E) \quad [M.6]$$

Equation of state:

$$p\alpha = RT \quad [M.7]$$

Hydrostatic equation:

$$\frac{\partial \Phi}{\partial \sigma} = \frac{-RT}{\sigma} \quad [M.8]$$

In the above equations,

\bar{V} = horizontal velocity

f = Coriolis parameter

\bar{k} = vertical unit vector

∇ = two dimensional gradient operator

α = specific volume

$\pi_L = P_s - P_I$

\bar{F} = horizontal frictional force

R = gas constant for dry air

T = temperature

θ = potential temperature

C_p = specific heat of dry air at constant pressure

Q = heating rate per unit mass

ϕ = gz = geopotential
q = water vapor mixing ratio
C = rate of condensation
E = rate of evaporation

4.0 Numerics

Finite difference methods are used to approximate the solution of the forecast equations.

4.1 Spacial Differencing

The distribution of variables on the horizontal grid corresponds to Arakawa's (1974) Scheme C as shown in Figure M-1. The horizontal differencing is constructed so as to maintain quadratic constraints analogous to the conservation of energy and mean square vorticity. Second-order, centered differencing is used in both the horizontal and vertical difference operators.

The change in the variables defined at the poles (π_L , T and q) is calculated by summing the meridional flux at all points on the latitude circle around the poles.

4.2 Temporal Differencing

Time differencing proceeds in half-hour cycles using a six minute time step. The first four steps of a cycle are centered time steps and the fifth is a Matsuno time step.

For computational economy, physical processes other than advection are only calculated every half hour of simulated time on the last time step of a cycle.

To avoid reducing the time step due to the convergence of the grid near the poles, the zonal mass flux and zonal pressure force are smoothed longitudinally. A three point averaging technique is used for latitudes such that $38^\circ \leq |\phi| \leq 70^\circ$, and a Fourier filtering technique is used for latitudes where $|\phi| \geq 74^\circ$. No smoothing is performed on latitude circles equatorward of 38° .

A characteristic of the model which is believed to be due to numerical truncation occurring in the finite difference computations, is a decrease in the globally averaged value of surface pressure with time. Therefore, a procedure is invoked to maintain the globally averaged value of surface pressure at each time step.

4.3 Boundary Conditions

The horizontal boundary conditions are periodicity in longitude and the poles are treated as mass points as explained in Section 4.1.

The vertical boundary conditions are $\dot{\sigma} = 0$ at $\sigma = -1$ and 1, and the upper pressure P_t is taken to be 1 mb.

5.0 Processes and Effects

5.1 Dynamics

Terms representing the horizontal and vertical advection and convergence/divergence of heat, moisture and momentum are included as are terms representing the pressure gradient and Coriolis forces in the momentum equations. Adiabatic temperature changes are also modeled.

Orography that is consistent with reality and the grid resolution is included to add realism to the flows.

Surface effects are evaluated as part of the planetary boundary layer parameterization which is based on the work of Deardorff (Arakawa et al., 1974).

5.2 Heat Sources/Sinks

The planetary boundary layer parameterization predicts both the height of the boundary layer and the temperature discontinuity at the top of the PBL. Quantities in the PBL are computed diagnostically. A surface discriminator is used to determine which type of surface is being considered (land-sea-ice). The ground temperature is predicted from the net surface energy flux. The ocean temperature varies spatially, but is held fixed in time.

Heating due to solar and terrestrial radiation is considered including ozone heating in the stratosphere. Cloudiness and surface effects are included.

Release of latent heat due to large scale precipitation is included.

A detailed parameterization of cumulus ensembles (moist convection) which is coupled to the PBL computations redistributes heat and moisture in the vertical. A dry convective adjustment procedure is included to preclude hydrostatic instability.

5.3 Moisture Sources/Sinks

The large scale precipitation algorithm removes supersaturated states from the model atmosphere and results in evaporation in non-saturated layers below the saturated layer and/or precipitation.

The cumulus parameterization process can result in the evaporation/condensation of moisture in the lower model layers.

The PBL parameterization predicts both the height of the boundary layer and the moisture discontinuity at the top of the PBL. Quantities in the PBL are computed diagnostically. Evaporation/condensation at the surface is evaluated and the soil moisture and snow cover is predicted.

6.0 Inputs

Since the UCLA general circulation model is used for numerical simulation experiments, and not for weather prediction, data is self generated by going through a spin-up period from an atmosphere at rest to generate "realistic" meteorological conditions. Experiments are then made using this initial data.

7.0 Outputs

An output cycle may be specified at any desired interval. Many outputs are built into the code in either grid-point format of a field, or printout of various diagnostic quantities. In addition to these types of output, the entire data base is saved on an output cycle for use either in restarting the computation, or for further processing.

8.0 Computer Information

The UCLA general circulation model is programmed mostly in Fortran IV (Level H Compiler) for the IBM 360/91 Computer System. Some specialized output routines are coded in assembly language. The execution time was approximately 2 hours and 40 minutes per model day for the version running in early 1976.

9.0 References

Arakawa, A., Y. Mintz, A. Katayama, J.W. Kim, W. Schubert, T. Tokioka, M. Schlesinger, W. Chao, D. Randall and S. Lord, "The UCLA Atmospheric General Circulation Model," Notes distributed at the Workshop 25 March - 4 April 1974, Department of Meteorology, University of California, Los Angeles, California.

N. ANMRC 5-Layer Hemispheric, Spectral Model

The ANMRC model was developed to study global-scale dynamics and numerical weather prediction and is an extension of Bourke's (1972) earlier one-level, primitive equation spectral model. The version of the model described here is dry and adiabatic although there is no fundamental limitation precluding the inclusion of detailed physical parameterizations. The model also uses a semi-implicit time integration of the spectral form of the governing equations to obtain a more efficient computation.

MODEL DESCRIPTION

1.0 Variables

1.1 Independent

The independent variables are the longitude, λ , the latitude, ϕ , sigma defined as:

$$\sigma = \frac{p}{p_*} \quad [N.1]$$

where p_* is the local surface pressure and time, t .

1.2 Dependent

1.2.1 Prognostic

The prognostic variables are the stream function, ψ , the velocity potential, χ , the temperature, T and the logarithm of surface pressure, $q = \ln(p_*)$.

1.2.2 Diagnostic

The diagnostic variables are the scalar velocities defined by

$$U = u \cos \phi \quad \text{and} \quad V = v \cos \phi \quad [\text{N.2}]$$

the geopotential, Φ , and the vertical velocity, $\dot{\sigma}$.

2.0 Domain

2.1 Horizontal

The horizontal domain is hemispheric (or global) with a $J=15$ wavenumber truncation (rhomboidal) coupled with a hemispheric transform grid of 20 Gaussian latitudes and 48 equispaced longitudes. The poles are regular points in this representation and variables are placed regularly on the transform grid.

2.2 Vertical

The vertical coordinate is sigma as defined by Equation [N.1]. Figure N-1 shows the model sigma surfaces and the placement of variables in the vertical.

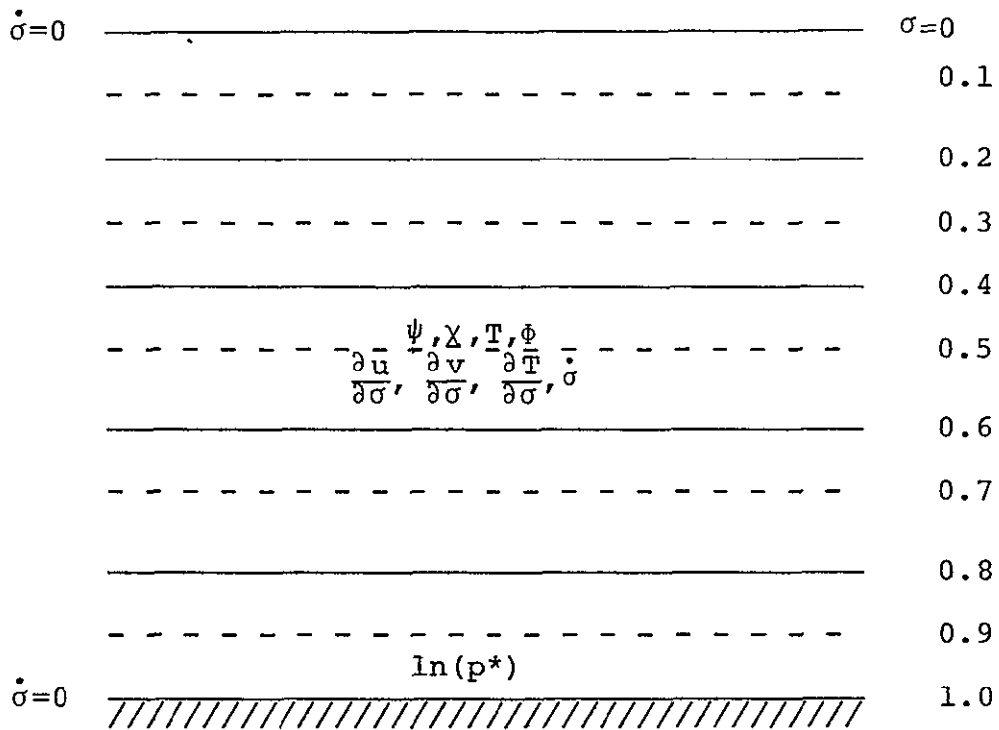


Figure N-1

Vertical Structure of the ANMRC 5-Layer Spectral Model (Repeated for all levels).

2.3 Temporal

Two time levels of data are required (except during the startup step) since a centered semi-implicit time differencing scheme is used with a sixty minute time step. There is no staggering of the variables in time.

3.0 Governing Equations

The governing partial differential equations written in spherical polar coordinates in the horizontal and a sigma coordinate in the vertical are listed below:

Vorticity equation:

$$\begin{aligned} \frac{\partial}{\partial t} \nabla^2 \psi = & - \frac{1}{a \cos^2 \phi} \left(\frac{\partial A}{\partial \lambda} + \cos \phi \frac{\partial B}{\partial \phi} \right) - 2\Omega \left(\sin \phi \nabla^2 \chi + \frac{V}{a} \right) \\ & + K_H \nabla^2 \left(\nabla^2 \psi + \frac{2\psi}{a^2} \right) \end{aligned} \quad [\text{N.3}]$$

Divergence equation:

$$\begin{aligned} \frac{\partial}{\partial t} \nabla^2 \chi = & \frac{1}{a \cos^2 \phi} \left(\frac{\partial B}{\partial \lambda} - \cos \phi \frac{\partial A}{\partial \phi} \right) + 2\Omega \left(\sin \phi \nabla^2 \psi - \frac{U}{a} \right) \\ & - \nabla^2 (E + \Phi' + RT_0 q) \end{aligned} \quad [\text{N.4}]$$

Thermodynamic energy equation:

$$\begin{aligned} \frac{\partial T}{\partial t} = & - \frac{1}{a \cos^2 \phi} \left(\frac{\partial UT'}{\partial \lambda} + \cos \phi \frac{\partial VT'}{\partial \phi} \right) + T' \nabla^2 \chi \\ & + \gamma \dot{\sigma} + \frac{RT}{C_p} [\overline{\nabla^2 \chi} + (\mathbf{W} + \overline{\mathbf{W}}) \cdot \nabla q] + K_H \nabla^2 T \end{aligned} \quad [\text{N.5}]$$

Pressure tendency equation:

$$\frac{\partial q}{\partial t} = \overline{\mathbf{W}} \cdot \nabla q + \overline{\nabla^2 \chi} + K_H \nabla^2 q \quad [\text{N.6}]$$

Hydrostatic relation:

$$\frac{\partial \phi}{\partial \sigma} = - \frac{RT}{\sigma} \quad [\text{N.7}]$$

Here:

$$U = - \frac{\cos \phi}{a} \frac{\partial \psi}{\partial \phi} + \frac{1}{a} \frac{\partial \chi}{\partial \lambda} \quad [\text{N.8}]$$

$$V = \frac{1}{a} \frac{\partial \psi}{\partial \lambda} + \frac{\cos \phi}{a} \frac{\partial \chi}{\partial \phi} \quad [\text{N.9}]$$

$$W = kx \nabla \psi + \nabla \chi$$

$$\begin{aligned} \dot{\sigma} = & (1-\sigma) \int_1^0 \nabla^2 \chi d\sigma - \int_1^\sigma \nabla^2 \chi d\sigma \\ & + [(1-\sigma) \int_1^0 W d\sigma - \int_1^\sigma W d\sigma] \cdot \nabla q \end{aligned} \quad [\text{N.10}]$$

$$A = \nabla^2 \psi U + \dot{\sigma} \frac{\partial V}{\partial \sigma} + \frac{RT'}{a} \cos \phi \frac{\partial q}{\partial \phi} - \frac{q}{p_*} \frac{\partial \tau_y}{\partial \sigma} \quad [\text{N.11}]$$

$$B = \nabla^2 \psi V - \dot{\sigma} \frac{\partial U}{\partial \sigma} - \frac{RT'}{a} \frac{\partial q}{\partial \lambda} + \frac{q}{p_*} \frac{\partial \tau_x}{\partial \sigma} \quad [\text{N.12}]$$

$$E = \frac{U^2 + V^2}{2 \cos^2 \phi} \quad [\text{N.13}]$$

the subscripted zero denotes a horizontal mean value and the superscripted prime the deviation from that mean; and the bar notation means $(\bar{\quad}) = \int_1^0 (\quad) d\sigma$.

In the above equations,

- U = $u \cos \phi$ = scalar zonal wind component
- V = $v \cos \phi$ = scalar meridional wind component
- ψ = stream function

χ = velocity potential
 q = $\ln(p_*)$ where p_* is the surface pressure
 T = $T_0 + T'$, temperature
 $\dot{\sigma}$ = vertical velocity
 γ = $\frac{RT}{\sigma C_p} - \frac{\partial T}{\partial \sigma}$ = static stability
 Φ = $\Phi_0 + \Phi'$ = geopotential height
 Ω = rotation rate of the earth
 τ_x = horizontal stress in the x direction
 τ_y = horizontal stress in the y direction

4.0 Numerics

A spectral representation in the horizontal coupled with finite differencing in the vertical and semi-implicit time differencing is used to approximate the solution of the model equations.

4.1 Spatial Representation

The essence of the transform procedures proposed by Orszag and Eliassen is to evaluate the nonlinear terms of the equations as simple products following a transform from the spectral to gridpoint domain; a subsequent inverse transform yields the spectral form of the requisite nonlinear term. The procedure may be more generally described as combining nonlocal (spectral) differentiations with local

(gridpoint) multiplications for evaluation of the nonlinear terms.

That is, the model considers the prognostic variables ψ , χ and T in terms of orthogonal spherical harmonics at each of five levels in the vertical; the diagnostic variables ϕ , U and V are similarly represented at these levels as is the prognostic variable q at the surface. Truncated expansions for the prognostic and diagnostic variables are required as follows:

$$\begin{aligned}
 \psi &= a^2 \sum_{m=-J}^J \sum_{\ell=|m|}^{|m|+J} \psi_{\ell}^m Y_{\ell}^m & \chi &= a^2 \sum_{m=-J}^J \sum_{\ell=|m|}^{|m|+J} \chi_{\ell}^m Y_{\ell}^m \\
 T &= \sum_{m=-J}^J \sum_{\ell=|m|}^{|m|+J} T_{\ell}^m Y_{\ell}^m & q &= \sum_{m=-J}^J \sum_{\ell=|m|}^{|m|+J} q_{\ell}^m Y_{\ell}^m \\
 U &= a \sum_{m=-J}^J \sum_{\ell=|m|}^{|m|+J+1} U_{\ell}^m Y_{\ell}^m & V &= a \sum_{m=-J}^J \sum_{\ell=|m|}^{|m|+J+1} V_{\ell}^m Y_{\ell}^m \\
 \phi &= a^2 \sum_{m=-J}^J \sum_{\ell=|m|}^{|m|+J} \phi_{\ell}^m Y_{\ell}^m & &
 \end{aligned}
 \tag{N.14}$$

where

a) The terms ψ_{ℓ}^m , etc. denote time dependent, generally complex, expansion coefficients, and the reality of the fields requires $(\psi_{\ell}^m)^* = (-1)^m \psi_{\ell}^{-m}$ and so forth.

- b) The spherical harmonics are given by $Y_{\ell}^m = P_{\ell}^m(\sin\phi)e^{im\lambda}$ where $P_{\ell}^m(\sin\phi)$ is an associated Legendre polynomial of the first kind normalized to unity.
- c) The wavenumber J denotes rhomboidal truncation.

Diagnostic relationships for U_{ℓ}^m and V_{ℓ}^m as obtained from Equations [N.8] and [N.9] are:

$$U_{\ell}^m = (\ell-1)\epsilon_{\ell}^m \psi_{\ell-1}^m - (\ell+2)\epsilon_{\ell+1}^m \psi_{\ell+1}^m + im\chi_{\ell}^m \quad [\text{N.15}]$$

$$V_{\ell}^m = -(\ell-1)\epsilon_{\ell}^m \chi_{\ell-1}^m + (\ell+2)\epsilon_{\ell+1}^m \chi_{\ell+1}^m + im\psi_{\ell}^m \quad [\text{N.16}]$$

where

$$\epsilon_{\ell}^m = [(\ell^2 - m^2)/(4(\ell)^2 - 1)]^{1/2}$$

The spectral representation of nonlinear products occurring in the prognostic and diagnostic equations requires spectral grid transforms. The nonlinear products are evaluated on a latitude-longitude grid (equally spaced in longitude, Gaussian in latitude) at each model level. These products are then expressed as truncated Fourier series at each latitude circle giving:

$$\nabla^2 \psi_U + \dot{\sigma} \frac{\partial V}{\partial \sigma} + \frac{RT'}{a} \cos \phi \frac{\partial q}{\partial \phi} - \frac{q}{p_*} \frac{\partial \tau_y}{\partial \sigma} = a \sum_{m=-J}^J A_m e^{im\lambda}$$

$$\nabla^2 \psi_V - \dot{\sigma} \frac{\partial U}{\partial \sigma} - \frac{RT'}{a} \frac{\partial q}{\partial \lambda} + \frac{q}{p_*} \frac{\partial \tau_x}{\partial \sigma} = a \sum_{m=-J}^J B_m e^{im\lambda}$$

$$E = a^2 \sum_{m=-J}^J E_m e^{im\lambda}$$

$$UT' = a \sum_{m=-J}^J F_m e^{im\lambda} \quad [N.17]$$

$$VT' = a \sum_{m=-J}^J G_m e^{im\lambda}$$

$$T' \nabla^2 \chi + \dot{\sigma} \gamma + \frac{RT'}{C_p} \left[\int_1^0 \nabla^2 \chi d\sigma + (\overline{W} + \int_1^0 \overline{W} d\sigma) \cdot \nabla q \right] = \sum_{m=-J}^J H_m e^{im\lambda}$$

$$\int_1^0 \overline{W} \cdot \nabla q d\sigma = \sum_{m=-J}^J Z_m e^{im\lambda}$$

The diagnostic evaluation of $\dot{\sigma}$ is required only at gridpoints and is not subsequently expressed spectrally.

With additional representations given by

$$(\)_{\ell}^m = \int_{-\frac{\pi}{2}}^{\frac{\pi}{2}} (\)_m P_{\ell}^m(\sin\phi) \cos\phi \, d\phi \quad [\text{N.18}]$$

where the integral is exactly evaluated by Gaussian quadrature and applied to E_m , H_m and Z_m thereby yielding E_{ℓ}^m , H_{ℓ}^m and Z_{ℓ}^m , the equations for the spectral amplitude tendencies for the stream function, velocity potential, temperature and logarithm of the surface pressure are found to be:

$$\begin{aligned} -l(l+1) \frac{\partial \psi_{\ell}^m}{\partial t} = & - \int_{-\frac{\pi}{2}}^{\frac{\pi}{2}} \frac{1}{\cos^2\phi} [1mA_m P_{\ell}^m(\sin\phi) - B_m \cos\phi \frac{\partial P_{\ell}^m(\sin\phi)}{\partial \phi}] \cos\phi \, d\phi \\ & + 2\Omega[l(l-1)\epsilon_{\ell}^m \chi_{\ell-1}^m + (l+1)(l+2)\epsilon_{\ell+1}^m \chi_{\ell+1}^m - v_{\ell}^m] \quad [\text{N.19}] \end{aligned}$$

$$\begin{aligned} -l(l+1) \frac{\partial \chi_{\ell}^m}{\partial t} = & \int_{-\frac{\pi}{2}}^{\frac{\pi}{2}} \frac{1}{\cos^2\phi} [1mB_m P_{\ell}^m(\sin\phi) + A_m \cos\phi \frac{\partial P_{\ell}^m(\sin\phi)}{\partial \phi}] \cos\phi \, d\phi \\ & - 2\Omega[l(l-1)\epsilon_{\ell}^m \psi_{\ell-1}^m + (l+1)(l+2)\epsilon_{\ell+1}^m \psi_{\ell+1}^m + U_{\ell}^m] \\ & + l(l+1) [E_{\ell}^m + \phi_{\ell}^m + \frac{RT}{a^2} q_{\ell}^m] \quad [\text{N.20}] \end{aligned}$$

$$\begin{aligned} \frac{\partial T_{\ell}^m}{\partial t} = & - \int_{-\frac{\pi}{2}}^{\frac{\pi}{2}} \frac{1}{\cos^2\phi} [1mF_m P_{\ell}^m(\sin\phi) - G_m \cos\phi \frac{\partial P_{\ell}^m(\cos\phi)}{\partial \phi}] \cos\phi \, d\phi \\ & + H_{\ell}^m \quad [\text{N.21}] \end{aligned}$$

$$\frac{\partial q_{\ell}^m}{\partial t} = z_{\ell}^m - \ell(\ell+1) \int_1^0 \chi_{\ell}^m d\sigma \quad [\text{N.22}]$$

The vertical derivatives appearing in the various non-linear terms and the vertical integrals are all evaluated by finite differencing at the half-levels. Full-level values are obtained by averaging half-level values where appropriate. Logarithmic variation of temperature between the lowest two levels is assumed in defining $\frac{\partial T}{\partial \sigma}$ at the lowest full and half-levels.

4.2 Temporal Differencing

A semi-implicit time integration algorithm based on the work of Robert (1969) is used in the model. The basic idea of the semi-implicit technique is to treat the gravity wave modes implicitly (unconditional stability) to give a much longer time step. This results in a time step of 60 minutes.

In order to facilitate description of the semi-implicit algorithm, it is convenient to rewrite the spectral prognostic equations in a simpler form. The prognostic equations for the velocity potential, temperature and logarithm of the surface pressure may be written as:

$$\frac{\partial D_{\ell}^m}{\partial t} = x_{\ell}^m + \ell(\ell+1) (\phi_{\ell}^m + R^* T_0 q_{\ell}^m) \quad [\text{N.23}]$$

$$\frac{\partial T_\ell^m}{\partial t} = Y_\ell^m + \gamma_0 \left[\int_1^0 D_\ell^m d\sigma - \int_1^\sigma D_\ell^m d\sigma \right] + \sigma \frac{\partial T_0}{\partial \sigma} \int_1^0 D_\ell^m d\sigma \quad [\text{N.24}]$$

$$\frac{\partial q_\ell^m}{\partial t} = z_\ell^m + \int_1^0 D_\ell^m d\sigma \quad [\text{N.25}]$$

where $D_\ell^m = -\ell(\ell+1) \chi_\ell^m$, the quantities x_ℓ^m , y_ℓ^m and z_ℓ^m denote the spectral representation of the nonlinear terms and other terms not explicit here, and R' denotes R/a^2 .

By writing the equations in matrix form where the vectors are column vectors over the number of levels, the prognostic equations may be written as:

$$\frac{\partial \underline{\Phi}}{\partial t} = R' \underline{A} \underline{y} + \Delta \sigma R' \underline{A} \underline{G} \underline{D} \quad [\text{N.26}]$$

$$\frac{\partial \underline{D}}{\partial t} = \underline{x} + \ell(\ell+1) [\underline{\Phi} + R' \underline{T}_0 \underline{q}] \quad [\text{N.27}]$$

$$\frac{\partial \underline{q}}{\partial t} = \underline{z} + \Delta \sigma \underline{I} \underline{D} \quad [\text{N.28}]$$

where $\underline{\Phi} = R' \underline{A} \underline{T}$ has been used to obtain the first equation.

Using a centered time difference and the semi-implicit operator of Robert, the finite difference equations may now be written as:

$$\underline{\Phi}^{\tau+1} = \underline{\Phi}^{\tau-1} + 2\Delta t R' \underline{A} \underline{y} + \Delta t \Delta \sigma R' \underline{A} \underline{G} (\underline{D}^{\tau+1} + \underline{D}^{\tau-1}) \quad [\text{N.29}]$$

$$\begin{aligned} \underline{D}^{\tau+1} = \underline{D}^{\tau-1} + 2\Delta t \underline{x} + \Delta t \ell(\ell+1) [(\underline{\phi}^{\tau+1} + \underline{\phi}^{\tau-1}) \\ + R' \underline{T}_0 (q^{\tau+1} + q^{\tau-1})] \end{aligned} \quad [\text{N.30}]$$

$$q^{\tau+1} = q^{\tau-1} + 2\Delta t z + \Delta t \Delta \sigma \underline{I} (\underline{D}^{\tau+1} + \underline{D}^{\tau-1}) \quad [\text{N.31}]$$

These three equations involve three unknowns that may be solved for the variable \underline{D} . Then by using Gauss elimination, the system is solved for \underline{D} and the other variables obtained by back substitution.

A forward time step is performed on the first time step.

4.3 Boundary Conditions

The representation of the variables in terms of spherical harmonics implies periodicity in longitude, and the poles, although not transform grid points, are regular points.

The vertical boundary conditions are $\dot{\sigma} \equiv 0$ at $\sigma = 1$ and 0.

5.0 Processes and Effects

5.1 Dynamics

Terms representing the horizontal and vertical advection and convergence/divergence of heat, vorticity and divergence are included as are terms representing the pressure gradient

and Coriolis forces in the vorticity and divergence equations. Adiabatic temperature changes are also modeled.

Orography that is consistent with reality and the transform grid resolution is included to add realism to the flows.

Horizontal stress is applied at the lowest level to simulate vertical momentum transport at the surface.

5.2 Heat Sources/Sinks

A dry, adiabatic fluid is considered; thus, there are only adiabatic heating terms.

5.3 Moisture Sources/Sinks

There are none since a dry, adiabatic fluid is considered.

6.0 Inputs

The model was originally tested with Phillips analytic initialization and found to have good phase speed characteristics as was expected of the spectral representation. The global integrals of total energy, angular momentum and mass showed good conservation properties.

Test integrations were performed with GARP data sets from the Melbourne WMC as analyzed by the method of Gauntlett, et al. (1972) which gives temperatures and winds at standard

levels and the surface pressure. The analyzed data is then interpolated to the transform lat-long grid and interpolated to the sigma surfaces. Fourier and associated Legendre transforms are then performed to obtain the initial spectral representation of the data fields.

7.0 Outputs

Fields at standard levels and the surface pressure are produced at variable output times.

8.0 Computer Information

The model is coded in FORTRAN (level-H Compiler) for the IBM 360/65 (185K bytes of storage required). The 5-layer, J=15 model requires 13 minutes to perform a 24-hour hemispheric forecast.

9.0 References

Bourke, William, "An Efficient, One-level, Primitive-Equation Spectral Model", Monthly Weather Review, Vol. 100, No. 9, September 1972, pp. 683-689.

Bourke, William, "A Multi-Level Spectral Model I. Formulation and Hemispheric Integrations", Monthly Weather Review, Vol. 102, No. 10, October 1974, pp. 687-701.

Gauntlett, D.J., R.S. Seaman, W.R. Kinninmonth, and J.C. Langford, "An Operational Evaluation of a Numerical Analysis-Prognosis System for the Southern Hemisphere", Australian Meteorological Magazine, 1972, Vol. 20, pp. 61-82.

Puri, Kamal and William Bourke, "Implications of Horizontal Resolution in Spectral Model Integrations", Monthly Weather Review, Vol. 102, No. 5, May 1974, pp. 333-347.

Robert, A.J., "Integration of a Spectral Model of the Atmosphere by the Implicit Method", Proc. WMO/IUGG Symposium on Numerical Weather Prediction, Tokyo, 26 November - 4 December 1968, Japan Meteorological Agency, Tokyo, 1969.

O. Canadian 5-Layer Hemispheric Spectral Operational Model

The model described here became the current operational large-scale forecast model of the Atmospheric Environment Service of Canada on 18 February 1976. The model traces its development to the work of Orszag and Eliassen (c. 1970), Bourke (1974) of the ANMRC and Robert (1972) of Canada and is probably the most complete spectral primitive equation model in existence today.

MODEL DESCRIPTION

1.0 Variables

1.1 Independent

The independent variables are the longitude, λ , the latitude, ϕ , sigma defined as

$$\sigma = \frac{p}{p^*} \quad [0.1]$$

where p^* is the local surface pressure and time, t .

1.2 Dependent

1.2.1 Prognostic

The prognostic variables are the vorticity, ζ , the divergence, D , an energy quantity, $P = \phi + RT_0 q$, the

logarithm of surface pressure, $q = \ln(p^*)$, and the dew point depression, $S = T - T_d$. A secondary prognostic variable is the precipitation.

1.2.2 Diagnostic

The diagnostic variables are the scalar velocities

$$U = \frac{u \cos \phi}{a} \quad \text{and} \quad V = \frac{v \cos \phi}{a} \quad [0.2]$$

the geopotential, Φ , and the vertical velocity, $\dot{\sigma}$.

2.0 Domain

2.1 Horizontal

The horizontal domain is hemispheric with a $J = 20$ wavenumber truncation (rhomboidal) coupled with a transform grid of 26 Gaussian latitudes and 64 equispaced longitudes. The poles are regular points in this representation and variables are placed regularly on the transform grid.

2.2 Vertical

The vertical coordinate is sigma as defined by Equation [0.1]. Figure 0-1 shows the model sigma surfaces and the placement of variables in the vertical.

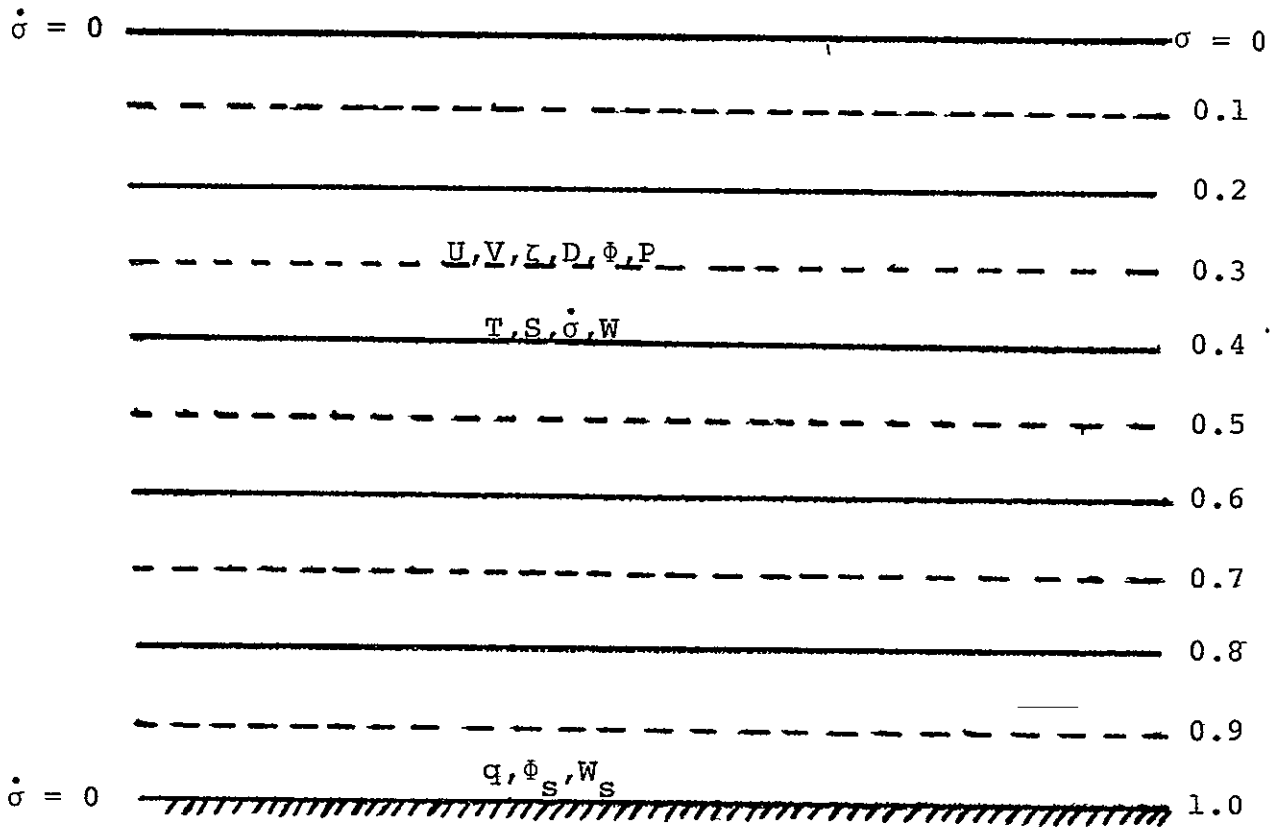


Figure O-1

Vertical Structure of the Canadian
5-Layer Spectral Model (Repeated for all Levels)

2.3 Temporal

Two time levels of data are required (except during the startup step) since a centered semi-implicit time differencing scheme is used with a forty minute time step. There is no staggering of the variables in time.

3.0 Governing Equations

The governing partial differential equations written in spherical polar coordinates in the horizontal and a sigma coordinate in the vertical are listed below.

Vorticity equation:

$$\frac{\partial \zeta}{\partial t} = -\alpha(A, B) \quad [0.3]$$

Divergence equation:

$$\frac{\partial D}{\partial t} + \nabla^2 P = \alpha(B, -A) - a^2 \nabla^2 E \quad [0.4]$$

Energy equation:

$$\sigma \frac{\partial^2 P}{\partial t \partial \sigma} + R Y_0 W = R \alpha(UT', VT') - RB_T \quad [0.5]$$

Pressure tendency equation:

$$\frac{\partial q}{\partial t} - W_S = 0 \quad [0.6]$$

Moisture equation:

$$\frac{\partial S}{\partial t} = -\alpha(US, VS) + B_S \quad [0.7]$$

Hydrostatic relation:

$$\sigma \frac{\partial \Phi}{\partial \sigma} = -RT \quad [0.8]$$

where

$$\alpha(A, B) = \frac{1}{\cos^2 \phi} \left[\frac{\partial A}{\partial \lambda} + \cos \phi \frac{\partial B}{\partial \phi} \right] \quad [0.9]$$

$$A = (\zeta + f)U + \dot{\sigma} \frac{\partial V}{\partial \sigma} + \frac{RT'}{a^2} \cos \phi \frac{\partial q}{\partial \phi} - \cos \phi \frac{F\phi}{a} \quad [0.10]$$

$$B = (\zeta + f)V - \dot{\sigma} \frac{\partial U}{\partial \sigma} - \frac{RT'}{a^2} \frac{\partial q}{\partial \lambda} + \cos \phi \frac{F\lambda}{a} \quad [0.11]$$

$$G = \frac{1}{\cos^2 \phi} \left[U \frac{\partial q}{\partial \lambda} + V \cos \phi \frac{\partial q}{\partial \phi} \right] \quad [0.12]$$

$$E = \frac{U^2 + V^2}{2 \cos^2 \phi} \quad [0.13]$$

$$\dot{\sigma} = (1 - \sigma)W_S + \int_{\sigma}^1 (G + D) d\sigma \quad [0.14]$$

$$B_T = T'D + \gamma' \dot{\sigma} + \frac{RT'}{C_p} W_S + \frac{RT'}{C_p} G + H_T \quad [0.15]$$

$$B_S = SD - \dot{\sigma} \frac{\partial S}{\partial \sigma} + \left[\frac{RT}{C_p} - \frac{RT^2}{\epsilon L (T_d)} \right] \left[\frac{\dot{\sigma}}{\sigma} + G + W_S \right] + H_T - H_M \quad [0.16]$$

$$W = \dot{\sigma} - \sigma \int_0^1 (G + D) d\sigma \quad [0.17]$$

$$W_S = - \int_0^1 (G + D) d\sigma \quad [0.18]$$

and the subscripted zero denotes a horizontal mean value and the superscripted prime the deviation from that mean.

In the above equations,

f = Coriolis parameter

U = $\frac{u \cos \phi}{a}$ = scalar zonal wind component

V = $\frac{v \cos \phi}{a}$ = scalar meridional wind component

ζ = vertical component of vorticity = $\overline{\mathbf{k} \cdot \nabla \times \mathbf{V}}$

D = horizontal divergence = $\nabla \cdot \overline{\mathbf{V}}$

T = $T_0 + T'$ = absolute temperature

q = $\ln(p^*)$ = logarithmic pressure

γ = $\gamma_0 + \gamma' = \frac{RT}{C_p \sigma} - \frac{\partial T}{\partial \sigma}$ = static stability

$\dot{\sigma}$ = vertical motion in sigma coordinates

ϕ = gz = geopotential

F_λ, F_ϕ = horizontal components of frictional force per unit mass

H_T = diabatic heating

R = gas constant for dry air
 C_p = the specific heat of dry air at constant pressure
 T_d = dewpoint temperature *
 S = $T - T_d$ is the dewpoint depression
 ϵ = ratio of the molecular weight of water vapor to effective molecular weight of dry air (0.622)
 $L(T_d)$ = latent heat of vaporization of water and ice
 H_M = moisture sources or sinks

4.0 Numerics

A spectral representation in the horizontal coupled with finite differencing in the vertical and semi-implicit time differencing is used to approximate the solution of the model equations.

4.1 Spatial Representation

The essence of the transform procedures proposed by Orszag and Eliassen is to evaluate the nonlinear terms of the equations as simple products following a transform from the spectral to gridpoint domain; a subsequent inverse transform yields the spectral form of the requisite nonlinear term. The procedure may be more generally described as combining nonlocal (spectral) differentiations with local (gridpoint) multiplications for evaluation of the nonlinear terms.

The spectral form of the governing equations is developed in a manner analogous to that of Machenhauer and Daley (1972) and, more specifically, Bourke (1974). The vorticity, ζ , for example, is expanded in the following truncated series of spherical harmonics:

$$\zeta = \sum_{m=-J}^J \sum_{\ell=|m|}^{|m|+J} \zeta_{\ell}^m Y_{\ell}^m \quad [0.19]$$

where

a) the terms ζ_{ℓ}^m denote time dependent, generally complex, expansion coefficients, and the reality of the fields requires $(\zeta_{\ell}^m)^* = (-1)^m \zeta_{\ell}^{-m}$

b) the spherical harmonics are given by $Y_{\ell}^m = P_{\ell}^m(\sin\phi) e^{im\lambda}$ where $P_{\ell}^m(\sin\phi)$ is an associated Legendre polynomial of the first kind normalized to unity

c) the wavenumber J denotes rhomboidal truncation. D , T , P , ϕ , S and W are expanded in the same manner as Equation [0.19]. The variable q is similarly expanded except that the q_{ℓ}^m are functions of time only.

In the expansions for U and V there is one extra component for each m , in order to be consistent with the expansions for ζ and D (Eliassen et al. 1970).

$$U = \sum_{m=-J}^J \sum_{\ell=|m|}^{|m|+J+1} U_{\ell}^m Y_{\ell}^m \quad V = \sum_{m=-J}^J \sum_{\ell=|m|}^{|m|+J+1} V_{\ell}^m Y_{\ell}^m \quad [0.20]$$

Diagnostic relations between U , V and D , ζ can be obtained through Helmholtz's theorem which states that an arbitrary wind field can be represented as the sum of the gradient of a potential function and the curl of a stream function; thus

$$\ell(\ell+1)U_{\ell}^m = -(\ell+1)\varepsilon_{\ell}^m \zeta_{\ell-1}^m + \ell\varepsilon_{\ell+1}^m \zeta_{\ell+1}^m - 1mD_{\ell}^m \quad [0.21]$$

and

$$\ell(\ell+1)V_{\ell}^m = (\ell+1)\varepsilon_{\ell}^m D_{\ell-1}^m - \ell\varepsilon_{\ell+1}^m D_{\ell+1}^m - 1m\zeta_{\ell}^m \quad [0.22]$$

where

$$\varepsilon_{\ell}^m = [(\ell^2 - m^2)/(4\ell^2 - 1)]^{1/2} \quad [0.23]$$

$U_0^0 = \varepsilon_1^0 \zeta_1^0$ and $V_0^0 = -\varepsilon_1^0 D_1^0$ are special cases.

Other diagnostic relations can be obtained from the hydrostatic equation; thus

$$T_{\ell}^m = -\frac{\sigma}{R} \frac{\partial P_{\ell}^m}{\partial \sigma} + \sigma \frac{\partial T}{\partial \sigma} \alpha_{\ell}^m \quad [0.24]$$

and

$$T_{\ell}^m = \frac{-\sigma}{R} \frac{\partial \Phi_{\ell}^m}{\partial \sigma} \quad [0.25]$$

The prognostic variables are ζ_ℓ^m , D_ℓ^m , P_ℓ^m , S_ℓ^m and q_ℓ^m . The variables T_ℓ^m , Φ_ℓ^m , U_ℓ^m and V_ℓ^m are all related to the prognostic variables by the diagnostic relations.

Introducing the operator

$$\{F\}_\ell^m = \frac{1}{2\pi} \int_{-\frac{\pi}{2}}^{\frac{\pi}{2}} \int_0^{2\pi} F(\lambda, \phi, \sigma, t) Y_\ell^{*m}(\lambda, \phi) \cos\phi d\lambda d\phi \quad [0.26]$$

the spectral form of the governing equations become

$$\frac{\partial \zeta_\ell^m}{\partial t} = -\{\alpha(A, B)\}_\ell^m \quad [0.27]$$

$$\frac{\partial D_\ell^m}{\partial t} - \frac{\ell(\ell+1)}{a^2} P_\ell^m = \{\alpha(B, -A) - a^2 \nabla^2 E\}_\ell^m \quad [0.28]$$

$$\sigma \frac{\partial^2 P_\ell^m}{\partial \sigma \partial t} + R Y_0 W_\ell^m = R\{\alpha(UT', VT') - B_T\}_\ell^m \quad [0.29]$$

$$\frac{\partial W_\ell^m}{\partial \sigma} + D_\ell^m = \{B_W\}_\ell^m \quad [0.30]$$

$$\frac{\partial q_\ell^m}{\partial t} - W_S^m = 0 \quad [0.31]$$

$$\frac{\partial S_\ell^m}{\partial t} = \{-\alpha(US, VS) + B_S\}_\ell^m \quad [0.32]$$

All variables required in the calculation of the right-hand sides of Equations [0.27-0.32] are first

synthesized onto the physical space transform grid. The nonlinear expressions are then evaluated and the integrals on the right-hand side are then simply calculated by exact numerical quadrature.

The transform grid consists of equally spaced longitudes and almost equally spaced Gaussian latitudes. In the synthesis from spectral to grid, an associated Legendre transform is first performed at each Gaussian latitude circle to produce Fourier coefficients. A discrete Fourier transform is then performed to produce functional values at each longitude of the transform grid. After the nonlinear calculations are carried out on the grid, the integrals on the right-hand sides of the equations are calculated by first performing a discrete inverse Fourier transform at each Gaussian latitude. The final step is the inverse associated Legendre transform performed by Gaussian quadrature.

The vertical finite-difference scheme is a somewhat more general form of the scheme used by Robert et al. (1972). The basic feature of the scheme is that the temperatures are carried at levels intermediate to the levels of the geopotentials. The vertical finite differencing involved in the right-hand sides of Equations [0.27-0.32] is conventional except that logarithmic differencing has generally been used, particularly with respect to the thermodynamic variables.

4.2 Temporal Differencing

A semi-implicit time integration algorithm following Robert et al. (1972) is used in the forecast model. The basic idea of the semi-implicit technique is to treat the gravity wave modes implicitly (unconditional stability) and the meteorological modes explicitly (conditional stability) to give a much longer time step. This results in a time step of forty minutes.

The time derivative is approximated by a centered difference (except at the initial time where a forward difference is used). The remaining terms on the left-hand sides of Equations [0.27-0.32] are handled implicitly by the application of the time averaging operator defined by

$$\bar{F}^t = 1/2 [F(t + \Delta t) + F(t - \Delta t)] \quad [0.33]$$

while the right-hand sides are calculated explicitly.

Two equations remain fully explicit. They are the vorticity and moisture equations:

$$\zeta_{\ell}^m(t+\Delta t) = -2\Delta t\{\alpha(A,B)\}_{\ell}^m + \zeta_{\ell}^m(t-\Delta t) \quad [0.34]$$

and

$$S_{\ell}^m(t+\Delta t) = 2\Delta t\{-\alpha(US,VS) + B_S\}_{\ell}^m + S_{\ell}^m(t-\Delta t) \quad [0.35]$$

The remaining equations are handled in a semi-implicit manner giving:

$$\begin{aligned} \overline{D}_\ell^m{}^t - \frac{\Delta t \ell(\ell+1)}{a^2} \overline{P}_\ell^m{}^t &= \Delta t \{ \alpha(B, -A) - a^2 \nabla^2 E \}_\ell^m \\ &+ D_\ell^m(t-\Delta t) \end{aligned} \quad [0.36]$$

$$\begin{aligned} \sigma \frac{\partial \overline{P}_\ell^m{}^t}{\partial \sigma} + \Delta t R \gamma_0 \overline{W}_\ell^m{}^t &= \Delta t R \{ \alpha(UT', VT') - B_T \}_\ell^m \\ &+ \sigma \frac{\partial P_\ell^m}{\partial \sigma}(t-\Delta t) \end{aligned} \quad [0.37]$$

$$\overline{q}_\ell^m{}^t - \Delta t \overline{W}_s^m{}^t = q_\ell^m(t-\Delta t) \quad [0.38]$$

and

$$\frac{\partial \overline{W}_\ell^m{}^t}{\partial \sigma} + \overline{D}_\ell^m{}^t = \{B_w\}_\ell^m \quad [0.39]$$

The integrals on the right-hand side are all evaluated at time t . Some of the terms in the integrals are forcing terms and should really be calculated at time $t-\Delta t$ to avoid the growth of a computational mode. This would require considerable additional computation, so the forcing terms are all calculated at time t and the

computational mode is suppressed with a very weak time filter (Asselin, 1972).

The implicit system of equations [0.36-0.39] is solved by eliminating \overline{D}_ℓ^m ; then \overline{W}_ℓ^m is eliminated from the resulting equations giving a diagnostic relation for \overline{P}_ℓ^m . This equation can then be solved for \overline{P}_ℓ^m and the remaining variables obtained by back substitution.

4.3 Boundary Conditions

The representation of the variables in terms of spherical harmonics implies periodicity in longitude, and the poles, although not transform grid points, are regular points.

The vertical boundary conditions are $\dot{\sigma} \equiv 0$ at $\sigma = 1$ and 0.

5.0 Processes and Effects

5.1 Dynamics

Terms representing the horizontal and vertical advection and convergence/divergence of heat, moisture, vorticity and divergence are included as are terms representing the pressure gradient and Coriolis forces in the vorticity and divergence equations. Adiabatic temperature changes are also modeled.

Orography that is consistent with reality and the transform grid resolution is included to add realism to the flows.

The skin friction F_λ and F_ϕ are calculated at the lowest level only using Cressman's drag formulation.

5.2 Heat Sources/Sinks

Sensible heating in the PBL is evaluated at the lowest model level over the open ocean. The term H_T depends on the windspeed and the difference between the extrapolated surface temperature obtained from the lowest sigma levels and the sea surface temperature. The sea surface temperature is spatially varying, but held constant during the forecast.

Release of latent heat due to large-scale precipitation is included.

A moist convective adjustment process based on the method of Manabe et al. modifies unstable vertical profiles of temperature and moisture conserving moist static energy. A dry convective adjustment procedure is included to preclude hydrostatic instability.

5.3 Moisture Sources/Sinks

The large scale precipitation process removes super-saturated states from the model atmosphere.

A moist convective adjustment process based on the method of Manabe et al. modifies unstable vertical profiles of temperature and moisture conserving moist static energy. This process may result in convective precipitation.

Evaporation in the PBL is evaluated at the lowest model level over the open ocean. The term H_M depends on the windspeed and the difference between the lowest layer mixing ratio and the saturated mixing ratio of air in contact with the sea.

6.0 Inputs

The forecast model is initialized from an objective analysis (Rutherford, 1976) which provides winds, heights, temperatures and dewpoint depressions at standard pressure levels and surface pressure on a 2805 point polar stereographic grid (381 km grid length at 60°N). This data is then interpolated with bi-cubic splines to the Gaussian transform grid. Some extrapolation is necessary in the tropics, and the symmetry conditions are used to determine the Southern Hemisphere.

The surface topography is then used to vertically interpolate the data to the model sigma surfaces. Finally, the spectral coefficients of the model variables are obtained by spectral analysis of the sigma surface data.

7.0 Outputs

The sea level pressure, precipitation and heights and temperatures at standard pressure levels are produced on a normal output cycle.

8.0 Computer Information

The forecast model is programmed mostly in CDC Fortran Extended (a dialect of FTN IV) for the CDC 7600. Approximately 25k words of SCM and 100k words of LCM are required for the SP20 hemispheric model. The running time is approximately five minutes for a 36 hour forecast.

9.0 References

-
- Asselin, R., "Frequency Filter for Time Integrations," Monthly Weather Review, Vol. 100, No. 6, June 1972, pp. 487-490.
- Bourke, W., "A Multi-Level Spectral Model. I - Formulation and Hemispheric Integrations," Monthly Weather Review, Vol. 102, No. 10, October 1974, pp. 687-701.
- Daley, R., C. Girard, J. Henderson and I. Simmonds, "Short-Term Forecasting with a Multi-Level Spectral Primitive Equation Model," Atmosphere, Vol. 14, No. 2, 1976, pp. 98-134.
- Eliassen, E.B., B. Machenhauer and E. Rasmussen, "On a Numerical Method for Integration of the Hydrodynamical Equations with a Spectral Representation of the Horizontal Fields," Institute of Theoretical Meteorology, University of Copenhagen, Report No. 2, 1970.

Robert, A., J. Henderson and C. Turnbull, "An Implicit Time Integration Scheme for Baroclinic Models of the Atmosphere," Monthly Weather Review, Vol. 100, No. 5, May 1972, pp. 329-335.

Rutherford, I.D., "An Operational Three-Dimensional Multivariate Statistical Objective Analysis Scheme," JOC Study Group Conference on Four-Dimensional Data Assimilation - Paris, 17-21 November 1975, Report No. 11, the GARP Programme on Numerical Experimentation, 1976, pp. 98-121.

P. Deutscher Wetterdienst 6-Layer Hemispheric Operational Model

The Deutscher Wetterdienst atmospheric prediction model is currently executed twice daily to produce four day forecasts for the Northern Hemisphere. Although the operational model described here is a dry model, a research version of the model also exists which contains moisture. The following description represents a snapshot of the state of the operational model as of mid-1976.

MODEL DESCRIPTION

1.0 Variables

1.1 Independent

The independent variables are x and y derived from a polar stereographic map projection in the horizontal, pressure in the vertical, p , and time, t .

1.2 Dependent

1.2.1 Prognostic

The prognostic variables are the x wind component, u ; the y wind component, v ; and, the potential temperature, θ .

Secondary prognostic variables are the geopotential of the 1000 mb surface, Φ_{1000} ; and the surface temperature over land or ice, T_s .

1.2.2 Diagnostic

The diagnostic variables are the geopotential, Φ , and the vertical velocity in pressure coordinates, ω .

2.0 Domain

2.1 Horizontal

The horizontal domain is a polar stereographic projection (true at 60°N) of the Northern Hemisphere north of 12°N (standard octagon) using x - y coordinates with map factor

$$m = \frac{1 + \sin 60^\circ}{1 + \sin \phi} \quad [P.1]$$

The grid resolution is 381 km at 60°N and the grid is shown in Figure P-1.

The variables are staggered in space and time according to the scheme of Eliassen (1956) which is shown in Figure P-2.

ORIGINAL PAGE IS
OF POOR QUALITY

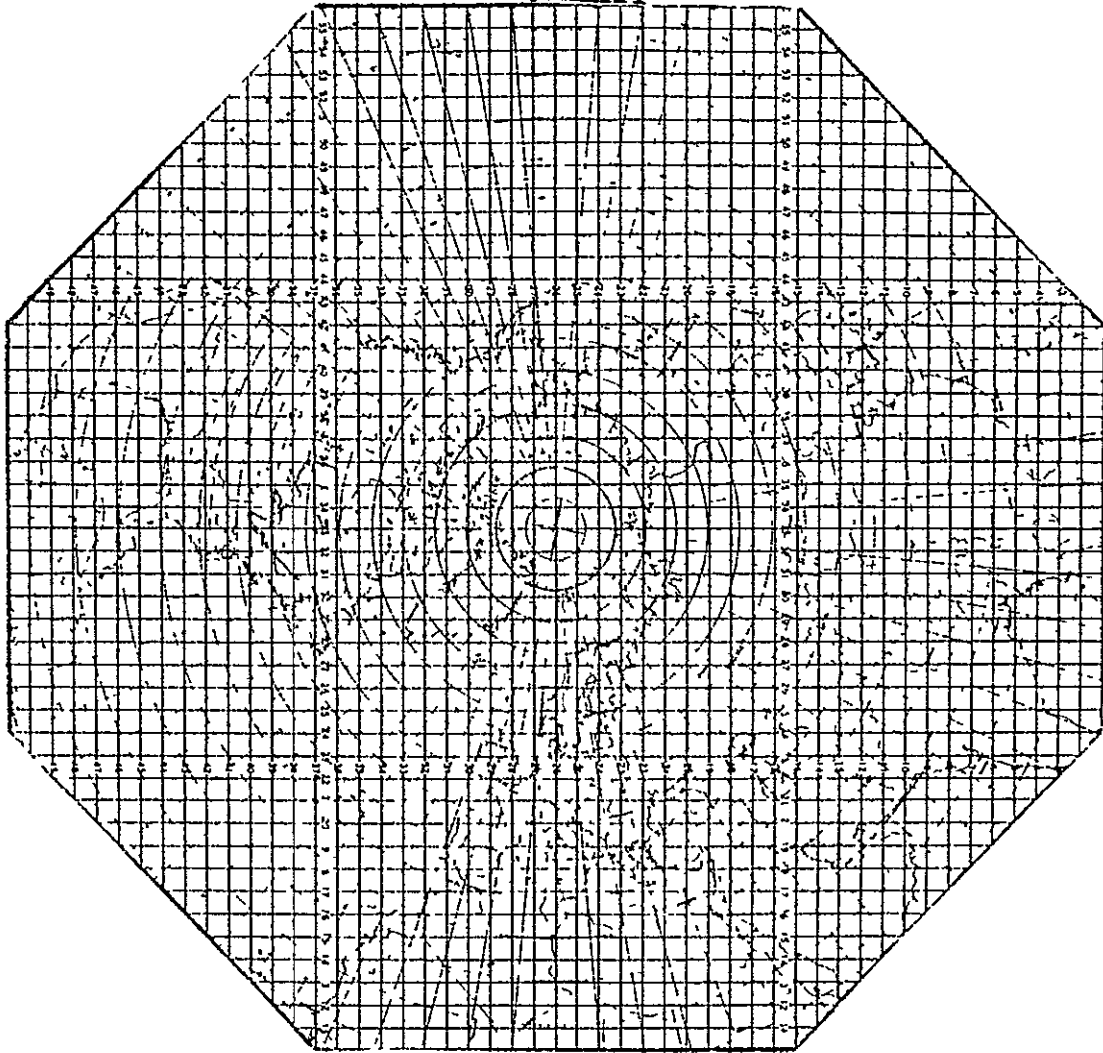
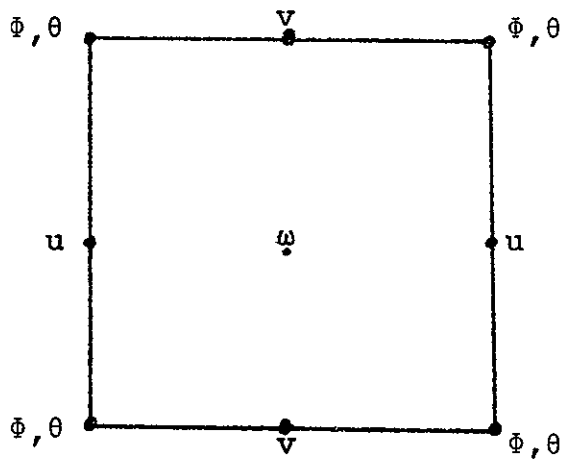
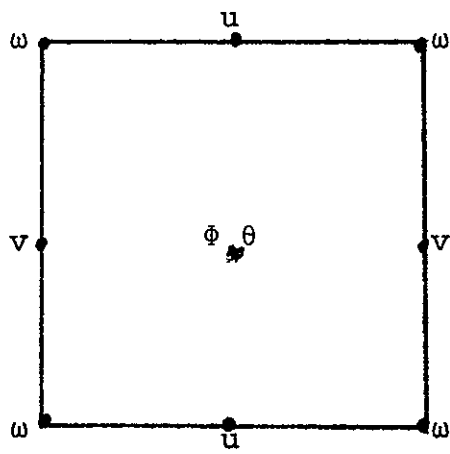


Figure P-1

Northern Hemisphere Polar Stereographic Grid
(standard Octagon)



even timestep



odd timestep

Figure P-2

Horizontal Staggering of Variables in Space and Time
for the Deutscher Wetterdienst Model
(Eliassen Grid)

2.2 Vertical

The vertical coordinate is pressure. Figure P-3 shows the vertical structure of the model and the placement of variables in the vertical.

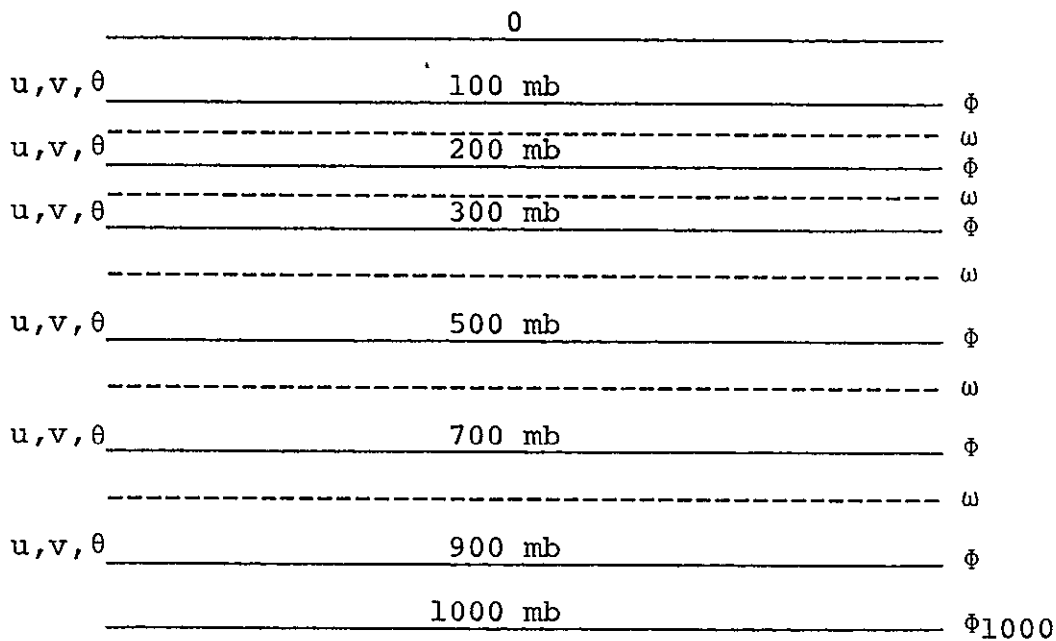


Figure P-3

Vertical Structure of the Deutscher Wetterdienst Prediction Model

2.3 Temporal

Two time levels of data are required since a centered time differencing scheme is used with a five minute time step. The variables are staggered in space and time according to the scheme of Eliassen (1956) as shown in Figure P-2.

3.0 Governing Equations

The governing partial differential equations, written in Cartesian coordinates in the horizontal and a pressure coordinate in the vertical, are listed below.

Wind component in the x direction:

$$\frac{\partial u}{\partial t} = -u \frac{\partial u}{\partial x} - v \frac{\partial u}{\partial y} - \omega \frac{\partial u}{\partial p} + fv - \frac{\partial \Phi}{\partial x} + D_u + F_x \quad [\text{P.2}]$$

Wind component in the y direction:

$$\frac{\partial v}{\partial t} = -u \frac{\partial v}{\partial x} - v \frac{\partial v}{\partial y} - \omega \frac{\partial v}{\partial p} - fu - \frac{\partial \Phi}{\partial y} + D_v + F_y \quad [\text{P.3}]$$

Thermodynamic energy equation:

$$\frac{\partial \theta}{\partial t} = -u \frac{\partial \theta}{\partial x} - v \frac{\partial \theta}{\partial y} - \omega \frac{\partial \theta}{\partial p} + D_T + H \quad [\text{P.4}]$$

Continuity equation:

$$\nabla \cdot \bar{V} + \frac{\partial \omega}{\partial p} = 0 \quad [\text{P.5}]$$

Hydrostatic equation:

$$\frac{\partial \Phi}{\partial p} = -\frac{1}{\rho} \quad [\text{P.6}]$$

Equation of state:

$$p = \rho RT \quad [\text{P.7}]$$

In the above equations,

u = x-component of wind velocity
 v = y-component of wind velocity
 \bar{V} = horizontal velocity vector
 ω = vertical (p) velocity
 θ = potential temperature
 ϕ = gz = geopotential
 f = Coriolis parameter
 D_u, D_v, D_T = horizontal diffusion terms
 F_x, F_y = stress components
 H = sensible heating term
 ρ = density
 R = gas constant for air

4.0 Numerics

Finite difference methods are used to approximate the solution of the forecast model primitive equations.

4.1 Spacial Differencing

Centered, second-order finite difference methods are used to approximate the horizontal and vertical derivatives. Since the staggered grid system of Eliassen is used, averaged values of the variables are required in the finite difference approximations. As an example of this procedure,

the finite difference form of the thermodynamic energy equation is given by

$$\frac{\partial \theta}{\partial t} = - \frac{\overline{xy}}{m^2} \left[\overline{U^x} \frac{\partial \theta}{\partial x} + \overline{V^y} \frac{\partial \theta}{\partial y} + \overline{\Omega \theta_{xp}^p} \right] + \frac{\overline{xy}}{m^2} A_h \nabla^2 \theta \quad [P.8]$$

where $U = \frac{u}{m^2}$, $V = \frac{v}{m^2}$, $\Omega = \frac{\omega}{m^2}$ and the bar notation

denotes averaging in the direction specified.

The lateral diffusion terms in the x and y component wind equations and thermodynamic energy equations take the form of

$$D\psi = A\nabla^2\psi \quad [P.9]$$

where both the n-1 and n time levels are used in the computation of the Laplacian.

4.2 Temporal Differencing

Centered, second-order time differencing is used to approximate the time derivatives with a time step of five minutes. The computation is started with a forward time step.

4.3 Boundary Conditions

The horizontal boundary conditions are that there is no flow normal to the boundary and no heat flux across the boundary.

The vertical boundary conditions are $\omega = 0$ at $p = 0$ at the model top, and $w_s = \bar{V}_s \cdot \nabla Z_s$ at the model surface.

5.0 Processes and Effects

5.1 Dynamics

Terms representing the three-dimensional advection of momentum and heat are included as are terms representing the pressure gradient and Coriolis forces in the equations of motion.

Orography that is consistent with reality and the grid resolution is included to add realism to the forecasts.

Friction based on the vertical derivative of the stress is applied at the lowest two model levels. The stress at the 1000 mb level is given by a drag coefficient formulation and at the 800 mb level by the wind shear.

5.2 Heat Sources/Sinks

Sensible heat exchange between the surface (ocean as well as continents) and the lowest model level is included. The ocean temperature is spatially varying, but held constant during a forecast.

5.3 Moisture Sources/Sinks

There are none since this is a dry model.

6.0 Inputs

The forecast model initial data is obtained from hemispheric analyses of the mass structure at the 850, 700, 500, 300, 200 and 100 mb levels using the iterative correction method. In addition, analyses are made of the surface pressure (smoothed in the tropics), the temperature at the two meter level and the ocean temperature.

Winds are obtained from the solution of the balance equation on the model pressure surfaces.

7.0 Outputs

A normal output cycle produces the surface pressure; ω on the 150, 250, 400, 600 and 800 mb surfaces; and the winds, geopotentials and temperatures on the 100, 200, 300, 500, 700 and 850 mb surfaces. An output cycle is made at the initial time plus 18, 24, 30 and 48 hours.

8.0 Computer Information

The forecast model is run on a Control Data Corporation 3800 Computer System. The model is normally executed twice daily and requires about two and one-half hours to produce a forty-eight hour forecast.

The model is written mainly in Fortran with some routines in assembly language and requires approximately 32K of central memory and 400K of mass storage.

9.0 References

Edelmann, W., Deutscher Wetterdienst, 1976 (personal communication).

Eliassen, A., "A Procedure for Numerical Integration of the Primitive Equations of the Two-Parameter Model of the Atmosphere," Science Report No. 4, Department of Meteorology, UCLA, 1956.

Q. Japan Meteorological Agency 6-Layer Limited Area Operational Model

The Japan Meteorological Agency operational fine-mesh limited area model (FLM) is executed twice daily to produce 24-hour prognostic charts for Japan and the surrounding area. As with all operational models, changes are continually being made to improve the quality of the forecasts produced and to better utilize the available computer resources; thus, this description is a snapshot of the forecast model as defined by the available reference documentation (1974).

MODEL DESCRIPTION

1.0 Variables

1.1 Independent

The independent variables are x and y derived from a polar stereographic map projection in the horizontal; pressure, p , in the vertical; and time, t .

1.2 Dependent

1.2.1 Prognostic

The prognostic variables are the surface pressure, p_s , the temperature, T , the specific humidity, q , the x wind component, u , and the y wind component, v . A secondary prognostic variable is the precipitation, P_r , obtained from both

the large-scale precipitation algorithm and the moist convective adjustment (cumulus parameterization).

1.2.2 Diagnostic

The diagnostic variables are the geopotential, ϕ , and the pressure coordinate vertical velocity, ω .

2.0 Domain

2.1 Horizontal

The horizontal domain is a polar stereographic projection of an area approximately 5600 by 5000 km centering on the Japan Islands using x-y coordinates with map factor:

$$m = \frac{1 + \sin 60^\circ}{1 + \sin \phi} \quad [Q.1]$$

The horizontal grid resolution is 152.4 km at 60°N. Figure Q-1 shows the fine-mesh limited area (FLM) grid nested in the coarse mesh grid from which boundary conditions for the FLM are obtained. There is no staggering of variables in the horizontal.

2.2 Vertical

The vertical coordinate is pressure. Figure Q-2 shows the model computational levels and the placement of the variables in the vertical.

FINAL PAGE IS
POOR QUALITY

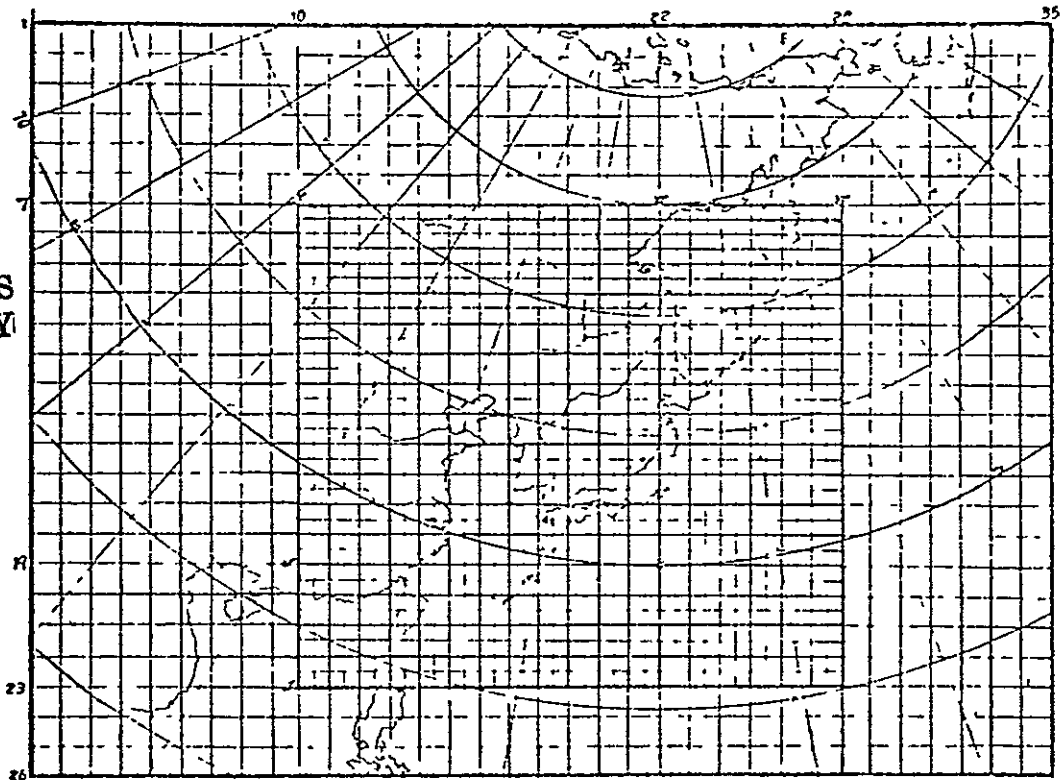


Figure Q-1

Japan Meteorological Agency Fine Mesh Limited
Area Grid Nested in the Coarse Mesh Grid

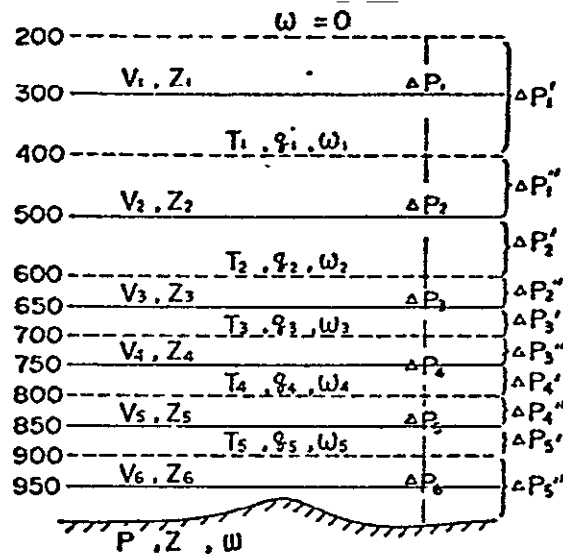


Figure Q-2

Vertical Structure of the Japan Meteorological
Agency Forecast Model

2.3 Temporal

One time level of data is required since the Euler-backward scheme is used. There is no staggering of variables in time.

3.0 Governing Equations

The governing partial differential equations, written for an x-y map projection with map factor m , are listed below.

Equation of motion in the x-direction:

$$\begin{aligned} \frac{\partial u}{\partial t} = & -m^2 \left[\frac{\partial}{\partial x} \left(\frac{uu}{m} \right) + \frac{\partial}{\partial y} \left(\frac{uv}{m} \right) \right] - \frac{\partial (u\omega)}{\partial p} - m \frac{\partial \phi}{\partial x} \\ & + fv + m^2 v \left[v \frac{\partial m}{\partial x} - v \frac{\partial m}{\partial y} \right] + F_x + D \end{aligned} \quad [Q.2]$$

Equation of motion in the y-direction:

$$\begin{aligned} \frac{\partial v}{\partial t} = & -m^2 \left[\frac{\partial}{\partial x} \left(\frac{uv}{m} \right) + \frac{\partial}{\partial y} \left(\frac{vv}{m} \right) \right] - \frac{\partial (v\omega)}{\partial p} - m \frac{\partial \phi}{\partial y} \\ & + fu - m^2 u \left[v \frac{\partial m}{\partial x} - v \frac{\partial m}{\partial y} \right] + F_y + D \end{aligned} \quad [Q.3]$$

Thermodynamic energy equation:

$$\begin{aligned} \frac{\partial T}{\partial t} = & -m^2 \left[\frac{\partial}{\partial x} \left(\frac{uT}{m} \right) + \frac{\partial}{\partial y} \left(\frac{vT}{m} \right) \right] - \frac{\partial (T\omega)}{\partial p} \\ & + \frac{\omega}{C_p} \frac{\partial \phi}{\partial p} - \frac{Q}{C_p} \end{aligned} \quad [Q.4]$$

Moisture equation:

$$\frac{\partial q}{\partial t} = - m^2 \left[\frac{\partial}{\partial x} \left(\frac{uq}{m} \right) + \frac{\partial}{\partial y} \left(\frac{vq}{m} \right) \right] - \frac{\partial (q\omega)}{\partial p} + M \quad [Q.5]$$

Surface pressure tendency equation:

$$\frac{\partial p_s}{\partial t} = - m \left[u \frac{\partial p_s}{\partial x} + v \frac{\partial p_s}{\partial y} \right] + \omega_s \quad [Q.6]$$

Continuity equation:

$$\frac{\partial \omega}{\partial p} = - m^2 \left[\frac{\partial}{\partial x} \left(\frac{u}{m} \right) + \frac{\partial}{\partial y} \left(\frac{v}{m} \right) \right] \quad [Q.7]$$

Hydrostatic equation:

$$\frac{\partial \phi}{\partial p} = - \frac{RT}{p} \quad [Q.8]$$

Equation of state:

$$p = \rho RT \quad [Q.9]$$

In the above equations,

u = x-direction wind component

v = y-direction wind component

T = temperature

q = specific humidity

ω = vertical velocity in p coordinates

f = Coriolis parameter

F_x, F_y = stress components
 D = diffusion term
 Q = diabatic heating/cooling term
 Φ = gz = geopotential
 ρ = density of air
 p_s = surface pressure
 R = gas constant for dry air
 C_p = specific heat of dry air at constant pressure

4.0 Numerics

Finite difference methods are used to approximate the solution of the forecast model equations.

4.1 Spacial Differencing

Centered, quasi-energy conserving, second-order finite difference operators are used to approximate the horizontal derivatives. Vertical derivatives are approximated by centered, second-order differences.

A horizontal smoothing operator is applied to the temperature, geopotential, specific humidity and surface pressure fields to control the computational noise. For the physical quantity A , the operator takes the form:

$$\frac{\partial A}{\partial t} + \dots = KV^4 A \quad [Q.10]$$

Where K is the smoothing coefficient (10^5xd^2). K is increased by a factor of eight and four, respectively, on the outermost and next to outermost line from the grid boundary.

The dissipation term in the equation of motion is given by:

$$D = k_1 \cdot \bar{k}_x \nabla \zeta + k_2 \nabla \mathcal{D} \quad [Q.11]$$

Where ζ and \mathcal{D} are the relative vorticity and horizontal divergence, respectively. The diffusion coefficients have the values $k_1 = 10^5$ and $k_2 = 10^6$ and are increased near the boundary in the same manner as the smoothing operator diffusion coefficient.

4.2 Temporal Differencing

Euler-backward time differencing is used to integrate the forecast model equations. This differencing technique gives additional control of the computational noise since it is dissipative.

The diabatic heating terms are evaluated every third time step to reduce the amount of computation.

The area mean surface pressure is kept constant throughout the forecast integration by adjusting the individual surface pressures.

4.3 Boundary Conditions

The horizontal boundary conditions for the FLM are obtained from the coarse-mesh model (QGM). A twenty-four hour integration is performed with the QGM and the coarse-mesh values are saved every hour for use in the FLM integration. The FLM boundary values are updated hourly and are obtained from the space interpolated QGM values through the following procedure:

a) ϕ , q , p_s and the tangential component of the wind with respect to the FLM grid boundary are replaced by the QGM values.

b) T is replaced as in a) at an inflow boundary point and is extrapolated from the FLM grid at an outflow boundary point.

c) The normal component of the wind with respect to the FLM grid is determined through an application of the continuity equation (Equation Q.7).

In addition, values of ϕ , p_s and T in the FLM next to the boundary are replaced by the QGM values hourly.

The vertical boundary conditions are $\omega \equiv 0$ at $p = 0$ and $\omega = \omega_s$ at the surface.

5.0 Processes and Effects

5.1 Dynamics

Terms representing the three-dimensional flux divergence of heat, moisture and momentum are included, as are terms representing the pressure gradient and Coriolis forces in the equation of motion. Adiabatic temperature changes are also modeled.

Orographic effects are also included to add realism to the forecast features.

Friction evaluated according to the vertical derivative of the stress is included at the lowest level. The stress at the surface depends on a drag coefficient and the surface wind.

5.2 Heat Sources/Sinks

Sensible heating is evaluated for the lowest model level over both ocean and land areas. Over the sea surface, the sensible heat flux is evaluated by the bulk method and the coefficient of sensible heat flux is treated as a function of the static stability and wind speed. A Bowen ratio (which depends on the temperature and relative humidity of the lowest layer) relationship is used over land areas.

A moist convective adjustment scheme is applied at grid points where the relative humidity is greater than 70% in order to estimate the heating due to the release of latent heat and the convective transport of heat. A dry convective adjustment procedure is applied at the remaining grid points to maintain hydrostatic stability.

5.3 Moisture Sources/Sinks

Evaporation from the surface (ocean and land) into the lowest model layer is treated in a manner similar to the sensible heat calculation described in Section 5.2.

A moist convective adjustment scheme is applied at points where the relative humidity is greater than 70% in order to estimate the precipitation and the convective transport of water vapor.

6.0 Inputs

The forecast model initial data is obtained from analyses of the mass structure, the moisture, the surface pressure and the sea surface temperature.

Initial winds are obtained by combining the non-divergent component obtained from the stream function through the balance equation using the geopotential, and the irrotational component obtained from the velocity potential

as calculated from the quasi-geostrophic vertical p-velocity satisfying the continuity equation.

7.0 Outputs

The twenty-four hour prognostic charts produced from the FLM forecast include:

- a) surface pressure,
- b) 24-hour rainfall,
- c) dew-point depression at 700 mb,
- d) vertical p-velocity (ω) at 700 mb,
- e) relative vorticity (ζ) at 700 mb, and
- f) geopotential contours and isotherms at 850 mb and at 500 mb.

8.0 Computer Information.

The 6L-FLM forecast model is run on a HITAC 8700/8800 Computer System and requires about 27-28 minutes to make a one-day forecast.

9.0 References

"Outline of Operational Numerical Weather Prediction at Japan Meteorological Agency", Electronic Computation Center, Japan Meteorological Agency, Feb. 1974, 44 pp.